HYDROPHOBICALLY MODIFIED POLYELECTROLYTES

SYNTHESIS, PROPERTIES AND INTERACTIONS WITH SURFACTANTS

Armanda C. Nieuwkerk

Promotor:	Dr. E. J. R. Sudhölter hoogleraar in de fysisch-organische chemie
Co-promotor:	Dr. A. T. M. Marcelis universitair docent bij het departement Biomoleculaire Wetenschappen

NN08201, 2394

Armanda C. Nieuwkerk

HYDROPHOBICALLY MODIFIED POLYELECTROLYTES

SYNTHESIS, PROPERTIES AND INTERACTIONS WITH SURFACTANTS

Proefschrift

ter verkrijging van de graad van doctor

op gezag van de rector magnificus

van de Landbouwuniversiteit Wageningen,

dr. C. M. Karssen,

in het openbaar te verdedigen

op vrijdag 20 februari 1998

des namiddags te vier uur in de Aula

ISN 952672

ISBN 90-5485-812-5

BIBLIOTHEEK
LANDBOUWUNIVERSITEIT
WAGENINGEN

This study was supported by the Netherlands Foundation for Chemical Research (SON) with financial aid from the Netherlands Organisation for Scientific Research (NWO).

NN08201, 2394

STELLINGEN

1) Het gebruik van surfactant selectieve elektrodes wordt alom beschreven als een zeer betrouwbare methode om de vrije surfactantconcentratie te bepalen. Hierbij is de kwaliteit van het zelfgemaakte elektrodemembraan echter essentieel.

Zana, R. *Surfactant Solutions. New Methods of Investigation*; Dekker, New York: 1987; Ch. 9.
Goddard, E. D. *J. Am. Oil Chem. Soc.* **1994**, *71*, 1.
Dit onderzoek.

2) Op grond van het type overdrachtsproces dat plaatsvindt bij Langmuir-Blodgett experimenten kan geen definitieve conclusie getrokken worden over de uiteindelijke ordening in de overgedragen lagen.

Dit onderzoek.
Ganguly, P.; Sastry, M.; Choudhury, S.; Paranjape, D. V. *Langmuir* **1997**, *13*, 6582.

3) Hoewel het gebruik van ^{14}N NMR zeker informatie kan verschaffen over het effect van oppervlaktekromming van vesikels en micellen op de beweeglijkheid van de kopgroepen van stikstofbevattende surfactanten, hebben Okamura *et al.* geen rekening gehouden met het feit dat de beweeglijkheid van diezelfde kopgroepen aan de binnenzijde van het membraan ook wordt bepaald door de oppervlaktekromming.

Okamura, E.; Wakai, C.; Matubayasi, N.; Nakahara, M. *Chem. Lett.* **1997**, 1061.

4) Het door Ortega *et al.* gevonden minimum in de geleidbaarheidsmetingen van een oplossing van Al^{3+} en bismuthiolaat als functie van de molfractie Al^{3+} leidt niet tot de door hun vermelde stoichiometrie van het gevormde polymeer van Al^{3+} en bismuthiolaat.

Ortega, P.; Vera, L. R.; Guzmán, M. E. *Macromol. Chem. Phys.* **1997**, *198*, 2949.

5) Bij de *in situ* omzetting van 'latent' naar onoplosbaar pigment in een *p*-hydroxy-polystyreen hars melden Zambounis *et al.* op basis van TEM metingen de vorming van goed gedispergeerde pigmentdeeltjes met een grootte kleiner dan 20 nm. Gezien de hoge concentratie pigment in het monster (40 %, w/w) is de individuele deeltjesgrootte echter niet goed te bepalen met deze techniek.

Zambounis, J. S.; Hao, Z.; Iqbal, A. *Nature* **1997**, *388*, 131.

6) De door Kamidate *et al.* aangedragen verklaring voor de opname van Cu^{2+} en Zn^{2+} door liposomen in afwezigheid van ionoforen is niet aannemelijk.

Kamidate, T.; Yamaguchi, J.; Suita, T.; Tani, H.; Watanabe, H. *Chem. Lett.* **1997**, 971.

7) Dynamische lichtverstrooiing is een geschikte methode om vesikelfusie te bestuderen.

Morgan, J. D.; Johnson, C. A.; Kaler, E. W. *Langmuir* **1997**, *13*, 6447.
Yatcilla, M. T.; Herrington, K. L.; Brasher, L. L.; Kaler, E. W.; Chirovolu, S.; Zasadzinski, J. A. *J. Phys. Chem.* **1996**, *100*, 5874.

8) Zonder fundamenteel onderzoek is er geen vooruitgang mogelijk.

9) Het zou goed zijn voor het milieubewustzijn van menigeen, wanneer men bij de slager bij ieder ons vlees een evenredige hoeveelheid mest mee zou krijgen.

10) Het is naïef te veronderstellen dat er op Mars alleen mannen zouden wonen.

11) Het helpen van met olie besmeurde vogels dient meer om het geweten van de mens te sussen dan dat het daadwerkelijk leidt tot het overleven van deze vogels.

12) Gezien het alcoholpercentage is zwaar bier lichter dan gewoon bier.

13) Het gelijke tred houden van het duurder worden van het openbaar vervoer en het autogebruik zal uiteindelijk leiden tot nog meer gebruik van de auto als vervoermiddel.

14) Windenergie is alleen een schone vorm van energie voor diegenen die ver van een windmolenpark af wonen.

Stellingen behorende bij het proefschrift

"Hydrophobically Modified Polyelectrolytes: Synthesis, Properties and Interactions with Surfactants"

Wageningen, 20 februari 1998 Armanda C. Nieuwkerk

Met dank aan M. D. E., A. T. M. M.

Voorwoord

Vier jaar heb ik gewerkt aan het in dit proefschrift beschreven onderzoek. Polymeren gesynthetiseerd, eigenschappen bestudeerd en de interacties met surfactanten onderzocht. Maar behalve deze interacties waren ook de interacties met de "mede" labgenoten (niet alleen de chemici), familie en vrienden van groot belang bij het slagen van het onderzoek. Bij deze wil ik daarom iedereen bedanken die op enigerlei wijze heeft bijgedragen aan het totstandkomen van dit proefschrift. Een aantal mensen wil ik in het bijzonder noemen.

Allereerst wil ik mijn promotor Ernst Sudhölter bedanken voor de mogelijkheid die hij mij geboden heeft om in zijn groep dit promotieonderzoek uit te voeren. Ernst, de vrijheid die ik kreeg om binnen het onderzoek mijn eigen(wijze) weg te gaan en het vertrouwen wat je in mij stelde heb ik zeer gewaardeerd.

Mijn co-promotor Ton Marcelis, wil ik bedanken voor de dagelijkse begeleiding de afgelopen jaren. Ton, jij was altijd aanspreekbaar bij kleine en grote chemische problemen, het liefst wel na de koffie, en je kwam vaak met nuttige suggesties en oplossingen. Ook was je altijd zeer snel, maar daarom niet minder kritisch, met de beoordeling van manuscripten. Bedank(t) hiervoor.

De leden van de promotiecommissie, prof. dr. A. Laschewsky, prof. dr. J. B. F. N. Engberts, prof. dr. M. A. Cohen Stuart en prof. dr. Æ. de Groot, ben ik erkentelijk voor hun inzet.

Op het gebied van synthese en zuivering was Arie Koudijs een geduldig leermeester. Arie, behalve voor de domme opmerkingen die de sfeer op en rond de labzaal verhoogden en de gezellige zwemuurtjes, wil ik je graag bedanken voor de synthese van de surfactanten en polymeren die in de verschillende hoofdstukken staan beschreven.

Ellen van Kan heeft middels een afstudeervak een bijdrage geleverd aan het onderzoek. De resultaten staan her en der verspreid in dit proefschrift. Ellen, bedankt voor je bijdrage en nimmer aflatende enthousiasme (trouwens, ik heb nog wat UV-reeksjes staan).

Voor de analyse van de gesynthetiseerde verbindingen kon ik altijd terecht bij Beb van Veldhuizen, Rien van Dijk en Hugo Jongejan. Alledrie bedankt hiervoor. Gert Jan Kuiper wil ik bedanken voor (de pogingen tot) het bepalen van de molekuulgewichten van de polymeren. Jan Kroon en Peter Kimkes ben ik dank verschuldigd voor de hulp bij de Langmuir-Blodgett en Brewsterhoekmicroscopie experimenten.

Jurrie Menkman, Gert Nieuwboer, Pleun van Lelieveld en Ronald de Bruin leverden het juiste chemische gereedschap, het glaswerk en de chemicaliën. Hannie van de Broek, Gerrie Muller en Gert Jan Kuiper leverden de koffie om op gang te blijven. Dit was regelmatig erg nodig. De dames van het secretariaat, Ineke de Wolf, Elly Geurtsen, Ien Wognum en Wikje Dijkwel, hebben vooral de laatste maanden de nodige hulp geboden. Allemaal heel veel dank hiervoor.

Mijn dank gaat ook uit naar een aantal mensen buiten de vakgroep organische chemie. Allereerst naar prof. dr. J. Lyklema (LUW, fysische chemie en kolloïdkunde) voor de discussies en getoonde belangstelling voor het onderzoek. Naar Remko Fokkink en prof. dr. M. A. Cohen Stuart (LUW, fysische chemie en kolloïdkunde) voor hun hulp bij de lichtverstrooiingsexperimenten. J. Groenewegen (LUW, virologie) heeft geholpen bij het maken van de electronenmicroscopische opnamen. H. Hey (LUW, bodemkunde) heeft met flash-fotolyse experimenten de aanwezigheid van kalium in de polymeren aangetoond. Prof. dr. G. J. Ashwell (Cranfield, UK) heeft de second harmonic generation experimenten uitgevoerd.

Alle (ex-)collega aio's, oio's, analisten en postdocs wil ik bedanken voor de gezelligheid tijdens de pauzes, de tripjes die we hebben gemaakt en het vrijdagmiddaggebeuren in Loburg. Dennis Piet en Peter Kimkes wil ik in het bijzonder bedanken voor de tijd die we samen als borrelcommissarissen doorbrachten. De BBQ's zijn onvergetelijk.

Als laatste wil ik mijn moeder en Marcel bedanken. Mam, jij zorgde voor mijn eerste kennismaking met de universiteit. Hoewel je weinig begreep van wat ik nu eigenlijk uitspookte achter die zuurkast heb je me altijd gesteund en veel belangstelling getoond. Heel veel dank hiervoor.

Marcel, behalve voor de vele nuttige discussies die we voerden over ons beider onderzoeken, wil ik je bedanken voor heel veel dingen buiten de chemie.

Cindy

Ter nagedachtenis aan mijn vader
Voor mijn moeder

Contents

Chapter 1 **General Introduction**

1.1 Liquid Crystalline Behaviour 2
1.1.1 Thermotropic liquid crystals 2
1.1.2 Lyotropic liquid crystals 4
1.1.3 Thermotropic liquid crystalline polymers 7
1.1.4 Lyotropic liquid crystalline polymers 9
1.2 Amphiphilic Polymers 10
1.2.1 Microdomain formation 10
1.2.2 Exciton coupling 12
1.2.3 Monolayer formation 14
1.2.4 Langmuir-Blodgett films 15
1.3 Polyelectrolyte-Surfactant Interactions 16
1.4 Outline of the Thesis 18
1.5 References 19

Chapter 2 **Synthesis and Characterisation of Maleic Anhydride Based Copolymers**

Abstract 23
2.1 Introduction 24
2.2 Some Theoretical Aspects 24
2.2.1 General aspects of radical polymerisation 24
2.2.2 Radical copolymerisation 26
2.2.3 Maleic anhydride copolymers 27
2.3 Results and Discussion 28
2.3.1 Monomer synthesis 28
2.3.2 Copolymerisation 30
2.3.3 Poly(maleic acid-*co*-alkyl vinyl ether)s 31
2.3.4 Poly(sulfonyl ethyl maleic acid monoamide-*co*-alkyl vinyl ether)s 31
2.3.5 Thermotropic Behaviour 32
2.4 Conclusions 36
2.5 Experimental 37
2.5.1 Materials 37
2.5.2 Methods 39
2.6 References 39

Chapter 3 **Behaviour of Negatively Charged Maleic Acid Based Polyelectrolytes in Aqueous Solution**

Abstract 41

3.1 Introduction 42

3.2 Results and Discussion 42

3.2.1 Potentiometric titrations 43

3.2.2 UV spectroscopy 47

3.2.3 Dynamic light scattering 50

3.3 Conclusions 53

3.4 Experimental 54

3.4.1 Materials 54

3.4.2 Methods 54

3.5 References 55

Chapter 4 **Interactions between Hydrophobically Modified Polyelectrolytes and Ammonium Surfactants**

Abstract 57

4.1 Introduction 58

4.2 Results and Discussion 59

4.2.1 Potentiometry 59

4.2.2 Surface tension measurements 64

4.2.3 UV spectroscopy 69

4.3 Conclusions 80

4.4 Experimental 81

4.4.1 Materials 81

4.4.2 Methods 81

4.5 References 82

Chapter 5 **Interactions between Chromophore Labelled Ammonium Surfactants and Hydrophobically Modified Polyelectrolytes**

Abstract 85

5.1 Introduction 86

5.2 Results and Discussion 86

5.3 Conclusions 101

5.4 Experimental 102

5.4.1 Materials 102

5.4.2 Methods 102

5.5 References 103

Chapter 6 **Self-assembly of Copolymers with Maleic Anhydride or Maleic Acid Moieties on Aqueous Subphases**

Abstract 105

6.1 Introduction 106

6.2 Results and Discussion 106

6.2.1 Polymers I-n 107

6.2.2 Polymers II-n 109

6.2.3 Subphase variation 113

6.2.4 Kinetics 120

6.2.5 Monolayer transfer 121

6.3 Conclusions 123

6.4 Experimental 123

6.4.1 Materials 123

6.4.2 Methods 123

6.5 References 124

Chapter 7 **Ion Pair Amphiphiles from Sodium Dodecyl Sulfate and Ammonium Amphiphiles Carrying Functionalised Azobenzene Units**

Abstract 127

7.1 Introduction 128

7.2 Results and Discussion 128

7.2.1 Ammonium amphotropes 128

7.2.2 Ion pair amphiphiles 131

7.2.3 Amphotrope aggregation in aqueous solution 132

7.2.4 Formation of ion pair amphiphiles in aqueous solution 135

7.3 Conclusions 138

7.4 Experimental 139

7.4.1 Materials 139

7.4.2 Methods 140

7.5 References 140

Summary 143

Samenvatting 147

Curriculum Vitae 151

List of Publications 153

General Introduction

Chapter 1

Aqueous systems containing polymers and surfactants are encountered in biological systems and everyday life. The interactions between these compounds are important in *e.g.* protein-lipid complexes in biomembranes.[1-4] Aqueous polymer-surfactant systems also find application in cosmetics, tertiary oil recovery, drug delivery, paint formulation and paper production.[5] The use of polymer-surfactant complexes in these applications is based on their ability to solubilize water-insoluble compounds within their apolar domains and on the possibility to adjust their rheological properties to a specific application. A special class of polymers are the hydrophobically modified charged polymers which can form micelle-like structures, so-called microdomains, in aqueous solution. The formation of the microdomains depends on the length and structure of the hydrophobic moiety and charge density of the polyelectrolyte.
In aqueous solution strong complexation occurs between hydrophobically modified polyelectrolytes and oppositely charged surfactants due to electrostatic and hydrophobic interactions. The effects of varying hydrophobicity and charge density of hydrophobically modified polyelectrolytes or surfactants on their mutual interactions are the main topics of this thesis.
Before going deeper into the interactions between hydrophobically modified polyelectrolytes and surfactants some general aspects of the individual constituents used in this study will be presented.

1.1 Liquid Crystalline Behaviour

Many of the polyelectrolytes and surfactants used in this study are labelled with rigid aromatic units which offer the possibility to monitor microdomain formation and polyelectrolyte-surfactant interactions in aqueous solution by UV spectroscopy. Furthermore, these rigid units can induce liquid crystalline phases. Liquid crystalline phases are anisotropic fluid phases characterised by long-range orientational order and varying degrees of spatial order. There is a large number of chemically different compounds forming different kinds of liquid crystalline phases, also called mesophases. The self-organisation into mesophases can occur upon heating of the pure compound (thermotropic liquid crystalline phases) or is induced by isotropic solvents (lyotropic liquid crystalline phases). The molecular structure of typical compounds forming thermotropic mesophases differs considerably from those forming lyotropic mesophases.

1.1.1 Thermotropic liquid crystals

Thermotropic liquid crystals usually consist of an anisometric rigid moiety (rod-like or disc-like) to which flexible alkyl chains are attached.[6-9] These rigid units are essential for the temperature induced mesophase formation, and are therefore called mesogenic units. The rod-

like molecules can form smectic and/or nematic mesophases as shown in Figure 1.1. The formation of these phases stems from the preference of the mesogens to arrange parallel to each other. The smectic phase can be divided into many subphases which differ in the way the molecules are packed within the layers. Disc-like molecules can give columnar structures, like columnar nematic, or discotic mesophases. Optically active molecules can give chiral nematic (or cholesteric) mesophases. In these mesophases a spontaneous twist in the phase is induced about an axis normal to the preferred molecular orientation.

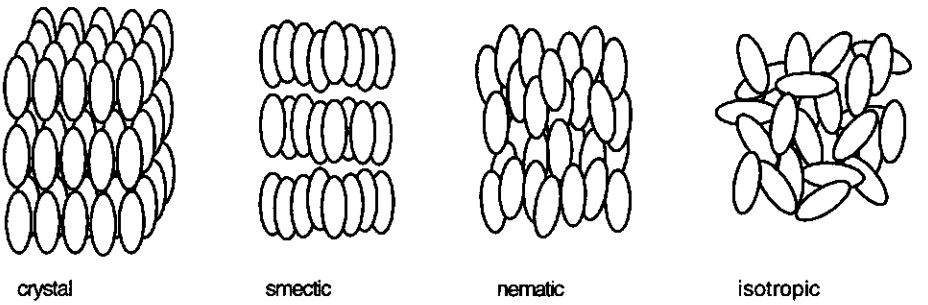

Figure 1.1 **Schematic representation of different thermotropic phases.**

The formation of mesophases can be studied by differential scanning calorimetry (DSC) and optical polarisation microscopy. With DSC the exact phase transition temperatures and the corresponding transition enthalpies can be determined. The reversibility of phase transitions can also be determined by DSC. Usually, little or no hysteresis is observed for liquid crystalline to liquid crystalline (lc → lc) and liquid crystalline to isotropic (lc → i) phase transitions, whereas solid to liquid crystalline (s → lc) or solid to isotropic (s → i) phase transitions may display considerable hysteresis. Transitions between different crystalline phases (s → s) depend on the history of the sample and may not appear in a second heating run.

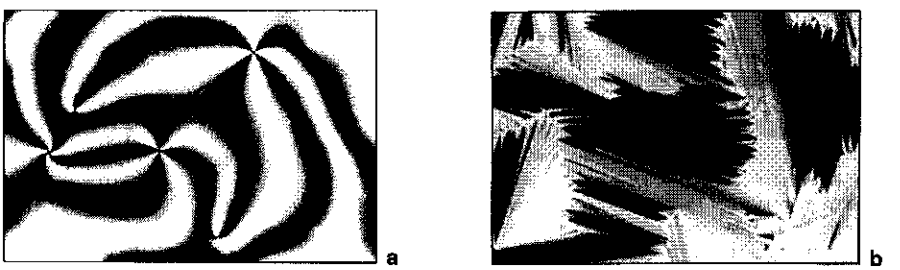

Figure 1.2 **Nematic Schlieren texture (a) and smectic fan-shaped focal-conic texture (b) viewed between crossed polarizers.**

By polarisation microscopy the textures of thin films of liquid crystalline material can be observed. These textures are characteristic for a given mesophase. A nematic phase is characterised by thread-like, marbled or Schlieren textures between crossed polarizers (see Figure 1.2a). For a smectic A phase a fan-shaped focal-conic texture as in Figure 1.2b is observed. Other smectic phases have a different appearance under the microscope, providing a possibility to distinguish them.

DSC and optical polarisation microscopy are complementary techniques in the sense that transitions that are not accompanied by a change in texture and are therefore invisible, often have a detectable transition enthalpy. On the other hand, phase transitions with a very low enthalpy may well be visible as a result of textural change.

1.1.2 Lyotropic liquid crystals

Compounds forming lyotropic mesophases usually consist of two chemically distinct regions, a flexible apolar part (the tail) and a polar (ionic or non-ionic) headgroup. These compounds are called amphiphiles, indicating that one part of the molecule likes a polar solvent and the other part prefers an apolar solvent. Due to their chemical structure they concentrate at the solvent-air interface, thus reducing the surface tension of a solvent. Therefore amphiphiles are also called SURFace ACTive AgeNTS or briefly surfactants. Some representative surfactants used in this study are shown in Scheme 1.1.

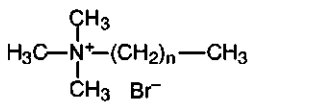

Alkyltrimethylammonium Bromide
DTAB n = 11, CTAB n = 15

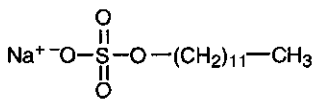

Sodium Dodecyl Sulfate
SDS

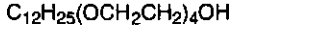

Polyoxyethyleen(4)lauryl ether
Brij 30

Scheme 1.1 **Some of the surfactant molecules used in this study.**

The hydrophobic part of a surfactant usually consists of one or more hydrocarbon chains, sometimes with various degrees of unsaturation or branching. The size and the length of the hydrocarbon chains may vary considerably, but must consist of at least 8 carbon atoms. The hydrophilic headgroups may be cationic, anionic, zwitterionic or non-ionic. Also the number of headgroups can be varied.[10-13] Self-aggregation of surfactants has been observed in polar solvents like water, hydrazine[14] and ethylene glycol[15], but also in apolar solvents like cyclohexane.[16] The common driving forces for aggregation are the solvent-solute immiscibilities (enthalpic force) that arise from differences in cohesive energy between solute

(amphiphile) and solvent.[17] The forces that govern the attraction between two or more molecules in water, the hydrophobic interactions, are however, up to now, not well understood. There is strong evidence that the hydrophobic interactions are caused by the extensive hydrophobic hydration shells that form around hydrophobic moieties in water. When the concentration of the hydrophobic molecules is increased above a certain value, the number of water molecules necessary to independently hydrate the hydrophobic groups becomes insufficient and the hydrophobic groups aggregate. Because the hydrophobic hydration shells are very large, cooperative interaction of, for example, surfactant molecules can indeed occur at very low surfactant concentrations (*i.e.* at the cmc).[18]

A delicate balance of the attractive interactions between the hydrophobic groups of the surfactants and the repulsive interactions between the hydrated surfactant headgroups determines the aggregate morphology. The molecular packing constraints within an aggregate are also very important. The surfactant parameter P, which was introduced by Israelachvili *et al.*[19], provides a qualitative prediction of the aggregate morphology of surfactants in water.

$$P = \frac{v}{a_o l_c}$$

In this equation v (= 27.5 + 27 n_c, in Å^3) is the volume of the hydrophobic moiety of the surfactant molecule, a_o the optimal headgroup area (Å^2) and l_c (= 1.5 + 1.27 n_c, in Å) the maximum length of the alkyl chains (n_c is the number of carbon atoms in the hydrophobic tail).[20] The headgroup area a_o can be estimated.

Table 1.1 **Dependence of aggregate type on the packing requirements of surfactant headgroup and chains.**

spherical micelles	P < 1/3
rod-like micelles	1/3 < P < 1/2
bilayers	1/2 < P < 1
inverted micelles	P > 1

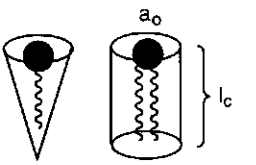

Cone shaped surfactants, like surfactants with one tail, can pack into highly curved aggregates like micelles, whereas double chained surfactants generally have a cylindrical shape (P = 1) and prefer to pack into bilayer structures (Table 1.1).

The monomer shape, and thus aggregate morphology, is affected by factors as the chemical structure of the monomer (hydrogen bonding capability, unsaturation of the alkyl chains), solvent and solvent ionic strength, pressure and temperature. Furthermore, the surfactant

concentration influences the morphology of the aggregates formed. Figure 1.3 shows some common aggregate morphologies.

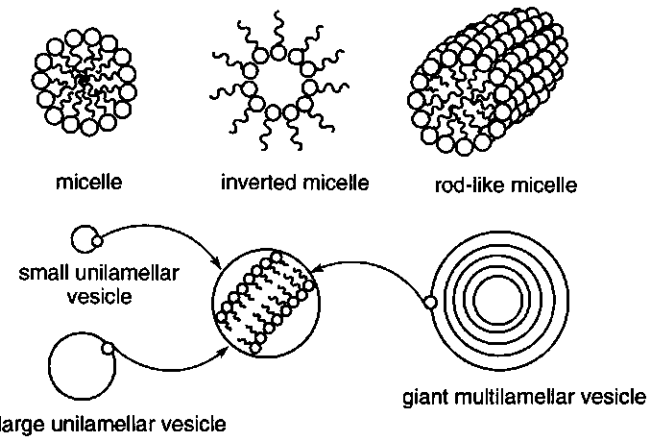

Figure 1.3 **Schematic representation of common aggregate morphologies.**

At higher surfactant concentrations lyotropic mesophases of the cubic, hexagonal, lamellar and nematic type can be formed.[21] These mesophases can be regarded as superstructures formed from micelles and bilayer fragments.

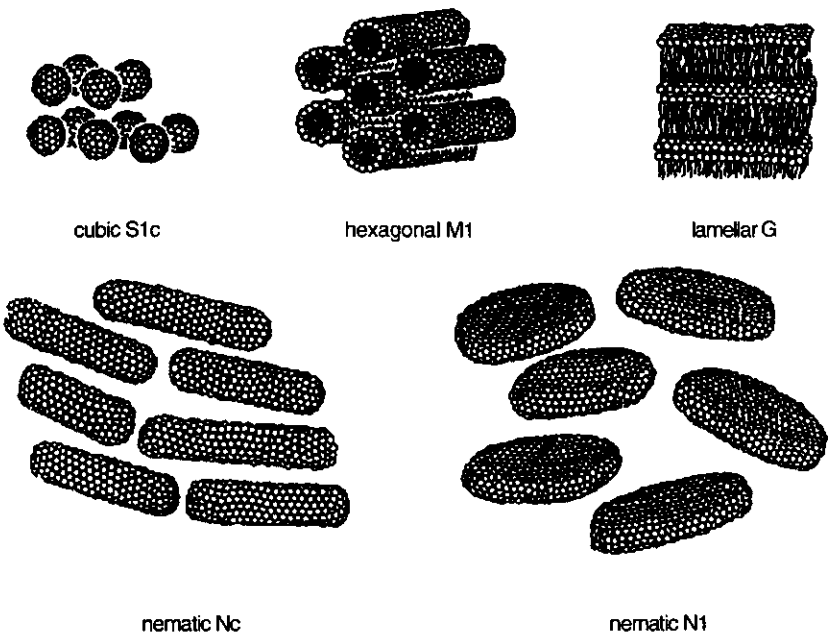

Figure 1.4 **Schematic representation of lyotropic mesophases. Taken from reference 48.**

The cubic phase *e.g.* is thought to be build up from spherical micelles arranged in a cubic lattice whereas the hexagonal M_1-phase is assumed to consist of rodlike micelles arranged in a hexagonal array. In the lamellar phases the molecules are arranged in planar sheets on top of each other. When the micellar units are only orientationally ordered nematic phases are formed. A schematic representation of these lyotropic phases is shown in Figure 1.4.

Ion pair amphiphiles form a specific class of amphiphiles. They consist of two oppositely charged single chained surfactant molecules and often form both thermotropic and lyotropic liquid crystalline phases.[22,23] For these compounds the formation of vesicles is usually observed.[24] The oppositely charged headgroups combine at the surface of the aggregate reducing the electrostatic repulsions between the alike species, and the alkyl chains concentrate in the interior of the bilayer structure.

A third class of compounds combines the possibility to form both lyotropic and thermotropic liquid crystalline phases, and are therefore called amphotropic liquid crystals. Amphotropic behaviour has *e.g.* been observed for some phospholipids[25], alkylated monosaccharides[26] and amphiphilic diols.[27]

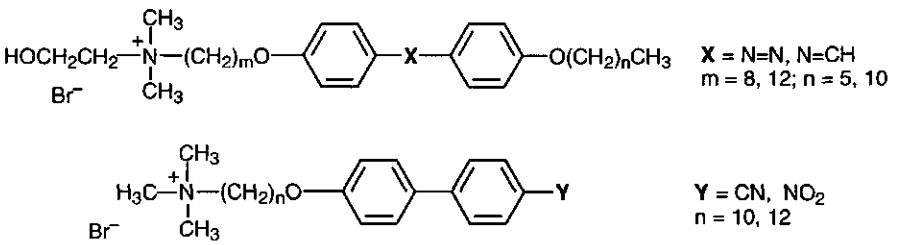

Scheme 1.2 **Amphotropes taken from references 28 and 29.**

By introducing rod- or disk-like building blocks into amphiphilic molecules the known amount of amphotropic molecules has increased considerably.[28-31] Some examples of these amphotropes are shown in Scheme 1.2. Amphotropism can also be observed in polymers when the structural units responsible for the formation of thermotropic and lyotropic mesophases are combined within the same polymer.

1.1.3 Thermotropic liquid crystalline polymers

Liquid crystalline polymers (LCPs) have become an important area of research effort because they combine the properties of low molar mass mesogens with the mechanical and thermal stability of the polymer main chain. Thermotropic liquid crystalline polymers can find applications in *e.g.* optical data storage, non-linear optics and in conductive LCP devices.[3,32,33] Liquid crystalline polymers are prepared by introducing rigid units into the polymers which tend to orient themselves into a particular direction. There are two major classes of LCPs, the main

chain and side chain liquid crystalline polymers (MCLCPs and SCLCPs, respectively). In the MCLCPs the mesogenic units are incorporated in the main chain and in SCLCPs the mesogens are attached to the polymeric backbone via a flexible spacer. Some examples are shown in Scheme 1.3.

The design of MCLCPs is based on lowering of the melting temperature of rigid polymers. In many MCLCPs this is accomplished by alternating the rigid-rod units with flexible spacers consisting of methylene or ethylene oxide groups.[34] The length and length-to-diameter ratio of the rigid units and the length of the flexible spacer influence the type of mesophase that is formed and its stability. Mesophase behaviour in otherwise rigid, nonmesogenic polymers can also be induced by introducing kinked bonds like *e.g.* -O-, -SO_2-, -CO- and -$C(CH_3)_2$- between the rigid units, or by introducing substituents on the rigid units.[35]

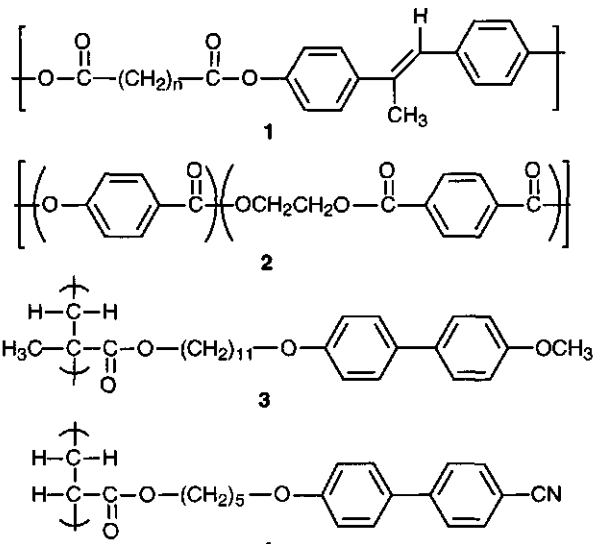

Scheme 1.3 **Examples of thermotropic liquid crystalline polymers.**[35-37]

The mesophase order in SCLCPs is mainly determined by the mesogenic group, allowing for incorporation in a wide variety of polymers with different backbones. Acrylates (**4**), methacrylates (**3**) and siloxanes (**5**) are backbones which are often used. The flexible spacer, connecting the mesogen with the backbone, usually consists of methylene units and decouples the motions of the polymer backbone and the mesogens.[38] An increase in spacer length leads to

the formation of more ordered mesophases, *e.g.* smectic instead of nematic, due to the increased freedom of the mesogens to attain their most favourable orientation.[39]

Although the mesophase order is mainly determined by the mesogenic unit, the flexibility of the main chain also is an important factor. A more flexible main chain, having a lower glass transition temperature T_g, allows for a broader temperature range of the mesophase. Other factors influencing the mesophase behaviour are the endgroup length, coupling unit, polymer tacticity, polymer molecular weight and polydispersity of the polymer. More ordered mesophases are favoured by increasing the molecular weight up to a degree of polymerisation of about 10, above which the mesophase order and transition temperatures remain rather constant.[37] Removal of oligomers from polymers is important because they have a strong influence on the mesophase formation, usually lowering the stability and order.[40]

1.1.4 Lyotropic liquid crystalline polymers

When immersed in a low molecular weight liquid like water, dioxane or benzene, some polymers form lyotropic mesophases. The self-ordering in these systems is caused by their amphiphilic character, *i.e.*, the presence of solvophobic (lyophobic) and solvophilic (lyophilic) groups in the polymer. Both SCLCPs and MCLCPs can form lyotropic mesophases.[41] The tobacco mosaic virus, DNA, collagen and cotton cellulose are biopolymers capable of forming lyotropic mesophases.[42]

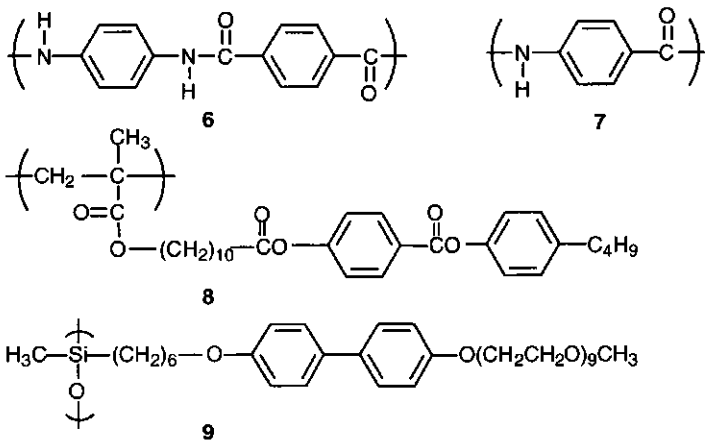

Scheme 1.4 **Polymers capable of forming lyotropic mesophases.**[43-45]

Some synthetic lyotropic LCPs are shown in Scheme 1.4. Lyotropic liquid crystalline polymeric systems are mainly used for fiber spinning.[46] An example is the mechanically very strong fiber poly(*p*-phenylene terephthalamide) (**6**) which is better known as Twaron and is commercially available from Akzo Nobel. A similar polymer is produced by Du Pont under the

name Kevlar. By preparing an anisotropic solution of the biopolymer cellulose in a phosphoric acid/water mixture products like *e.g.* flame retarding fibers or additives for paints and laundry detergents can be produced.[47]

By varying the solubilisation quality of the solvent (by using various solvents, solvent mixtures or by varying temperature) the extent of inter- and/or intramolecular aggregation between the alike groups may be altered leading to various lyotropic phases. Other factors influencing lyotropic behaviour are the polymer molecular weight, polydispersity and chain rigidity.[43]

1.2 Amphiphilic Polymers

Polymers bearing hydrophilic and hydrophobic fragments, so-called amphiphilic polymers, have been known for a long time. They have attracted much attention due to their resemblance to biopolymers and their strong tendency for self-organisation in aqueous solution (lyotropic mesomorphism). The conformational behaviour of amphiphilic polymers is intriguing from the point of protein science. The secondary structure of these polymers is of course much simpler than that found in proteins, but the factors controlling the secondary structure are similar. Hydrophobic interactions, electrostatic repulsions between headgroups, and excluded volume interactions play an important role in both systems. Furthermore, both systems undergo conformational changes upon addition of free surfactants. This makes amphiphilic polymers attractive model systems for proteins. By incorporation of different surfactants in a polymer chain proteins may be mimicked (Figure 4.1).[48] Amphiphilic polymers are often called 'micellar polymers' because of their resemblance in both properties and structures of surfactant micelles. Both systems have a high solubilisation capacity for non water-soluble molecules and have low viscosities in aqueous solution due to hydrophobic aggregation.

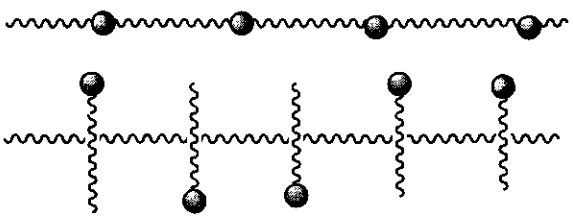

Figure 1.4 **Schematic representation of amphiphilic polymers.**

1.2.1 Microdomain formation

Amphiphilic polymers are characterised by versatile molecular architectures. An important class of amphiphilic polymers are the polysoaps in which the hydrophilic and hydrophobic groups are scattered all over the macromolecule. The amphiphilic character stems from the presence of many independent, surfactant-like structural units which are covalently linked as depicted in

Figure 1.4. The ionic groups can be incorporated in an otherwise hydrophobic backbone or be present in side chains. Many types of hydrophilic headgroups have been employed in polysoaps, covering non-ionic, cationic, anionic and zwitterionic ones. Also a variety of side chains have been used. Some examples are shown in Scheme 1.5.

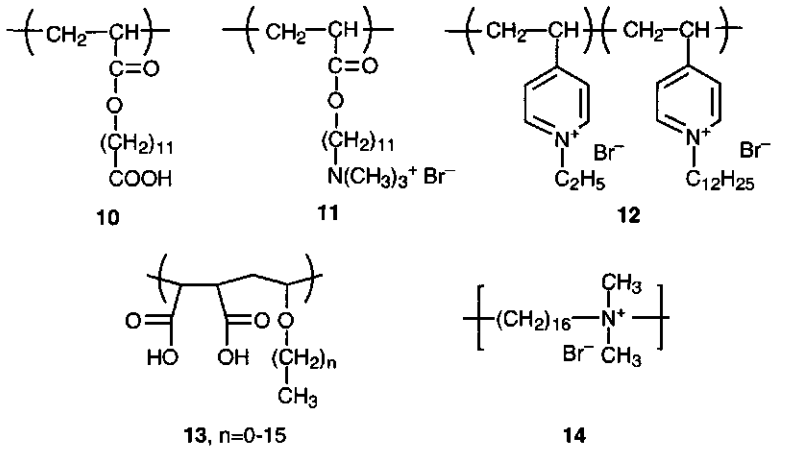

Scheme 1.5 **Amphiphilic polymers.**[49-52]

A well known class of polysoaps are the poly(maleic acid-*co*-alkyl vinyl ether)s **13** which have been studied to a great extent by Zana *et al.*[53-55] and Strauss *et al.*[56-59] In aqueous solution the ionic groups prefer to be hydrated by the surrounding water molecules, whereas the hydrophobic side chains shy from the water molecules by forming so-called microdomains. The charge density on the polyelectrolyte backbone and the size of the hydrophobic side chains govern the formation of microdomains. The electrostatic interactions between the charged groups on the backbone favour the stretching of the polyelectrolyte chain in order to decrease the repulsions between the chain segments. Opposing this are the hydrophobic interactions between the side chains. Increasing alkyl chain length will increase the intramolecular hydrophobic interactions favouring a more compact polymer coil.[60] This is schematically depicted in Figure 1.5.

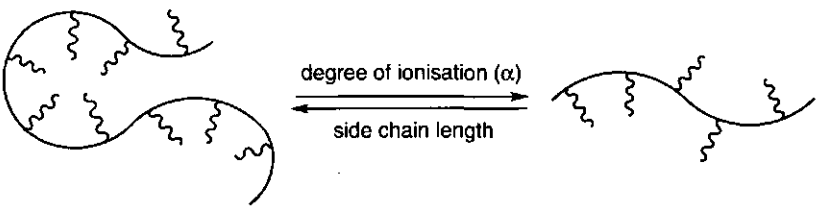

Figure 1.5 **Polymer conformation as function of charge density and side chain length.**

For n = 0 or 1 polysoap **13** behaves as a normal hydrophilic polyelectrolyte which undergoes progressive conformational expansion when the charge density is increased. The increase in charge density is obtained by deprotonation of the carboxylic acid groups. For $2 < n < 9$ an increase in charge density results in a conformational transition whereby the copolymer coil goes from a compact globular conformation stabilised by hydrophobic interactions at low charge density (low α), to a normal extended polyelectrolyte conformation at high charge density (high α). The transition takes place within a fairly narrow range of α which increases with n. For $n \geq 9$ the polysoaps appear to retain the compact conformation in the whole range of α. Similar results are obtained for poly(1-alkene-*co*-maleic acid)s upon varying charge density and alkyl chain length.[61-63]

The presence of hydrophobic microdomains has been ascertained by techniques like viscometry[64,65], surface tensiometry[66] and fluorescence probing.[51,54] This last technique makes use of probe molecules of which small amounts are added to the solution or are covalently linked to the polysoap. The disadvantage of these systems is that the probe molecules do not form an intrinsic part of the system, and can therefore affect the microdomain formation. When the probe molecules are regularly distributed along the polymer chains, *e.g.* on each side chain, they form an intrinsic part of these polymers and play a role in determining the physical properties. Aggregation of the probe molecules, also called chromophores, can then be used to monitor the microdomain formation.

1.2.2 Exciton coupling

Spectroscopic techniques like NMR, UV/VIS and fluorescence spectroscopy are very helpful in elucidating conformational transitions in both synthetic and biopolymers.[67] In lyotropic systems the formation of highly ordered aggregates is usually accompanied by an increase in linewidth of the NMR peaks due to restricted molecular motions, changes in relaxation times and changes in chemical shifts due to a different chemical surrounding.[68] In UV/VIS and fluorescence experiments use is made of spectral changes, like shifts in absorption maxima, peak widths and peak asymmetry, which result from a different micropolarity (solvatochromic shifts) or from exciton formation. As many polymers have no UV sensitive or fluorescent groups, labelling with chromophores can be helpful in elucidating physical changes.[69]

The close proximity and preferred orientation of molecules within an aggregate structure lead to intermolecular interactions which affect the energies of both the ground and excited states. Under these conditions molecules do not behave as isolated species but participate in an extended electronic network. Kasha proposed the "molecular exciton theory" to explain the observed spectral changes upon aggregation.[70-73] This model, which neglects the electronic overlap of the π-systems, is based on the interaction between localised transition dipole moments. The coupling between the dipole moments results in a splitting of the monomer

excited state into a higher energy and a lower energy state. The resulting transition energy ($E^{\pm}$) is related to the energy of the monomer, E_m, by

$$E^{\pm} = E_m \pm E_{ex} + D$$

in which D is the dispersion or Van der Waals interaction energy reflecting the change in environment from monomer to oligomer, and E_{ex} is the exciton splitting energy.

For parallel transition dipole moments only the in-phase transition dipole arrangement, with the transition to the higher energy level (E^+), is allowed. Transition to the lower energy level (E^-), with out-of-phase transition dipole arrangement, is forbidden because the transition dipoles cancel each other. Parallel chromophore orientation therefore results in a shift of the UV absorption maximum to lower wavelengths (blue shift) with respect to the monomer absorption maximum. These types of aggregates are also called H-aggregates.

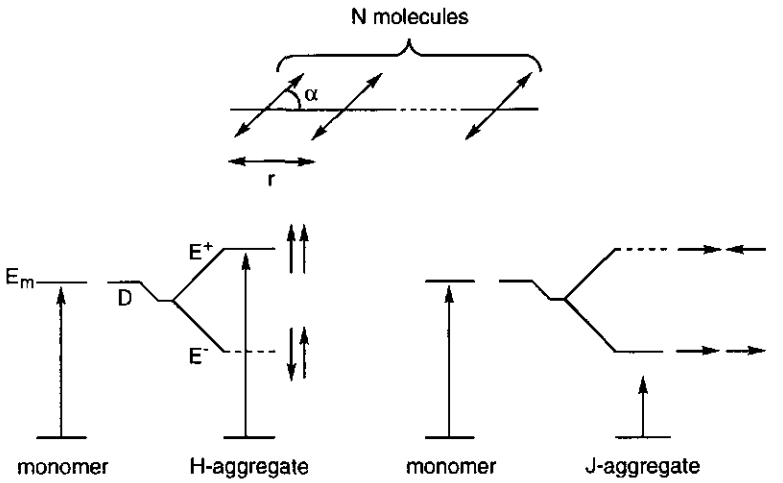

Figure 1.6 **Molecular exciton model. Taken from reference 74.**

For in-line transition dipole moments only the transition to the lowest energy level, with the in-phase transition dipole arrangement, is allowed. In-line chromophore orientation, also called J-aggregation, thus results in a shift of the UV absorption maximum to higher wavelengths (red shift).

The spectral shift (in wavenumber, $\Delta\nu$) for an aggregate consisting of N monomers with respect to the monomer absorption is given by[73]:

$$\Delta\nu = \frac{2}{hc}\frac{N-1}{N}\frac{\mu^2}{r^3}\left(1-3\cos^2\alpha\right)$$

in which μ is the magnitude of the transition dipole moment, r is the centre-to-centre distance between the dipoles and α is the angle between the chromophore long axes and the chromophore centre-to-centre line. $\Delta\nu$ is believed to be mainly governed by r and α. As for the *tilt* angle α, a blue shift means H-aggregation having a relatively large α value and a red shift means J-aggregation having a relatively small α value.

1.2.3 Monolayer formation

Due to their distinct hydrophilic and hydrophobic parts amphiphilic polymers do not only aggregate in aqueous solution, but they can also aggregate at an air-water interface. A technique used to prepare these ordered layers is the Langmuir technique.

Accumulation of polar organic molecules, like surfactants or polyelectrolytes, at the air-water interface may result in the formation of well-ordered molecular films, the so-called Langmuir films. These Langmuir films can be prepared on a Langmuir trough. A small quantity of an amphiphilic compound is dissolved into a volatile organic solvent and spread onto a purified subphase (usually water). When the solvent has evaporated the compound remains at the interface. The use of moveable barriers allows compression and expansion of the film at the air-water interface and the surface pressure and available area can be simultaneously recorded. The surface pressure is the difference between the surface tension of pure subphase and that of the subphase covered with a monolayer. Since the total number of molecules and the total area that the monolayer occupies are known, the available area per molecule can be calculated and a surface pressure-area (π-A) isotherm can be constructed.[75]

The π-A isotherms give information on the molecular cross-section, orientational behaviour of the compounds and information about the interactions with substances dissolved in the subphase. Monolayer films can exhibit a multiplicity of phases depending on the area available per molecule, the temperature and composition of the subphase and the nature of the compound (Figure 1.7).[76-78]

For compounds with strong headgroup repulsions a liquid expanded phase is formed at large molecular areas. Upon compression the intermolecular distance decreases and a liquid condensed (Figure 1.7c) or crystalline phase (Figure 1.7a,b) can be adopted. This phase sometimes coexists with the liquid expanded phase. When all molecules are in the condensed or crystalline phase all rotational freedom is lost. Further compression of the monolayer results in a steep rise in surface pressure followed by collapse of the monolayer due to mechanical instability. Upon collapse a sharp decrease in surface pressure is usually observed. Nonionic amphiphiles form isolated crystalline or amorphous domains at large molecular areas due to their self-assembling characteristics. The crystalline domains can assemble as a large homogeneous crystalline monolayer (Figure 1.7d) or as a polycrystalline monolayer without crystallographic orientation due to the thermal molecular motion at the domain bounderies

(Figure 1.7e). The amorphous monolayer can not be crystallised upon compression due to collapse before reaching the surface pressure at which the monolayer can be crystallised at a given subphase temperature (Figure 1.7f).

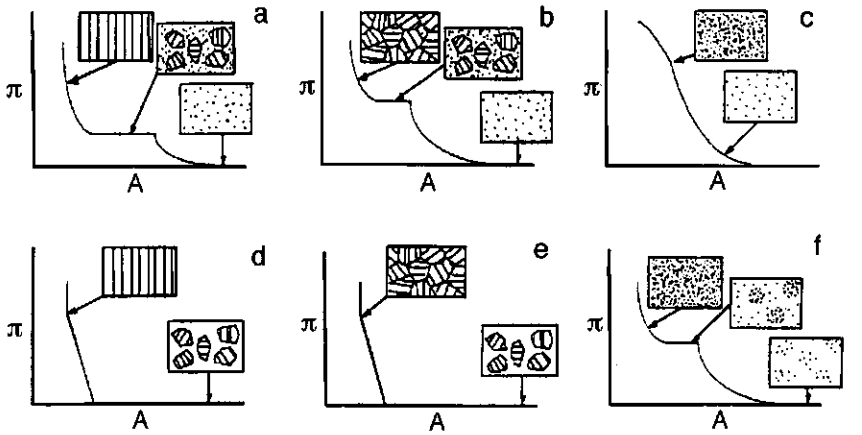

Figure 1.7 **Surface pressure-area isotherms for compounds with strong (a,b,c) and weak (d,e,f) headgroup repulsion as a function of temperature. The temperature increases from left to right. The monolayer can be amorphous or crystalline. Taken from reference 77.**

To prepare polymeric monolayers the interactions of the hydrophilic groups in the polymer with the subphase must be strong enough to make it energetically favourable for the polymer molecules to uncoil and to become relatively ordered at the water-air interface. In this respect polymers with frequent and regular placement of the hydrophilic and lipophilic groups like *e.g.* alternating copolymers of maleic anhydride or maleic acid with various comonomers comprise an interesting class of polymers for the formation of stable monolayers.

With Brewster Angle Microscopy (BAM) it is possible to visualise the morphology and domain structures of a monolayer at the air-water interface.[79,80] The principle of this technique is the almost zero reflectivity of the water surface for light polarised in the plane of incidence and incident at the Brewster angle (53°). This means that the surface will appear dark. If a polarised laser beam is directed to a monolayer-covered surface at 53°, the Brewster angle is slightly different, and therefore the reflectivity from the interface is not zero. The reflected beam can be imaged by a CCD camera and contrast is provided by local differences in the thickness and optical dispersion properties of the monolayer.

1.2.4 Langmuir-Blodgett films

Organised films necessary for electronic and electro-optical applications can be prepared by the Langmuir-Blodgett technique. If the surface pressure (surface tension) of the monolayer is held

constant in a liquid condensed phase and a stable monolayer is obtained, a monomolecular film can be transferred from the surface onto a suitable solid substrate by dipping the latter through the monolayer-air interface. In this way highly ordered (multilayer) films can be obtained where the thickness can be controlled exactly by the number of dipping cycles. Arrays of molecules are formed, preferably with cooperative properties different from those of the individual molecular components and perhaps possessing some functional enhancement. Liquid crystals are a well-known example of a cooperative function, nowadays used in numerous applications.[81]

Commonly used substrates are glass and quartz slides, silicon wafers and mica. Depending on the interactions between the polar and nonpolar parts of the molecules and the nature of the interaction between the first layer and the substrate several deposition modes are possible. These include X-type (film transfer on downstroke only), Z-type (transfer on upstroke only) and Y-type deposition (transfer on both the upstroke and downstroke). Y-type deposition is the most commonly observed deposition mode and yields stable, centrosymmetric multilayers. However, for non-linear optics (NLO), piezoelectric and pyroelectric devices non-centrosymmetrical structures are required. The X- and Z-type multilayers may have sufficient asymmetry, but they often transform into Y-type multilayers due to molecular turnaround.[75] So far only few monomeric materials have been reported to produce genuine X- or Z-type multilayers.[82-84] When deposited in a X- or Z-type fashion polymeric materials are more attractive for use in non-linear optics than low molecular weight materials due to their superior thermal and mechanical stability.[85-88]

1.3 Polyelectrolyte-Surfactant Interactions

A large number of studies have been dedicated to polymer-surfactant interactions.[89,90] These studies provide information on biological processes, like protein denaturation by surfactants and the binding of proteins to biological tissues like membranes.[91,92] Biopolymers like bovine serum albumin (BSA) and collagen, bind strongly to oppositely charged surfactants like sodium dodecyl sulfate (SDS).[92,93] Various researchers have *e.g.* studied the interaction of DNA with cationic surfactants.[94,95] Recently, the interaction between DNA and cationic liposomes has become a focus of interest. These liposomes were shown to be promising gene delivery systems.[96] The use of synthetic polymers in biological systems is also gaining interest. The synthetic polymer polyethyleenglycol (PEG) has been used to coat red blood cells which makes it possible to use the blood for transfusion to patients irrespective of their blood type. Experiments using mice have shown that the coated blood cells are accepted by all blood types because the immune system does not recognize the antigens of the injected blood cells.[97]

Polyelectrolytes and oppositely charged surfactants provide a good model system to study the binding of biopolymers to individual or aggregated surfactant molecules.[98] The binding of surfactants to polymers usually starts at concentrations far below the critical aggregation concentration of the surfactants in pure water and is highly cooperative. The electrostatic forces between the oppositely charged components are reinforced by a cooperative process involving aggregation of the alkyl chains of the bound surfactant molecules.[68]

For many polyelectrolyte-surfactant systems of opposite charge, it has been found that the interaction strength increases with surfactant chain length and polyelectrolyte hydrophobicity and that binding is a cooperative process.[94,99,100] For inorganic compounds anticooperative binding to polyelectrolytes is observed, which means that the presence of the polyelectrolyte counterion does not stimulate a next counterion to bind in its proximity. This suggests that there are not only electrostatic interactions involved in the process of surfactant binding, but also hydrophobic interactions between bound surfactant molecules.[99]

The cooperativity of binding suggests that the surfactants bind to the polyelectrolytes in the form of micelle-like aggregates.[101] The polyelectrolyte serves as the counterion in these complexes, shielding the inner part of the micelles from the surrounding water molecules.[102–104] This usually results in critical aggregation concentrations far below the critical micelle concentrations observed without polyelectrolytes.

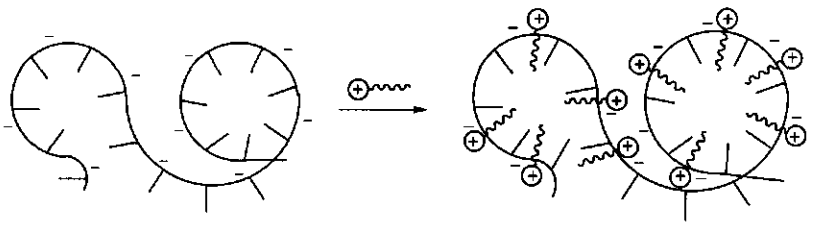

Figure 1.8 **Schematic representation of the binding of cationic surfactants to a polysoap which forms intramolecular microdomains in aqueous solution.**

For hydrophobically modified polyelectrolytes the interaction is also seen to increase in strength upon increasing polyelectrolyte and/or surfactant hydrophobicity, but the cooperativity of the interaction decreases. Hydrophobically modified polyelectrolytes are capable of forming microdomains by aggregation of the polyelectrolyte side chains themselves. Due to electrostatic attraction and hydrophobic interactions a surfactant molecule will preferably incorporate into a microdomain. A next surfactant molecule tends to incorporate in another microdomain for entropic reasons and, to a lesser extent, because the first surfactant molecule has reduced the overall electrical charge of the microdomain.[105] This is thought to lead to the decrease in cooperativity upon surfactant binding to the oppositely charged hydrophobically modified polyelectrolyte and finally leads to the formation of mixed aggregates as depicted in Figure 1.8.

In these aggregates the charged headgroups of the surfactants are located close to the polymer's charged groups, that replace the surfactant counterions, while the surfactant alkyl chains swell the microdomains.

Several systematic investigations of the effect of polymer hydrophobicity and electrical charge density on the polyelectrolyte-surfactant interaction have been performed using techniques like fluorescence probing[106] and potentiometry using surfactant selective electrodes.[107] Using this last technique Zana *et al.* have extensively studied the interaction between alternating poly(maleic acid-*co*-alkyl vinyl ether)s **13**, and ammonium amphiphiles.[51,105,108] For these systems the strength of binding indeed increases upon increasing polyelectrolyte hydrophobicity and the cooperativity of binding decreases due to surfactant binding to the microdomains formed by the polyelectrolyte itself.

1.4 Outline of the thesis

Although many studies have been performed on polyelectrolyte-surfactant interactions the precise influence of variables in polyelectrolyte and/or surfactant structure on the interactions can still not be predicted accurately and the structures of the complexes are not yet completely elucidated. The study described in this thesis is performed to gain a better insight into the mutual interactions and factors influencing these interactions. This has been done by designing and synthesising a new series of hydrophobically modified polyelectrolytes in which the side chain lengths and the charge density can be varied relatively easy. Chromophores have been attached to the ends of the hydrophobic side chains to be able to monitor changes in the interior of the microdomains formed by these polyelectrolytes upon varying hydrophobicity, charge density and upon interaction with surfactants. Furthermore, these chromophores, which consist of rigid aromatic units, can induce the formation of liquid crystalline mesophases.

In *Chapter 2* the synthesis of the used polyelectrolytes is described and their thermotropic behaviour is discussed. *Chapter 3* describes the polyelectrolyte behaviour in aqueous solution as a function of side chain length, charge density and polyelectrolyte headgroup. Furthermore, the sizes and nature of the formed aggregates are discussed.

Chapters 4 and 5 deal with polyelectrolyte-surfactant interactions. In *Chapter 4* the interaction between polyelectrolytes and surfactants as studied with a dodecyltrimethylammonium cation selectieve electrode, surface tensiometry and UV spectroscopy is described. In this chapter surfactants and polyelectrolytes are discussed in which chromophores are introduced in the polyelectrolyte or in the surfactant or in both components. In *Chapter 5* interactions between chromophore labelled surfactants and polyelectrolytes with and without chromophores are discussed.

In *Chapter 6* the monolayer formation of the polyelectrolytes as studied with the Langmuir technique is presented, together with the observed effects of the interaction with simple salts and surfactants which are added to the subphase. Also, the results of some transfer experiments of the polyelectrolytes onto various substrates are presented.

Chapter 7 describes the formation of ion pair amphiphiles between chromophore labelled ammonium surfactants and oppositely charged sodium dodecyl sulfate. Their amphotropism is presented and the formation of vesicles is described.

The thesis is concluded with a *Summary* containing the most relevant results and conclusions.

1.5 References

1 Goddard, E. D. *Colloids Surf.* **1986**, *19*, 255.
2 Ringsdorf, H.; Schlarb, B.; Venzmer, J. *Angew. Chem.(Int. Ed. German)* **1988**, *100*, 117.
3 Ahlers, M.; Müller, W.; Reichert, A.; Ringsdorf, H.; Venzmer, J. *Angew. Chem. (Int. Ed. German)* **1990**, *102*, 1310.
4 Breuer, M.; Strauss, U. P. *J. Phys. Chem.* **1960**, *64*, 228.
5 Hayakawa, K.; Shinohara, S.; Sasawake, S.; Satake, J.; Kwak, J. C. T. *Bull. Chem. Soc. Jpn.* **1995**, *68*, 2179.
6 Vertogen, G.; De Jeu, W. H. *Thermotropic Liquid Crystals, Fundamentals*, Springer-Verlag: Berlin; 1988, part I.
7 Stegemeyer, H. *Topics in Physical Chemistry: Liquid Crystals*, Steinkopff: Darmstadt; 1994.
8 Chandrasekhar, S. *Liquid Crystals*, Cambridge University Press: Cambridge; 1992, p. 1-8.
9 Tschierske, C. *Prog. Polym. Sci.* **1996**, *21*, 775.
10 Satake, I.; Fukunaga, T.; Maeda, T.; Soeda, Y.; Hayakawa, K. *Bull. Chem. Soc. Jpn.* **1993**, *66*, 1618.
11 Danino, D.; Talmon, Y.; Zana, R. *Langmuir* **1995**, *11*, 1448.
12 Zana, R.; Levy, H.; Papoutsi, D.; Beinert, G. *Langmuir* **1995**, *11*, 3694.
13 Esumi, K.; Taguma, K.; Koide, Y. *Langmuir* **1996**, *12*, 4039.
14 Ramadan, M.; Evans, D. F.; Lumry, R.; Philion, S. *J. Phys. Chem.* **1985**, *89*, 3405.
15 Garibi, H.; Palepu, R.; Tiddy, G. J. T.; Hall, D. G.; Wyn-Jones, E. *J. Chem. Soc., Chem. Commun.* **1990**, 115.
16 Ishikawa, Y.; Kuwahara, H.; Kunitake, T. *J. Am. Chem. Soc.* **1994**, *116*, 5579.
17 Kunitake, T. *MRS Bull.* **1995**, 22.
18 Blokzijl, W.; Engberts, J. B. F. N. *Angew. Chem. (Int. Ed. Engl.)* **1993**, *32*, 5145.
19 Israelachvili, J. N.; Mitchell, D. J.; Ninham, B. W. *J. Chem. Soc., Faraday Trans. II* **1976**, *72*, 1525.
20 Tanford, C. *J. Phys. Chem.* **1972**, *76*, 3020.
21 Hoffmann, H. *Ber. Bunsenges. Phys. Chem.* **1984**, *88*, 1078.
22 Kaler, E. W.; Murthy, A. K.; Rodriguez, B. E.; Zasadzinski, J. A. N. *Science* **1989**, *245*, 1371.
23 Fukuda, H.; Kawata, K.; Okuda, H. *J. Am. Chem. Soc.* **1990**, *112*, 1635.
24 Yatcilla, M. T.; Herrington, K. L.; Brasher, L. L.; Kaler, E. W.; Chiruvolu, S.; Zasadzinski, J. A. *J. Phys. Chem.* **1996**, *100*, 5874.
25 Gray, G. W.; Winsor, O. A. in *Liquid Crystals and Plastic Crystals*, Vol 1, Horwood, E., ed.: Chichester: 1974.
26 Jeffrey, G. A. *Acc. Chem. Res.* **1985**, *19*, 168.
27 Tschierske, C.; Brezesinski, G.; Wolgast, S.; Kuschel, F.; Zaschke, H. *Mol. Cryst. Liq. Cryst. Lett.* **1990**, *7*, 131.
28 Shimomura, M.; Ando, R.; Kunitake, T. *Ber. Bunsenges. Phys. Chem.* **1983**, *87*, 1134.
29 Everaars, M. D.; Marcelis, A. T. M.; Kuijpers, A. J.; Laverdure, E.; Koronova, J.; Koudijs, A.; Sudhölter, E. J. R. *Langmuir* **1995**, *11*, 3705.
30 Nishimi, T.; Ishikawa, Y.; Ando, R.; Kunitake, T. *Recl. Trav. Chim. Pays-Bas* **1994**, *113*, 201.
31 Fuller, S.; Shinde, N. N.; Tiddy, G. J. T.; Attard, G. S.; Howell, O. *Langmuir* **1996**, *12*, 1117.
32 Möhlmann, G. R.; Van der Vorst, C. P. J. M. in *Side Chain Liquid Crystal Polymers*, McArdle, C. B., ed., Chapmann and Hall: New York; 1989, Ch.12.

33 McArdle, C. B. in *Side Chain Liquid Crystal Polymers*; McArdle, C. B., ed., Chapman and Hall: New York; 1989, Ch. 13.
34 Jin, J. I.; Antoun, S.; Lanz, R. W. *Br. Polym. J.* **1980**, *12*, 132.
35 MacDonald, W. A. in *Liquid Crystal Polymers: From Structures to Applications*, Collyer, A. A., ed., Elsevier Applied Science: London and New York; 1992, Ch. 8.
36 Roviello, A.; Sirigu, A. *Macromol. Chem.* **1982**, *183*, 895.
37 Percec, V.; Pugh, C. in *Side Chain Liquid Crystal Polymers*, McArdle, C. B., ed., Chapmann and Hall: New York; 1989, Ch. 3.
38 McArdle, C. B. in *Side Chain Liquid Crystal Polymers*; McArdle, C. B., ed., Chapman and Hall: New York; 1989, p. 39.
39 Donald, A. M. Windle, A. H. in *Liquid Crystalline Polymers*, Cambridge University Press: 1992.
40 Simmonds, D. J. in *Liquid Crystal Polymers: From Structures to Applications*, Collyer, A. A., ed., Elsevier Applied Science: London and New York; 1992, Ch. 7.
41 Platé, N. A. *Liquid-Crystal Polymers*, Plenum Press: New York; 1993, p.1.
42 Baird, D. G. in *Liquid Crystalline Order in Polymers*, Blumstein, A., ed., Academic Press: New York; 1987, Ch.7.
43 Shibaev, V. P.; Platé, N. A. *Adv. Polym. Sci.* **1984**, *60/61*, 238.
44 Kwolek, S. L.; Morgan, P. W.; Schaefgen, J. R.; Gulrich, L. W. *Macromolecules* **1977**, *10*, 1390.
45 Lühmann, B.; Finkelmann, H.; Rehage, R. *Makromol. Chem.* **1985**, *186*, 1059.
46 Northolt, M. G.; Sikkema, D. J. in *Liquid Crystal Polymers: From Structures to Applications*, Collyer, A. A., ed., Elsevier Applied Science: London and New York; 1992, Ch. 6.
47 Recently, Akzo Nobel has introduced a new process using anisotropic solutions of cellulose. *Chemisch Weekblad* **1997**, *93 (april 12)*, 1.
48 Borisov, O. V.; Halperin, A. *Langmuir* **1995**, *11*, 2911.
49 Paleos, C. M.; Tsiourvas, D.; Anastassopoulou, J.; Theophanides, T. *Polymer* **1992**, *33*, 4047.
50 Jorgenson, H. E.; Strauss, U. P. *J. Phys. Chem.* **1961**, *65*, 1873.
51 Benrraou, M.; Zana, R.; Varoqui, R.; Pefferkorn, E. *J. Phys. Chem.* **1992**, *96*, 1468.
52 Kunitake, T.; Nakashima, H.; Takanabe, K.; Nagai, M.; Tsuge, A.; Yanagi, H. *J. Am. Chem. Soc.* **1981**, *103*, 5945.
53 Binana-Limbelé, W.; Zana, R. *Macromolecules* **1987**, *20*, 1331.
54 Binana-Limbelé, W.; Zana, R. *Macromolecules* **1990**, *23*, 2731.
55 Anthony, O.; Zana, R. *Macromolecules* **1994**, *27*, 3885.
56 Strauss, U. P.; Schlesinger, M. S. *J. Phys. Chem.* **1978**, *82*, 571.
57 Strauss, U. P.; Schlesinger, M. S. *J. Phys. Chem.* **1978**, *82*, 1627.
58 Strauss, U. P.; Vesnaver, G. *J. Phys. Chem.* **1975**, *79*, 1558.
59 Strauss, U. P.; Vesnaver, G. *J. Phys. Chem.* **1975**, *79*, 2426.
60 Upon increasing the alkyl chain length the intermolecular hydrophobic interactions will also increase.
61 Shih, L. B.; Sheu, E. Y.; Chen, S. H. *Macromolecules* **1988**, *21*, 1387.
62 Shih, L. B.; Mauer, D. H.; Verbrugge, C. J.; Wu, C. F.; Chang, S. L.; Chen, S. H. *Macromolecules* **1988**, *21*, 3235.
63 Chu, D. Y.; Thomas, J. K. *Macromolecules* **1987**, *20*, 2133.
64 Morishima, Y.; Kobayashi, T.; Nozakura, S. *Polymer J.* **1989**, *21*, 267.
65 Ito, K.; Ono, H.; Yamashita, Y. *J. Colloid Sci.* **1964**, *19*, 28.
66 Maltesh, C.; Xu, Q.; Somasundaran, P.; Benton, W. J.; Nguyen, H. *Langmuir* **1992**, *8*, 1511.
67 Sun, S. F. *Physical Chemistry of Macromolecules*, John Wiley & Sons: New York; 1994, Ch. 14 & 16.
68 Sugai, S.; Nitta, K.; Ohno, N. in *Microdomains in Polymer Solution*, Dubin, P., ed., Plenum Press: New York; 1985, Ch. 3.
69 See *e.g.* Winnik, F. M. *Chem. Rev.* **1993**, *93*, 587; Li, Y.; Bloor, D. M.; Wyn-Jones, E. *Langmuir* **1996**, *12*, 4476; Kido, J.; Hiyoshi, M.; Endo, C.; Nagai, K. *J. Colloid Interface Sci.* **1991**, *142*, 326.
70 Mc Rae, E. G.; Kasha, M. *J. Chem. Phys.* **1958**, *28*, 721.
71 Kasha, M. *Radiat. Res.* **1963**, *20*, 55.
72 Kasha, M.; Rawls, H. R.; Ashraf El-Bayoumi, M. *Pure Appl. Chem.* **1965**, *11*, 371.
73 Shimomura, M.; Aiba, S.; Tajima, N.; Inoue, N.; Okuyama, K. *Langmuir* **1995**, *11*, 969.
74 Shimomura, M. *Prog. Polym. Sci.* **1993**, *18*, 295.
75 Clint, J. H. *Surfactant Aggregation*, Blackie: Glasgow and London; 1992, Ch. 3.
76 Kajiyama, T.; Oishi, Y.; Uchida, M.; Takashima, Y. *Langmuir* **1993**, *9*, 1978.
77 Oishi, Y.; Takashima, Y.; Suehiro, K.; Kajiyama, T. *Langmuir* **1997**, *13*, 2527.
78 Everaars, M. D. *Ammonium Amphiphiles Carrying Mesogenic Units - Synthesis, Properties, Applications*, Ph. D. Thesis; Wageningen Agricultural University, 1997.

79 Cohen Stuart, M. A.; Wegh, R. A. J.; Kroon, J. M.; Sudhölter, E. J. R. *Langmuir* **1996**, *12*, 2863.
80 Mul, M. N. G. de; Mann Jr., J. A. *Langmuir* **1994**, *10*, 2311.
81 Petty, M. C.; Wood, S. *Int. Laboratory* **1997**, *27*, 8.
82 Popovitz-Biro, R.; Hill, H.; Shavit, E.; Hung, D. J.; Lahav, M.; Leiserowitz, L.; Sagiv, J.; Hsiung, H.; Meredith, G. R.; Vanherzeele, H. *J. Am. Chem. Soc.* **1990**, *112*, 2498.
83 Ashwell, G. J.; Jackson, P. D.; Crossland, W. A. *Nature* **1994**, *368*, 438.
84 Ledoux, I.; Josse, D.; Vidakovic, P.; Zyss, J.; Hann, R. A.; Gordon, P. F.; Bothwell, B. D.; Gupta, S. K.; Allen, S.; Robin, P.; Chastaing, E.; Dubois, J. C. *Europhys. Lett.* **1987**, *3*, 803.
85 Carr, N.; Goodwin, M. J.; McRoberts, A. M.; Gray, G. W.; Marsden, R.; Scrowstoon, R. M. *Makromol. Chem., Rapid Commun.* **1987**, *8*, 487.
86 Ringsdorf, H.; Schlarb, B.; Venzmer, J. *Angew. Chem.* **1988**, *27*, 113.
87 Senoh, T.; Sanui, K.; Ogata, N. *Chem. Lett.* **1990**, 1849.
88 Burland, D. M.; Miller, R. D.; Walsch, C. A. *Chem. Rev.* **1994**, *94*, 31.
89 Picullel, L.; Guillemet, F.; Thuresson, K.; Shubin, V.; Ericsson, O. *Adv. Colloid Interface Sci.* **1996**, *63*, 1.
90 Goddard, E. D. *Colloids Surfaces* **1986**, *19*, 301.
91 Borisov, O. V.; Halperin, A. *Macromolecules* **1996**, *29*, 2612.
92 Turro, N. J.; Lei, X.-G.; Ananthapadmanabhan, K. P.; Aronson, M. *Langmuir* **1995**, *11*, 2525.
93 Henriquez, M.; Lissi, E.; Abuin, E.; Ciferri, A. *Macromolecules* **1994**, *27*, 6834.
94 Hayakawa, K.; Santerre, J. P.; Kwak, J. C. T. *Biophys. Chem.* **1983**, *17*, 175.
95 Shirohama, K.; Takashima, K.; Takisawa, N. *Bull. Chem. Soc. Jpn.* **1987**, *60*, 43.
96 Lasic, D. D.; Strey, H.; Stuart, M. C. A.; Podgornik, R.; Frederik, P. M. *J. Am. Chem. Soc.* **1997**, *119*, 832 and references therein.
97 *Intermediair* **1997**, *33 (19)*, 39.
98 Decher, G.; Kuchinka, E.; Ringsdorf, H.; Venzmer, J.; Bitter-Suermann, D.; Weisgerber, C. *Angew. Makromol. Chem.* **1989**, *166/167*, 71.
99 Hayakawa, K.; Kwak, J. C. T. *J. Phys. Chem.* **1983**, *87*, 506.
100 Thalberg, K.; van Stam, J.; Lindblad, C.; Almgren, M.; Lindman, B. *J. Phys. Chem.* **1991**, *95*, 8975.
101 Malovikova, A.; Hayakawa, K.; Kwak, J. C. T. *J. Phys. Chem.* **1984**, *88*, 1930.
102 Fundin, J.; Hansson, P.; Brown, W.; Lidegran, I. *Macromolecules* **1997**, *30*, 1118.
103 Hansson, P.; Almgren, M. *J. Phys. Chem.* **1995**, *99*, 16684 & 16694.
104 Hansson, P.; Lindman, B. *Current Opinion Colloid Interface Sci.* **1996**, *1*, 604.
105 Anthony, O.; Zana, R. *Langmuir* **1996**, *12*, 3590.
106 Winnik, F. M.; Regismond, S. T. *Colloids Surf. A: Physicochem. Eng. Aspects* **1996**, *118*, 1.
107 Shimizu, T.; Kwak, J. C. T. *Colloids Surf. A: Physicochem. Eng. Aspects* **1994**, *82*, 163.
108 Anthony, O.; Zana, R. *Langmuir* **1996**, *12*, 1967.

Synthesis and Characterisation of Maleic Anhydride Based Copolymers

Chapter 2

Novel alternating copolymers were obtained by radical copolymerisation of maleic anhydride and alkyl vinyl ethers with spacer lengths of 6 to 12 methylene units and terminal (cyanobiphenylyl)oxy moieties. These polymers were hydrolysed to the corresponding poly(maleic acid-co-alkyl vinyl ether)s. By reaction of the maleic anhydride groups with 2-aminoethanesulfonic acid copolymers with both a carboxylic acid and a sulfonic acid moiety were synthesised.

The maleic anhydride and maleic acid copolymers display liquid crystalline behaviour. The transition temperatures are lower for the more rigid poly(maleic anhydride-co-alkyl vinyl ether)s. The enthalpy gain associated with the phase transition increases with decreasing rigidity of the polymeric backbone and with increasing spacer lengths.

For the polymers with a maleic acid and a potassium sulfonate moiety no liquid crystalline phases have been observed.

2.1 Introduction

In the past decade numerous papers have appeared on liquid crystalline polymers. These polymers have better mechanical and thermal stability as compared to the low molar mass liquid crystals. Possible applications in data storage, non-linear optics and conductive materials have increased the efforts to synthesise new liquid crystalline polymers.[1] The main chain liquid crystalline polymers combine rigid units and flexible spacers within the main chain, whereas in side chain liquid crystalline polymers the rigid units are coupled to the polymeric backbone via a flexible spacer. Above a certain length of the flexible spacer the motion of the rigid mesogens and the backbone become decoupled. In this way mesophase formation is largely determined by the mesogen and a large number of different mesogens can relatively easy be introduced into a specific polymer.[2]

Some main chain and side chain LCPs are capable of forming lyotropic mesophases. In these systems the thermodynamic quality of the solvent determines the extent of intra- and intermolecular aggregation between the alike groups within the polymers.

In an effort to obtain both thermotropic and lyotropic liquid crystallinity, copolymers of maleic anhydride and alkyl vinyl ethers carrying a (cyanobiphenylyl)oxy mesogen are synthesised. In a water/THF mixture these copolymers are hydrolysed to the corresponding maleic acid copolymers. By reacting the maleic anhydride copolymers with 2-aminoethanesulfonic acid copolymers with a carboxylic acid and a sulfonic acid moiety are obtained. In this chapter the synthesis and thermal behaviour of these three classes of new copolymers is described.

2.2 Some Theoretical Aspects

2.2.1 General aspects of radical polymerisations

The general reaction scheme for free radical polymerisation can be expressed as drawn in Scheme 2.1. In this scheme I represents an initiator molecule and R· a free radical produced thermally or photochemically in the initial step. Usually the initiator is a peroxide or aliphatic azo compound, such as benzoyl peroxide, cumene hydroxyperoxide and azobisisobutyronitrile (Scheme 2.2).

The radical produced from the initiator attacks a double or triple bond of a monomer to form a radical which can then react with other compounds having a double or triple bond, resulting in chain propagation. Chain termination can occur by chain transfer, disproportionation or recombination of radicals. In chain transfer the polymer chain is terminated by transfer of the radical centre to a monomer, polymer, solvent or even to the initiator. This does not affect the overall rate of polymerisation, but the molecular weight distribution broadens.

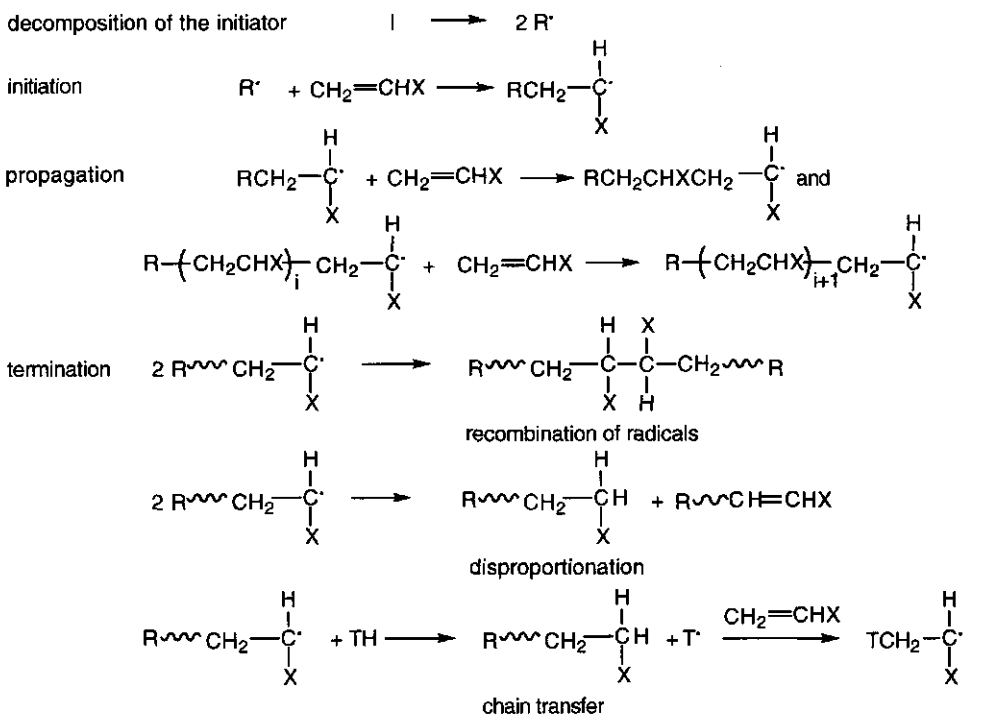

Scheme 2.1 **General reaction scheme for radical polymerisation.**

By disproportionation two radicals combine yielding short chains with saturated and unsaturated chain ends. The preferred chain termination occurs by recombination of radicals belonging to two identically initiated chains, or by use of a chain inhibitor like *e.g.* quinone, O_2 or nitrobenzene.[3-5]

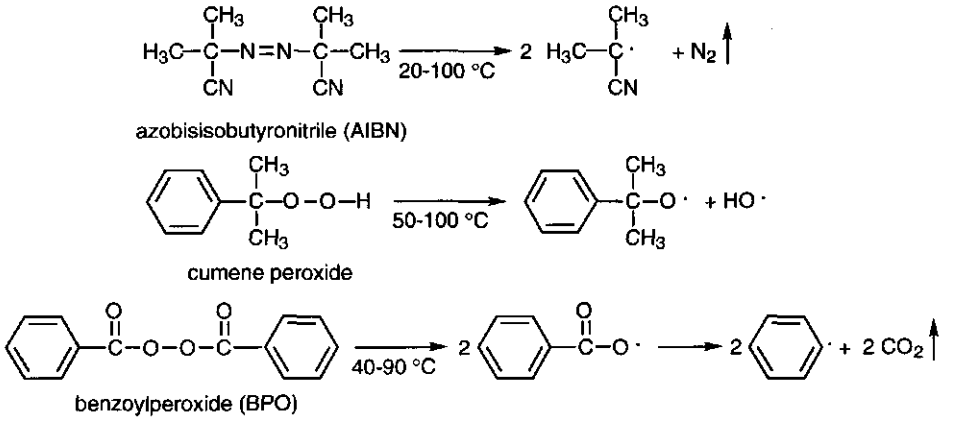

Scheme 2.2 **Common initiators for radical polymerisations.**

2.2.2 Radical copolymerisation

When two monomers copolymerise a competition in the propagation reaction will occur, as visualised in Scheme 2.3. In this Scheme, r_1 and r_2 are the reactivity ratios which control the copolymer composition. They can be determined by analyzing the composition of the copolymer formed from a number of comonomer mixtures with various [A]/[B] ratios at low conversion (5 to 10%).

From Scheme 2.3 it can be seen that there is an increasing tendency to form alternating copolymers when the product $r_1.r_2$ approaches zero. This is found for copolymers of maleic anhydride with acrylonitrile ($r_1.r_2$ = 0.04) or maleic anhydride with methacrylate ($r_1.r_2$ = 0.02).[6,7]

Reactivity ratios of maleic anhydride with various vinyl ethers, like butyl vinyl ether and dodecyl vinyl ether (both with $r_1.r_2$ = 0), confirm the tendency of these monomer pairs to form perfectly alternating copolymers.[8]

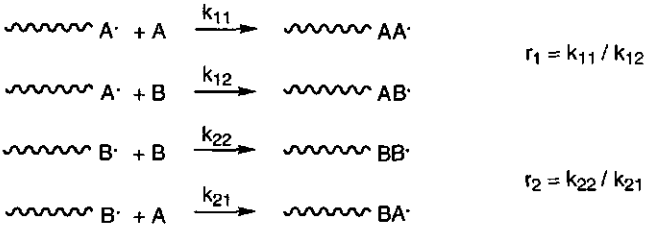

Scheme 2.3 **Competing copolymerisation reactions.**

Monomer reactivities in radical copolymerisations depend on factors like resonance stability, polarity and steric effects. If, in a vinyl monomer (CH_2=CHR), the group R is capable of aiding in the delocalisation of the radical, the radical stability will increase, decreasing its reactivity. Styrene and acrylonitrile, both conjugated monomers, are examples of highly reactive monomers but they will form relatively stable radicals leading to a decrease in reactivity. Nonconjugated monomers like ethylene and vinylacetate are, on the other hand, relatively unreactive towards free radicals, but they will form a highly unstable adduct which is very reactive.

The polarity is, like the resonance stability, largely determined by the substituents. Electron withdrawing substituents like -COOR, -CN, $-COCH_3$, all decrease the electron density of the double bond of a monomer relative to ethylene, whereas electron donating substituents like $-CH_3$, -OR, $-OCOCH_3$, increase the electron density of the double bond. Strongly alternating copolymers are obtained when comonomers which differ widely in polarity are reacted. The polar interactions between two comonomers can be so strong that steric hindrance between the comonomers is overcome and alternating copolymerisation is observed.

2.2.3 Maleic anhydride copolymers

Even though maleic anhydride does not easily homopolymerise it is known to copolymerise readily with a variety of electron rich monomers to yield alternating copolymers.[9-12] It can copolymerise with sterically hindered monomers if strong electron donating substituents are present on these monomers resulting in an electron rich double bond. *Trans*-stilbene is an example of such a sterically hindered compound which has an electron rich double bond and forms an alternating copolymer with maleic anhydride.[13] The strong electron deficient double bond of maleic anhydride makes it a powerful electron acceptor ready to react with a wide variety of donor molecules, like vinyl ethers, olefins and styrenes, to produce perfectly alternating copolymers. The formation of these alternating copolymers of maleic anhydride and various donor molecules has led to the suggestion that electron transfer from a donor radical to an acceptor monomer, or vice versa, in an activated charge transfer complex (CTC) may account for the alternation tendencies.[10,14]

In solution, when a CTC is formed between an electron donor (ED) and an electron acceptor (EA) monomer pair an equilibrium occurs:

$$ED + EA \rightleftharpoons [(ED...EA) + (ED^{+}EA^{-})]$$

In the ground state the complex (ED...EA) is the most abundant complex whereas in the excited state the complex ($ED^{+}EA^{-}$) is present in excess.[14] The constant K for this equilibrium is expressed by

$$K = \frac{[CTC]}{[ED][EA]}$$

where [CTC], [ED] and [EA] are the concentrations of the respective species.

The nature of the charge-transfer complexes of maleic anhydride are considered to be of the π-donor-π-acceptor type and the equilibrium is not only determined by the donor and acceptor strength of the respective monomers but also by resonance stabilization, steric effects, Van der Waals forces and hydrogen bonding. Temperature, additives and donor solvents also influence the equilibrium.

For copolymerisation of maleic anhydride with isobutyl vinyl ether in dichloroethane a K of 1.05 L/mol is reported by Rätzsch.[15] Culbertson reports a K of 0.56 for maleic anhydride-*n*-butyl vinyl ether copolymerisation in tetrachloromethane.[8] A charge transfer complex is likely formed during the copolymerisation of various alkyl vinyl ethers with maleic anhydride, but the exact participation of this CTC in the reaction mechanism is not yet clear.

For the alternating copolymerisation between maleic anhydride and isobutyl vinyl ether Bortel *et al.*[16] proposed the formation of a reactive charge transfer donor-acceptor complex

shown in Scheme 2.4. Maleic anhydride can even be copolymerised with isobutyl vinyl ether without addition of an initiator. The electron donating capacity of isobutyl vinyl ether is apparently high enough to bring about complexation between the two species.

Although there has been much controversy on the CTC formation in alternating copolymerisation, nowadays the most common view holds that the reaction occurs by preliminary formation of a CTC between monomers or a CTC between the propagating radical and the monomer.[15,17] Copolymerisation occurring via successive combinations of monomers with greatly differing polarity without CTC formation is another possible manner to obtain alternating copolymers.[18,19]

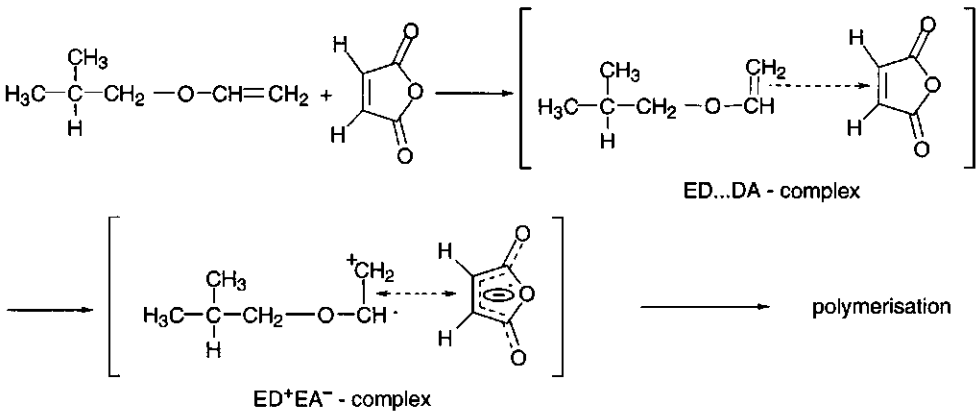

Scheme 2.4 **CTC formation as proposed by Bortel *et al.*[13]**

2.3 Results and Discussion

Both the maleic acid copolymers and the copolymers with a carboxylic acid and a sulfonic acid moiety are prepared from the same parent polymer, the copolymer of maleic anhydride with an alkyl vinyl ether. In this section the complete synthetic pathways and the thermotropic phase behaviour of the polymers are described.

2.3.1 Monomer synthesis

The vinyl ethers have been synthesised as depicted in Scheme 2.5. In the first step the *n*-[(4-cyano-4'-biphenylyl)oxy]alcohol is formed via a S_N2 reaction. In the second step the vinyl ether is prepared by a transetherification reaction. Route A describes the reaction as performed by McKeon *et al.*[20,21] which is catalysed by palladium. The overall reaction is stereospecific and proceeds with *trans-cis* isomerisation. The proposed mechanism is shown in Scheme 2.6.

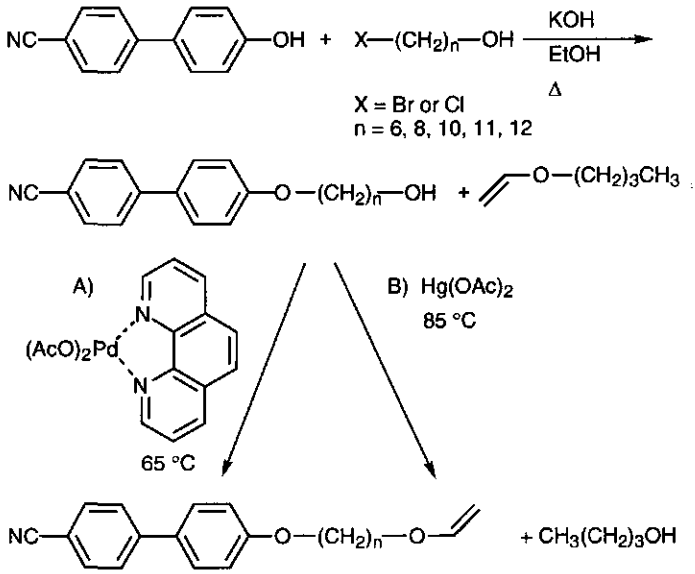

Scheme 2.5 **Preparation of the vinyl monomers.**

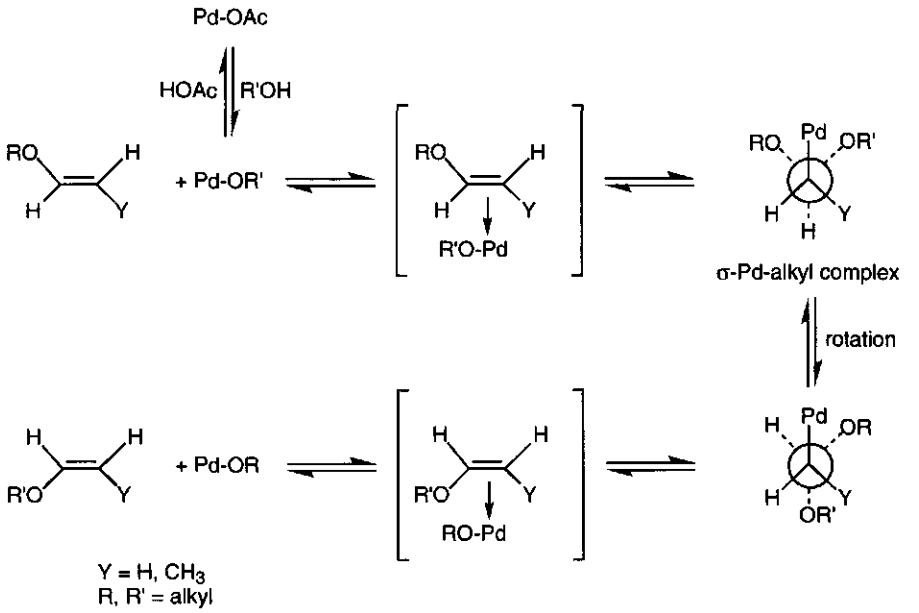

Scheme 2.6 **The reaction mechanism of transetherification using a palladium catalyst.**[21]

The addition of a palladiumalkoxide across the double bond of the vinyl ether results in a σ-Pd-alkyl complex. Rotation about the C-C bond followed by the elimination of a palladiumalkoxide then gives the product. Elimination without rotation would result in the starting material. Since the overall reaction proceeds with *trans-cis* isomerisation, the stereochemistry in the addition step and the elimination step must be the same, probably *syn* addition and *syn* elimination. Also, since the overall reaction is stereospecific, both steps must be concerted.[21,22]

The palladium complex is very sensitive to water so dry reaction conditions are very important for this reaction. The products are obtained in an average yield of 48 % when a 10-fold excess of *n*-butyl vinyl ether is used.

Higher yields are obtained in the transetherification reaction when mercuric salts of weak acids, *e.g.* mercuric acetate, are used.[23] The mechanism is shown in Scheme 2.7. This mechanism is essentially a reversible alkoxymercuration. Important is the formation of an intermediate which is essentially symmetric, so that the reverse reaction can lead to either the starting reactants or to the desired products.[23] In the course of the reaction the mixture is equilibrated, and because of the removal of unreacted *n*-butyl vinyl ether and *n*-butanol under reduced pressure an average yield of 75 % is obtained.[24]

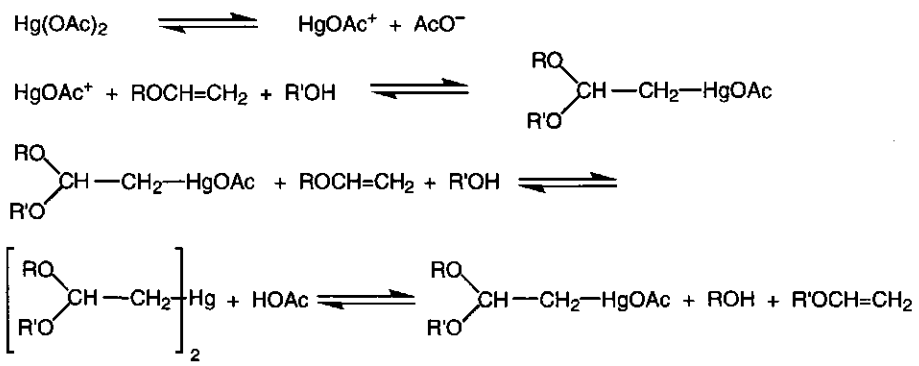

Scheme 2.7 **The proposed reaction mechanism of the transetherification reaction using a mercuric acetate catalyst.[23]**

2.3.2 Copolymerisation

The synthesis of the polymers is outlined in Scheme 2.8. The parent poly(maleic anhydride-*co*-alkyl vinyl ether)s **I-n** are synthesised by radical copolymerisation using azobisisobutyronitrile (AIBN) as the initiator. As solvent benzene was used in which both starting materials are soluble and the insoluble product forms a transparent sticky mass. The radical polymerisation of alkyl vinyl ethers with maleic anhydride is known to give perfectly alternating copolymers as already described in section 2.2.3.

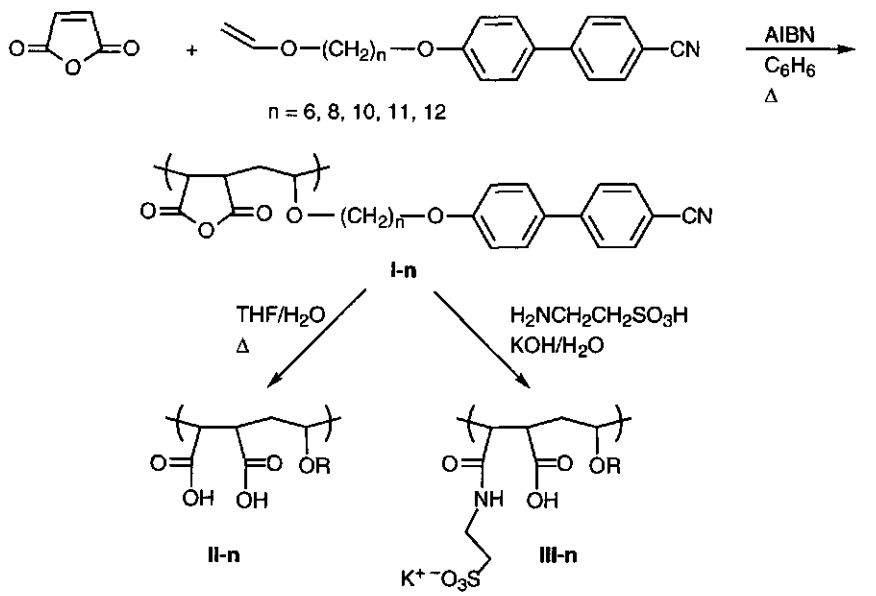

Scheme 2.8 **Synthetic pathway to the polymers I-n, II-n and III-n.**

2.3.3 Poly(maleic acid-*co*-alkyl vinyl ether)s

Zhao *et al.*[25] have reported the partial hydrolysis of polyacrylates bearing (cyanobiphenylyl)oxy units by use of sodium hydroxide. The acrylate ester bond was hydrolysed, yielding a polyelectrolyte with a random distribution of (cyanobiphenylyl)oxy and carboxylic acid groups. Hydrolysis of **I-n** with dilute potassium hydroxide at elevated temperatures resulted in the hydrolysis of the cyano moiety to the amide as was shown in the FTIR spectrum by the disappearance of the CN stretching vibration at 2226 cm^{-1}. Milder hydrolysis of **I-n** in a neutral aqueous THF solution gave the maleic acid copolymer **II-n**.

The FTIR spectra in Figure 2.1 clearly show the formation of the maleic acid moiety without the loss of the CN stretch vibration. The symmetric and antisymmetric bands typical for an anhydride at 1861 and 1780 cm^{-1} completely disappeared and the C=O stretching band characteristic for a carboxyl group at 1733 cm^{-1} appeared, showing the completion of the hydrolysis reaction.[26,27]

2.3.4 Poly(sulfonyl ethyl maleic acid monoamide-*co*-alkyl vinyl ether)s

Polymers carrying both a sulfonic acid and a carboxylic acid moiety were obtained by reaction of the parent polymer **I-n** with an excess of 2-aminoethanesulfonic acid in alkaline water at room temperature. The reaction is depicted in Scheme 2.8. The 2-aminoethanesulfonic acid reacts with one of the carbonyl groups of the anhydride leaving the other unit as a carboxylic acid.

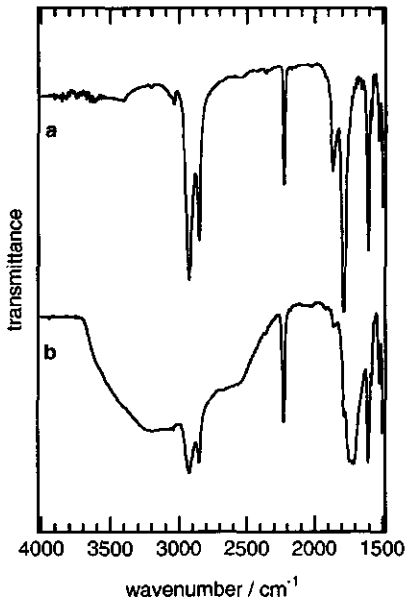

Figure 2.1 **FTIR spectra of polymers I-12 (a) and II-12 (b).**

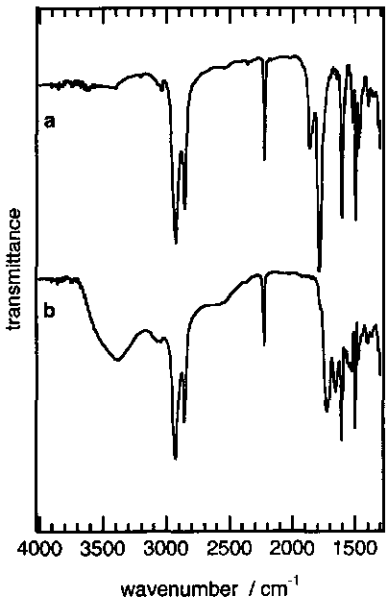

Figure 2.2 **FTIR spectra of polymers I-12 (a) and III-12 (b).**

The polyelectrolytes were purified by dialysis against ultrapure water at neutral pH to remove the excess of 2-aminoethanesulfonic acid and potassium hydroxide.

The FTIR spectra of **I-12** and **III-12** are shown in Figure 2.2. The disappearance of the symmetrical and antisymmetrical stretching bands of the anhydride is clearly observed. The formation of the amide bond is confirmed by the appearance of the carbonyl stretching vibration at 1657 cm^{-1} and the NH bending vibration at 1595 cm^{-1}, typical for a monosubstituted amide moiety. Additional evidence for the presence of sulfonyl ethyl monoamide moieties was obtained from elemental analysis on sulfur.

Under the conditions used the potassium ions form the counterions of the sulfonic acid and carboxylic acid moieties. This can be seen in the FTIR spectra which show the formation of carboxylate ions having symmetrical and antisymmetrical bands at 1601 and 1395 cm^{-1}. Furthermore, flame photolysis on the final products confirmed the presence of potassium ions in all samples. To remove more potassium ions an attempt was made to dialyse the polyelectrolytes **III-n** at pH ~ 4. However, the solubility of polyelectrolytes **III-n** is too low to dialyse the samples at this pH without precipitation.

2.3.5 Thermotropic behaviour

The formation of liquid crystalline phases by the [(cyanobiphenylyl)oxy]alcohols and [(cyanobiphenylyl)oxy]alkyl vinyl ethers has already been studied by others.[28-30] They report

the formation of nematic phases for both series of compounds with spacer lengths between 6 and 12 methylene units. For 11-[(4-cyano-4'-biphenylyl)oxy]undecanol also a smectic A phase is observed.

The thermotropic phase transition temperatures of the polymers were investigated by hot-stage polarisation microscopy and DSC. Figure 2.3 shows the second cooling (a) and third heating cycles (b) for polymers **II-n**.

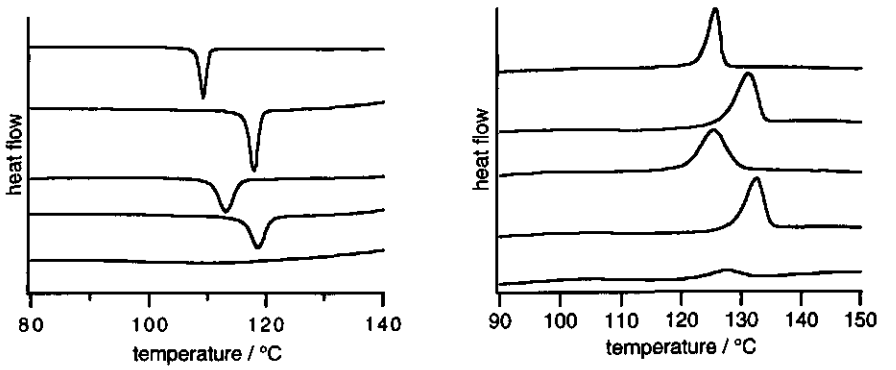

Figure 2.3 **DSC thermograms of compounds II-n: second cooling scans (left) and third heating scans (right). From top to bottom II-12, II-11, II-10, II-8 and II-6.**

Copolymers **I-n** and **II-n** display a reversible liquid crystalline to isotropic phase transition by both DSC and polarisation microscopy, except for compounds **I-6** and **II-6** for which no transition was observed in the cooling trace of the DSC. The textures observed by polarisation microscopy indicate the formation of smectic mesophases for both series of polymers.

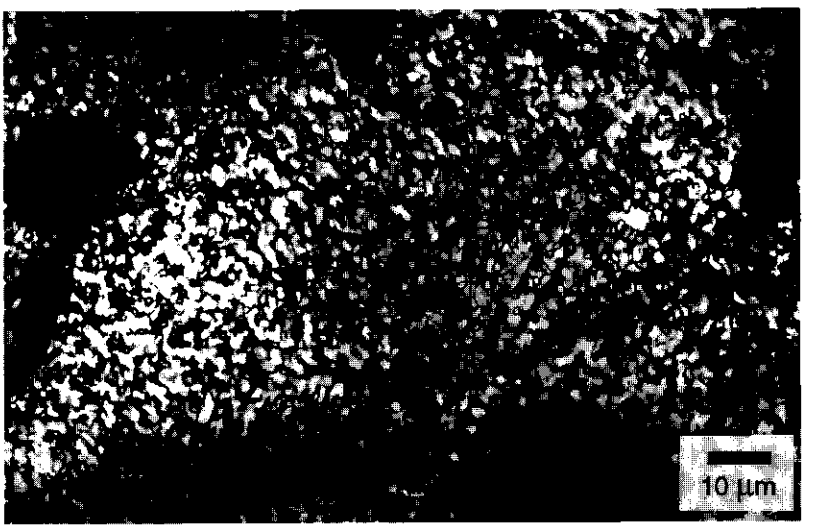

Figure 2.4 **Texture of the smectic A phase of II-11 observed between crossed polarizers.**

Table 2.1 **Liquid crystalline to isotropic phase transition temperatures for polymers I-n (°C) and their corresponding enthalpy changes, ΔH (kJ/mol of repeating unit).**

polymer	polarisation microscopy lc -> i	DSC lc -> i	ΔH
I-6	95	82	0.3
I-8	120	116	0.5
I-10	102	112	2.0
I-11	110	110	2.0
I-12	117	116	3.1

The isotropisation temperatures for compounds **I-n** are lower than for compounds **II-n**. The polymer backbone influences the isotropisation temperatures as a result of incomplete decoupling of the backbone and mesogenic moieties.[31] Isotropisation temperatures generally increase with increasing backbone flexibility.[32,33] Compounds **I-n** have maleic anhydride units in the backbone making the backbone more rigid than in compounds **II-n**. This rigidity hampers the interactions between the mesogens and makes the liquid crystalline state of **I-n** relatively less stable and lowers the isotropisation temperature as compared to **II-n**.
The enthalpy gain upon isotropisation is lower for polymers **I-n** than for **II-n**. Since the more rigid backbone of **I-n** restricts the motions of the mesogens, ordering of these mesogens is less than in the more flexible polymers **II-n**. This results in a lower enthalpy for isotropisation for the more rigid **I-n** polymers.

Table 2.2 **Liquid crystalline to isotropic phase transition temperatures for polymers II-n (°C) and their corresponding enthalpy changes, ΔH (kJ/mol of repeating unit).**

polymer	polarisation microscopy lc -> i	DSC lc -> i	ΔH
II-6	100	105	0.5
		128	0.3
II-8	125	132	1.5
II-10	121	127	2.2
II-11	127	131	2.5
II-12	158	151	4.4

With increasing spacer length the enthalpy gain increases for both series of polymers as is usual for liquid crystalline monomers and polymers.[27,34-39] Compared to the values for homopolymers of alkyl vinyl ethers with (cyanobiphenylyl)oxy units the enthalpy gain is lowered when these monomers are copolymerised with maleic anhydride and hydrolysed to

the maleic acid copolymers.[31-33] Enthalpy changes reported for homopolymers of (cyanobiphenylyl)oxy alkyl vinyl ethers with hexyl, octyl, decyl and undecyl spacers are 0.8, 2.1, 2.9 and 3.3 kJ / mol repeating unit respectively.[30,37,38] This implies a lesser extent of ordering for **I-n** and **II-n** as compared to the homopolymers, which can be attributed to changes in the backbone flexibility and the relative dilution of the mesogenic units of **I-n** and **II-n**.

Polymer molecular weight can influence phase transition temperatures, therefore differences in isotropisation temperature as a result of molecular weight differences can not be completely excluded.[30,32] The molecular weight distribution can also influence the thermal properties of side-chain liquid crystalline polymers.[40] It is reported that both the isotropisation temperature and the glass transition temperature of poly(vinyl ether)s depend on the molecular weights of the polymers.[41] However, a strong molecular weight dependence is usually only seen for degrees of polymerisation of less than 12.[31,39,42] The degrees of polymerisation of **I-n** were found to be at least 250, so no influence of the molecular weights is expected on the thermotropic properties.

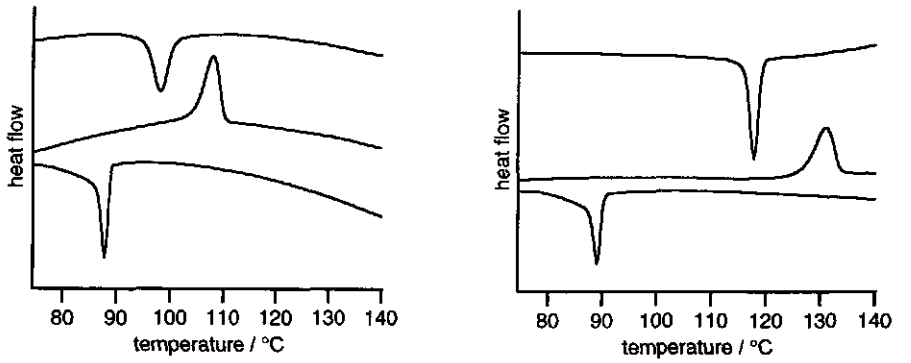

Figure 2.5 **DSC thermograms of compounds I-11 (left) and II-11 (right). From top to bottom, second cooling scan, third heating scan and cooling scan after heating at 210 °C.**

DSC measurements showed a decrease in isotropisation temperature for **II-n** after heating at 210 °C (Figure 2.5). FTIR investigations of the heated samples showed the partial reappearance of the anhydride stretch vibrations. This indicates that at higher temperatures the polyelectrolytes are partially dehydrated. However, the maleic anhydride copolymers **I-n** also showed a decrease in isotropisation temperature after heating at 210 °C. This lowering in the isotropisation temperature might be caused by a partial degradation of the polymers. Another possibility is the formation of anhydride cross-links within the same or between different polymeric backbones.

The copolymers **III-n** which were isolated as fluffy white powders, show no transitions upon heating up to 230 °C, the temperature where the polymers decompose. Polymers **III-n** have

potassium counterions included in the polyelectrolyte structure, as is confirmed by flame-photolysis. Salts usually have high melting temperatures, since strong interactions between positively and negatively charged groups prevent a fast break up of the salt structure.

As the polymers **I-n** and **II-n** were isolated in their glass state, no crystal to liquid crystalline phase transitions were observed. We were not able to detect a T_g between -50 °C and 210 °C for all polymers. One possibility is that the T_g's of polymers **I-n** and **II-n** lie in the same temperature range as the liquid crystalline to isotropic phase transitions. It is known from literature that poly(maleic anhydride-*co*-alkyl vinyl ether)s with octyl and decyl side chains have T_g's of 120 and 104 °C respectively.[25]

It is also known that as the spacer length is increased, the heat capacity change associated with the glass transition becomes smaller.[34] For our polymers the minimum spacer length, with 6 methylene units, might already be too long to observe the change in heat capacity.

The kind of mesophase formed also influences the T_g. The T_g of poly(biphenyl methacrylate)s could only be observed if the polymer exhibited a nematic phase whereas for the smectic polymers the change in specific heat at the glass transition is too low to be detected by DSC.[25] The low change in heat capacity is probably caused by the restricted motions of the polymeric backbone due to the lamellar smectic structure of the mesogenic side chains. This might give an indication for the formation of smectic mesophases by **I-n** and **II-n**, resulting in a low specific heat change upon cooling into the glass state.

The glass transition is also known to be dependent on the polymer molecular weight, usually only showing a strong dependence for degrees of polymerisation of 12 and lower.[25,37] However, no reports were found which mention the effect of the molecular weight on the change in the specific heat capacity. For **III-n** a T_g was not expected because of the powder like appearance of the isolated product even at high temperatures and because of the presence of the potassium counterions.

2.4 Conclusions

Novel side chain liquid crystalline copolymers with a perfect alternating distribution of the mesogenic moieties have been synthesised by a convenient method. The polymers **I-n** and **II-n** show liquid crystalline behaviour, the isotropisation temperature being higher for the more flexible **II-n** polymers. The enthalpy changes associated with the phase transition are higher for **II-n** than for **I-n** and increase with increasing spacer length.

For polymers **III-n** the presence of potassium sulfonate groups prevents the formation of liquid crystalline phases due to the increase in the melting temperatures.

No glass transitions are observed for all polymers. For **I-n** and **II-n** this is probably due to the low change in specific heat capacity at this transition caused by the rigidity of the backbones.

The strong interactions between the mesogens in the liquid crystalline state enhance the rigid structure of the polymers. The potassium ions in polymers **III-n** cause the formation of a more salt-like polymer which does not show a glass transition.

2.5 Experimental

2.5.1 Materials

The *n*-[(4-cyano-4'-biphenylyl)oxy]alcohols were synthesised as described before.[30]

Diacetato-(1,10-phenanthroline)palladium(II)

A solution of 1,10-phenanthroline (10 mmol) in dry benzene (75 mL) was added dropwise with stirring to a solution of palladium(II)acetate (10 mmol) in benzene (60 mL). The precipitate was washed with petroleum ether (bp 40-60 °C). After drying at 100 °C *in vacuo* a pale yellow solid was obtained in 95 % yield (dec. 234 °C).

***n*-[(4-Cyano-4'-biphenylyl)oxy]alkyl vinyl ethers (route A)**

The appropriate *n*-[(4-cyano-4'-biphenylyl)oxy]alcohol (0.01 mol) was added to a mixture of diacetato-(1,10-phenanthroline)palladium(II) (1 mmol), *n*-butyl vinyl ether (15 mL) and dry chloroform (3.85 mL). The mixture was heated at 60 °C for 20 hours. After cooling and filtration to remove the catalyst, the solvent was evaporated under reduced pressure. The product was purified by column chromatography (silica gel, CH_2Cl_2:petroleum ether (bp 40-60 °C) 3:1 v/v). Average yield 48 %.

^{1}H NMR ($CDCl_3$, TMS, δ, ppm): 1.3 (s, 2n-8 H, $(CH_2)_{2n-8}$), 1.6 (qui, 2 H, CH_2), 1.8 (qui, 2 H, CH_2), 3.7 (t, 2 H, CH_2O), 4.0 (t, 2 H, CH_2OPh), 4.1 (dd, 2 H, $CH=CH_2$), 6.6 (dd, 1 H, $CH=CH_2$), 7.0 (d, 2 aromatic H, *o* to alkoxy), 7.5 (d, 2 aromatic H, *m* to alkoxy), 7.7 (2 d, 4 H, *o* and *m* to CN).

***n*-[(4-Cyano-4'-biphenylyl)oxy]alkyl vinyl ethers (route B)**

The appropriate *n*-[(4-cyano-4'-biphenylyl)oxy]alcohol (0.014 mol) was dissolved in *n*-butyl vinyl ether (35 mL). Mercuric(II)acetate (0.9 mmol) was added and the reaction mixture was refluxed for 24 hours. After cooling the *n*-butyl vinyl ether was removed under reduced pressure. The residue was dissolved in dichloromethane and purified by column chromatography on silica gel using CH_2Cl_2:petroluem ether (bp 40-60 °C) 3:1 (v/v) as eluent. Average yield 75 %.

Poly(maleic anhydride-*co*-(n-[(4-cyano-4'-biphenyl)oxy]alkyl vinyl ether)s I-n.

Dry benzene (5-10 mL) was added to an equimolar mixture of the appropriate alkyl vinyl ether and freshly sublimated maleic anhydride. To the resulting mixture 0.1 mol% of azobisisobutyronitrile (AIBN) dissolved in dry benzene was added. The polymerisations were performed in sealed glass flasks under a nitrogen atmosphere at 60 °C for at least 24 hours. After completion, the benzene was evaporated under reduced pressure. The polymers were dissolved in a small amount of THF and precipitated in a large volume of cold methanol. The polymer was filtered, dried *in vacuo* and the procedure was repeated until all monomer was removed. Yields varied between 57 and 85 %.

^{1}H NMR (DMSO-d_6, δ, ppm): 1.2-1.6 (2n-4 H, $(CH_2)_{n-2}$), 3.3 (4H, OCH_2 and CHCO), 3.8 (3H, CH_2OPh and CHO), 6.9 (2 aromatic H, *o* to alkoxy), 7.5 (2 aromatic H, *m* to alkoxy), 7.7 (4H, *o* and *m* to -CN).[43] FTIR (KBr): ν_{CH} 2929, 2856, ν_{CN} 2225, $\nu_{O=COC=O}$ 1861, 1780 cm^{-1}.[44]

GPC measurements of **I-n** show a degree of polymerisation of at least 250.

Table 2.1 **Elemental analyses of polymers I-n.**

	calculated			found			
polymer	**C**	**H**	**N**	**C**	**H**	**N**	**mol H_2O**
I-6	68.63	6.22	3.20	68.67	5.55	3.16	1
I-8	69.93	6.70	3.02	69.89	6.06	2.98	0.9
I-10	70.82	7.13	2.85	70.96	6.58	2.84	0.9
I-11	71.49	7.32	2.78	71.40	6.73	2.80	0.9
I-12	71.37	7.54	2.69	71.24	6.88	2.72	1

Poly(maleic acid-*co*-(n-[(4-cyano-4'-biphenyl)oxy]alkyl vinyl ether)s II-n.

I-n was dissolved in a mixture of freshly distilled THF and water (10/1 v/v), and refluxed until the anhydride was completely hydrolysed (6 to 12 hours). The solvent was evaporated under reduced pressure and the residue was subsequently stirred in CH_2Cl_2. The precipitate was filtered and dried *in vacuo*. For further purification it was sometimes necessary to redissolve the product in THF, evaporate the solvent, followed by stirring in CH_2Cl_2 and filtration.

^{1}H NMR (DMSO-d_6, δ, ppm): 1.2, 1.6 (2n-4 H, $(CH_2)_{n-2}$), 2.8 (2 H, CHCOOH), 3.3 (2H, OCH_2), 3.8 (3H, CH_2OPh and CHO), 6.9 (2 aromatic H, *o* to alkoxy), 7.5 (2 aromatic H, *m* to alkoxy), 7.7 (4H, *o* and *m* to CN), 12.2 (2H, COOH).[43] FTIR (KBr): ν_{OH} 3500-2500, ν_{CH} 2930, 2855, ν_{CN} 2226, $\nu_{C=O}$ 1733 cm^{-1}.

Table 2.2 **Elemental analyses of polymers II-n.**

	calculated			found			mol
polymer	**C**	**H**	**N**	**C**	**H**	**N**	**CH_2Cl_2**
II-6	63.81	5.88	2.92	63.60	6.18	2.85	0.5
II-8	65.88	6.42	2.80	65.55	6.57	2.72	0.4
II-10	66.93	6.84	2.66	66.92	6.85	2.62	0.4
II-11	66.59	6.96	2.55	66.95	6.91	2.49	0.5
II-12	66.35	7.30	2.54	66.33	7.23	2.42	0.5

Poly[(sulfonyl ethyl maleic acid monoamide)-*co*-*n*-[(4-cyano-4'-biphenylyl)oxy]-alkyl vinyl ether]s III-n.

0.5 mmol of the appropriate poly(maleic anhydride-*co*-*n*-[(4-cyano-4'-biphenylyl)oxy]alkyl vinyl ether) was added to an excess of potassium hydroxide (0.01 mol) and 2-aminoethanesulfonic acid (0.01 mol) in 4 mL of water. The mixture was stirred for at least 24 hours. The reaction was stopped when the polymer was completely dissolved. The mixture was dialysed against ultra pure water for 24 hours twice to remove the excess of 2-aminoethanesulfonic acid and potassium hydroxide. The residue was lyophilised to obtain the solid white **III-n** in an average yield of 30 %.

^{1}H NMR (DMSO-d_6/ TFA, δ, ppm): 1.3-1.6 (2n-4 H, $(CH_2)_{n-2}$), 2.7 (4 H, CHCO and CH_2S), 3.4 (4 H, CH_2NH and CH_2O), 3.8 (3 H, CH_2OPh and CHO), 6.9 (2 aromatic H, *o* to alkoxy), 7.5 (2 aromatic H, *m* to alkoxy), 7.6 (4 aromatic H, *o* and *m* to CN).[43] FTIR (KBr): ν_{NH} 3600-3100, ν_{CH} 2929, 2853, ν_{CN} 2228, ν_{CONH} 1657, ν_{NH} 1557, ν_{RCOO^-} 1601, 1395, ν_{CH} 1489 cm^{-1}.

2.5.2 Methods

The elemental analyses on C, H, N were performed on a Carlo Erba elemental analyser 1106. The elemental analyses on S were performed at Mikroanalytisches Labor Pascher in Germany. ^{1}H NMR (200 MHz) spectra were recorded on a Bruker AC200 spectrometer. FTIR spectra were recorded on a BioRad FTS-7 spectrometer. A Perkin-Elmer DSC-7 differential scanning calorimeter was used to determine the thermal transition enthalpies and temperatures, which are reported as the maxima of their endothermic peaks. In all cases, heating and cooling rates were 10 °C/min and the samples were annealed at 80 °C for 15 minutes before scanning, to obtain identical thermal histories for all compounds. Polarisation microscopy was performed using an Olympus BH-2 microscope equipped with a Mettler FP82HT hot-stage and a FP80HT temperature controller.

The molecular weights (M_W) of the polymers **I-n** were determined by gel permeation chromatography (GPC; Waters ^{TM} column: HR 4E + HR 5E, eluent: THF + 5% (v/v) acetic acid) equipped with an Applied Biosystems 759A Absorbance Detector set at 297 nm. The molecular weights were calculated with the use of a polystyrene calibration curve.

2.6 References

1 Jansson, J.-F. in *Liquid Crystal Polymers: From Structures to Applications*, Collyer, A. A., ed., Elsevier Applied Science: London and New York; 1992, Ch. 9.

2 Percec, V.; Pugh, C. in *Side Chain Liquid Crystal Polymers*; McArdle, C. B., ed., Chapmann and Hall: New York; 1989, Ch. 3.

3 Sun, S. F. *Physical Chemistry of Macromolecules: Basic Principles and Issues*, John Wiley & Sons, Inc.: New York; 1994, Ch. 2.

4 Challa, G. *Polymeer Chemie*, Rijksuniversiteit Groningen; 1973, Ch. 6.

5 Odian, G. *Principles of Polymerization*, 3rd ed., John Wiley & Sons, Inc.: New York; 1991, Ch. 3.

6 Cowie, J. M. G. in *Polymers: Chemistry & Physics of Modern Materials*, 2nd ed., Chapmann & Hall: New York; 1991, Ch. 5.

7 Jenner, G.; Kellou, M. *Makromol. Chem. Rapid Commun.* **1980**, *1*, 275.

8 Culbertson, B. M. in *Encyclopedia of Polymer Science and Engineering: Volume 9.* John Wiley & Sons: New York; 1987, p. 225-294.

9 Trivedi, B. C. in *Maleic Anhydride*, Trivedi, B. C.; Culbertson, B. M., ed., Plenum Press: New York; 1982, Ch. 8.

10 Sackmann, G. in *Methoden der Organischen Chemie*, Houben-Weyl, Thieme Verlag: New York; 1987, Ch. 2.

11 Lang, J. L.; Pavelich, W. A.; Clarey, H. D. *J. Polym. Sci., Part A* **1963**, *1*, 1123.

12 Gaylord, N. G. *J. Macromol. Sci., Revs. Macromol. Chem.* **1975**, *C13*, 235.

13 Wagner-Jauregg, T. *Chem. Ber.* **1930**, *B63*, 3213.

14 Trivedi, B. C. in *Maleic Anhydride*, Trivedi, B. C.; Culbertson, B. M., ed., Plenum Press: New York; 1982, Ch. 10.3.

15 Rätzsch, M. *Prog. Polym. Sci.* **1988**, *13*, 277.

16 Bortel, E.; Kochanowski, A.; Witek, E. *J. M. S. - Pure Appl. Chem.* **1995**, *A32*, 73.

17 Kokubo, T.; Iwatsuki, S.; Yamashita, Y. *Macromolecules* **1968**, *1*, 482.

18 Martin, M. M.; Jensen, N. P. *J. Org. Chem.* **1962**, 1201.

19 Butler, G. B.; Olson, K. G.; Tu, C.-L. *Macromolecules* **1984**, *17*, 1884.

20 McKeon, J. E.; Fitton, P.; Griswold, A. A. *Tetrahedron* **1972**, *28*, 227.

21 McKeon, J. E.; Fitton, P. *Tetrahedron* **1972**, *28*, 233.

22 Volger, H. C. *Recl. Trav. Chim. Pays-Bas* **1968**, *87*, 481.

23 Watanabe, W. H.; Conlon, L. E. *J. Am. Chem. Soc.* **1956**, *79*, 2828.

24 Brekke, O. L.; Kirk, L. D. *J. Am. Chem. Soc.* **1960**, *37*, 568.

25 Zhao, Y.; Lei, H. *Macromolecules* **1994**, *27*, 4525.

26 Rim, P. B. *J. Macromol. Sci., Phys.* **1984**, *B24 (4-6)*, 549.

27 Rim, P. B. *Polym. Commun.* **1986**, *27*, 199.

28 Percec, V.; Lee, M. *Macromolecules* **1991**, *24*, 1017.

29 Percec, V.; Lee, M. *Macromolecules* **1991**, *24*, 2780.

30 Percec, V.; Lee, M.; Jonsson, H. *J. Polym. Sci., Part A: Polym. Chem.* **1991**, *29*, 327.

31 Finkelmann, H.; Happ, M.; Portugal, M.; Ringsdorf, H. *Makromol. Chem.* **1978**, *179*, 2541.
32 Imrie, C. T.; Schleeh, T.; Karasz, F. E.; Attard, G. S. *Macromolecules* **1993**, *26*, 539.
33 Imrie, C. T.; Karasz, F. E.; Attard, G. S. *Macromolecules* **1993**, *26*, 3803.
34 Shibaev, V. P.; Kostromin, S. G.; Platé, N. A. *Eur. Polym. J.* **1982**, *18*, 651.
35 Imrie, C. T.; Karasz, F. E.; Attard, G. S. *Macromolecules* **1993**, *26*, 545.
36 Sagane, T.; Lenz, R. W. *Macromolecules* **1989**, *22*, 3763.
37 Percec, V.; Lee, M. *Macromolecules* **1991**, *24*, 1017.
38 Percec, V.; Lee, M. *Macromolecules* **1991**, *24*, 2780.
39 Percec, V.; Tomazos, D.; Pugh, C. *Macromolecules* **1989**, *22*, 3259.
40 Sagane, T.; Lenz, R. W. *Polym. J.* **1988**, *20*, 923.
41 Heroquez, V.; Schappacher, M.; Papon, E.; Deffieux, A. *Polym. Bull.* **1991**, *25*, 307.
42 Stevens, H.; Rehage, G.; Finkelmann, H. *Macromolecules* **1984**, *17*, 851.
43 The two remaining backbone protons from the alkyl vinyl ether could not be seen in the NMR spectra due to the broadness of their resonances and their chemical shift, ~ 1.5 ppm.
44 Polymers **I-n** could also be obtained from **II-n** by drying *in vacuo* at 100 °C over P_2O_5 for about 7 days.

Behaviour of Negatively Charged Maleic Acid Based Polyelectrolytes in Aqueous Solution

Chapter 3

The dissociation behaviour of poly(maleic acid-co-alkyl vinyl ether)s and poly(sulfonyl ethyl maleic acid monoamide-co-alkyl vinyl ether)s with and without chromophoric labels in aqueous solution has been studied using potentiometry, dynamic light scattering (DLS) and UV spectroscopy. The maleic acid polyelectrolytes show two distinct (apparent) pK_a^{app} values of 3.3 and 6.5 respectively. The pK_a^{app} values of the sulfonic acid containing polyelectrolytes could not be determined with enough accuracy. DLS measurements show the formation of large aggregates in which the polymer chains are highly entangled. The formed aggregates are highly ordered as can be deduced from the blue shift of the absorption maxima of the chromophores by UV spectroscopy. Upon increasing the charge density on the polyelectrolyte backbones or decreasing the hydrophobicity of the polyelectrolyte, the aggregates become more open and less ordered. For most polyelectrolytes this is accompanied by an increase in aggregate size.

3.1 Introduction

Although known since the 1950s, amphiphilic polymers or polysoaps have only recently become the object of growing research activity.[1-3] These polymers, bearing hydrophilic and hydrophobic fragments, have attracted much attention due to their resemblance to biological systems and their strong tendency for self-aggregation in aqueous solution. The secondary structure of amphiphilic polymers is much simpler than the secondary structure of proteins or DNA, but the factors controlling it are alike. Hydrophobic interactions, electrostatic repulsion between charged groups and excluded volume effects play an important role in both systems. Furthermore, the addition of surfactants can induce conformational changes in both systems, making amphiphilic polymers model systems for proteins.[4] Polysoaps also resemble surfactants, both in properties and structures of their formed aggregates. In aqueous solution the ionic groups prefer to be solvated by the surrounding water molecules, whereas the hydrophobic side chains shy from water by forming so-called microdomains. Due to this microdomain formation polysoaps exhibit low viscosity in aqueous media and within the microdomains water-insoluble compounds can be solubilised indicating possible applications in the field of *e.g.* detergency and tertiary oil recovery.[1,5]

In this chapter the microdomain formation of poly(maleic acid-*co*-alkyl vinyl ether)s **Cn acid** and **II-n**, and poly(sulfonyl ethyl maleic acid monoamide-*co*-alkyl vinyl ether)s **Cn sulfonate** and **III-n** in water is described. These polymers are well suited to study the opposing effects of hydrophobic and electrostatic interactions in the behaviour of hydrophobically modified polymers. The dissociation constants (pK_a values) and hydrodynamic radii of these polyelectrolytes have been determined. The aggregational state of the polyelectrolytes **II-n** and **III-n** has been studied by UV spectroscopy using the shifts in absorption maxima observed for the (cyanobiphenylyl)oxy chromophores upon aggregation.

3.2 Results and Discussion

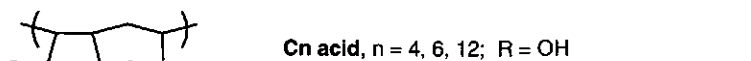

Cn acid, n = 4, 6, 12; R = OH
Cn sulfonate, n = 6, 12; R = $NHCH_2CH_2SO_3^-K^+$

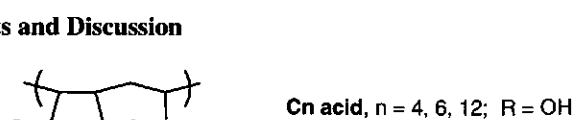

II-n, n = 6, 8, 10, 11, 12; R = OH
III-n, n = 6, 8, 10, 11, 12; R = $NHCH_2CH_2SO_3^-K^+$

Scheme 3.1 **Polyelectrolytes described in this Chapter.**

3.2.1 Potentiometric titration

In general the dissociation behaviour of polyelectrolytes, characterised by the dissociation constant K_a, is analysed from titration experiments. For a diprotic acid the pK_a values can be determined directly from the titration curve by using the equations given in Figure 3.1.[6] In this Figure a typical titration curve for polymers **II-n** is presented. Due to their low solubility in water at pH < 7 the polymers were first dissolved in alkaline water and then titrated with HCl.

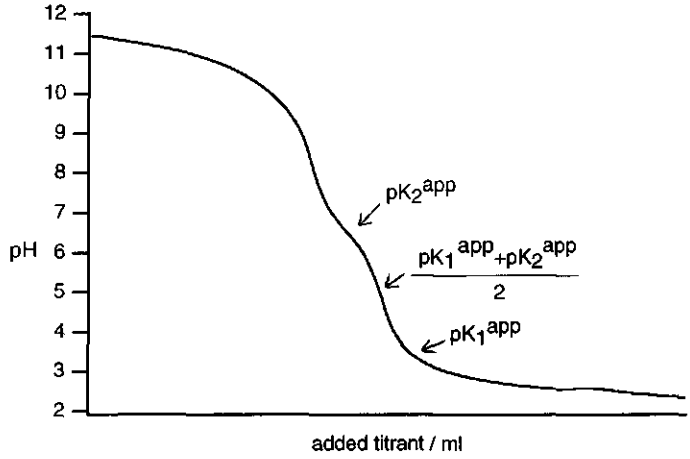

Figure 3.1 **Typical titration curve for polymers II-n.**

The polymers appear to dissociate in two steps in the same way as other alternating copolymers of maleic acid.[7,8] Using the equations in Figure 3.1 the two apparent pK_a values, pK_1^{app} and pK_2^{app}, of polymers **II-n** were determined to be 3.3 ± 0.3 and 6.5 ± 0.1, in accordance with the pK_a values of 3.8 and 6.6 reported for poly(maleic acid-*co*-alkyl vinyl ether)s with ethyl, butyl and hexyl side chains.[8,9] For all spacer lengths the titration curves of solutions of **II-n** in 5 mM KCl are the same, indicating that there is no influence of the chain length on the apparent pK_a values. The fact that two pK_a values are observed suggests that the two carboxylic acid moieties within a monomeric unit mainly have strong nearest neighbour interactions. The deprotonation of the first carboxylic acid within a maleic acid unit takes place while the neighbouring carboxylic acid group stays completely protonated.[10] It is known that the presence of neighbouring dipoles favours the dissociation of carboxylic acid groups.[11] For instance, the pK_a of the carboxyl group in R-CH_2-COOH is 4.87 when R = CH_3 and 1.7 when R = COOH. The formation of a hydrogen bond between the two carboxylic acid moieties also influences the dissociation behaviour. Kawaguchi *et al.*[12] found, by resolving FTIR spectra, that upon increasing the degree of dissociation (α) of poly(isobutylene-*co*-maleic acid) dissociation of the first acid group instantaneously leads to the formation of a

3.4 displays the pK_a^{app} values of **II-n** as a function of α, using the aforementioned equations.[16]

For polyelectrolytes **II-n** no conformational transitions, as observed for copolymers of maleic acid with linear and branched alkyl vinyl ethers consisting of 3 to 10 and 4 to 7 methylene units respectively, are found.[8,14,17,18] For these side chains a conformational transition from the compact to the random coil conformation is seen to occur between $0 < \alpha < 1$ in pK_a vs. α curves. The conformational transition of these polymers is confirmed by viscosity measurements.[8,18] For the 4-methylhexyl side chains the conformational transition is only observed by viscosity measurements at $\alpha > 1$, whereas for the 1-methylheptyl side chains no effect of α on the viscosity is observed at all indicating the absence of a conformational transition.[18] Unfortunately, the pK_a values as a function of α at $\alpha > 1$ were not determined for these polymers. However, below $\alpha < 1$ a similar pK_a *vs.* α plot is observed for polymers **II-n** as for the copolymers of maleic acid with 4-methylhexyl and 1-methylheptyl vinyl ether. This indicates that for polyelectrolytes **II-n** a conformational transition does also not occur below $\alpha = 1$, and similar compact microdomains are formed for all polymers.

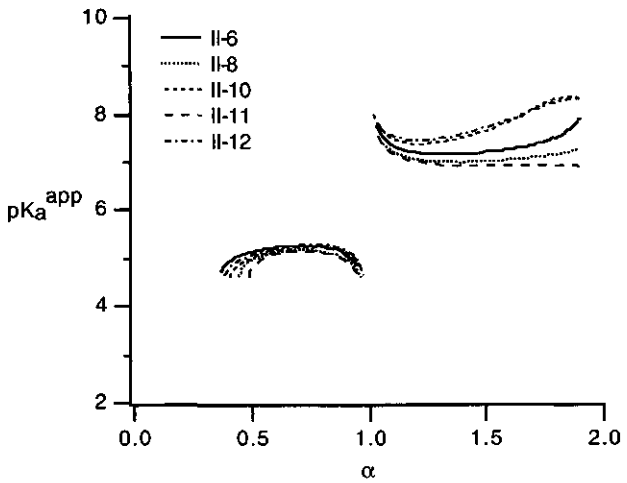

Figure 3.4 **Apparent pK_a values of polymers II-n in 5 mM KCl at 25 °C.**

Because of the low solubility of the polyelectrolytes **II-n** in water at pH values below 7, polyelectrolytes which were expected to have an improved water solubility were synthesised. Within these polyelectrolytes **III-n** one of the carboxylic acid moieties is substituted by a sulfonic acid containing group. Indeed the solubility was improved and polyelectrolytes **III-n** could be solubilised in water down to pH 4.0.

However, the interpretation of the data from the titration experiments of polyelectrolytes **III-n** was not straightforward due to the presence of potassium as counterions of the sulfonic acid

moieties and the strength of this acidic group. Furthermore, the precipitation made the experiments unreliable at low pH.

Due to the similarity in local surrounding of the carboxylic acid group in polyelectrolytes **II-n** and **III-n**, the pK_2^{app} of **III-n** is expected to be similar to the pK_2^{app} of the polyelectrolytes **II-n**, namely 6.5. For the sulfonic acid group the pK_1^{app} will be of the same order as for the 2-aminoethanesulfonic acid from which it is prepared, *i.e.* 1.5. However, because all measurements with polyelectrolytes **III-n** are performed at pH 4 and higher the sulfonic acid units will be taken as deprotonated in all experiments.

3.2.2 UV spectroscopy

pH dependence In an organic solvent like THF the UV spectra of polyelectrolytes **II-n** and **III-n** display a maximum absorption, λ_{max}, at 297 nm, which corresponds to the absorption of monomeric, non-aggregated (cyanobiphenylyl)oxy chromophores. In water the monomerically dispersed (cyanobiphenylyl)oxy chromophores have their absorption maximum at 292 nm.[19] This difference in wavelength of the absorption maximum is due to the solvent effect on the chromophores. Usually a more polar solvent like water results in a lower λ_{max}, whereas a more apolar solvent like THF results in a higher λ_{max}.

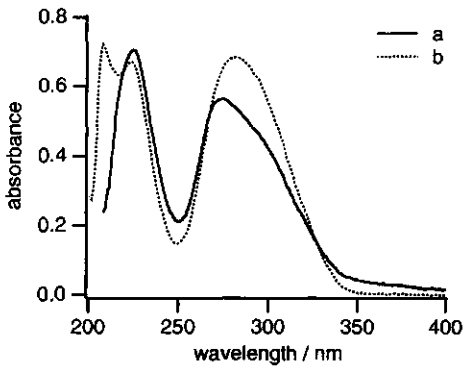

Figure 3.5 **UV absorption spectra of polyelectrolyte II-12 in water at pH 1.9 (a) and 12 (b).**

The absorption maxima of compounds **II-n** are dependent on the pH. From Figure 3.5 it is clear that upon increasing pH the absorption maximum of **II-12** shifts from 270 nm at pH 1.9 to about 282 nm at pH 12.[20] For the shortest spacer, with 6 methylene units, a shift from 278 nm at pH 3.4 to 286 nm at pH 12 is found. In aqueous solution at low pH a blue shift of the absorption maximum is thus observed for these polyelectrolytes. According to the exciton model proposed by McRae and Kasha[21,22], the blue shift of the π–π^* absorption band is indicative of linear chromophore aggregation with their transition dipole moments parallel to each other and ordered perpendicular to the stacking direction (so-called H-aggregates). The wavelength shift depends on the degree of aggregation, which is determined by the mutual orientation and the aggregation number of the chromophores, and the distance between the chromophores. The observation of a blue shift is indicative for the formation of ordered microdomains in water. The microdomains are stabilised by hydrophobic interactions between the side chains and

additionally by π–π stacking interactions between the (cyanobiphenylyl)oxy units (see also section 1.2.2).

Upon increasing the pH the electrostatic interactions on the polymeric backbones start to dominate the hydrophobic and π–π stacking interactions, resulting in the loss of stacking interactions between the (cyanobiphenylyl)oxy chromophores. For polyelectrolyte **II-6** the absorption maximum starts to shift to higher wavelengths at pH 8, indicating the beginning of the transition from rather compact microdomains to a more open conformation at higher pH. With elongation of the spacer connecting the chromophore and the polymeric backbone the transition to a less ordered, more open conformation starts at higher pH values. As can be seen in Figure 3.6, the pH to reach the midpoint of the transition to a more extended conformation increases with increasing spacer length.

This effect of the spacer length on the stabilisation of the microdomains is also seen at neutral pH where the absorption maximum for **II-12** exhibits the largest blue shift as a result of the strongest interaction between the (cyanobiphenylyl)oxy units. This results from the increase in hydrophobicity by increasing the spacer length, thus favouring microdomain formation, and the chromophores on this polyelectrolyte have the largest amount of freedom to attain the most favourable mutual π–π stacking interactions.

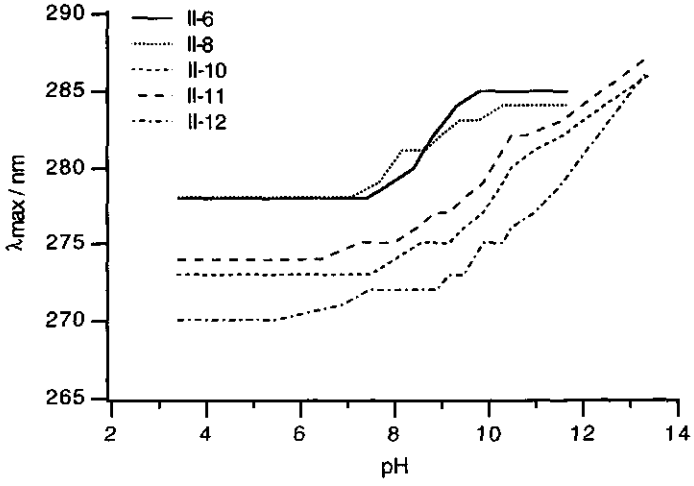

Figure 3.6 **Absorption maxima of II-n as a function of the pH.**

Similar results are obtained for polyelectrolytes **III-n** (Figure 3.7). As the pH increases, a shift in absorption maximum from 275 nm at pH 3.0 to 285 nm at pH > 11 is observed for **III-12**. For the undecyl and decyl spacers a shift of about 5 nm is observed, whereas for the octyl and hexyl spacers the absorption maximum is hardly affected by the increasing pH. The absorption maxima at high pH correspond to the values observed for mainly non-aggregated

(cyanobiphenylyl)oxy chromophores. For **III-12** the absorption maximum starts to shift to higher wavelengths at pH 6, indicating the start of a conformational transition. Upon increasing pH electrostatic repulsion on the polyelectrolyte backbone starts to dominate the hydrophobic and stacking interactions between the side chains resulting in the loss of stacking interactions between the chromophores. For the shortest spacer the more open conformation is also observed at low pH.

At neutral pH the effect of spacer length on the stabilisation of the microdomains is clearly seen from Figure 3.7. Upon decreasing spacer lengths the blue shift at this pH is seen to decrease. The largest blue shift is observed for polyelectrolyte **III-12** as a result of the strongest interactions between the chromophores. The spacer length of this polyelectrolyte favours the formation of more compact aggregates by hydrophobic interactions. Furthermore, the long spacer decouples the chromophores from the backbone giving them the largest amount of freedom to attain the most favourable mutual π–π stacking interactions.

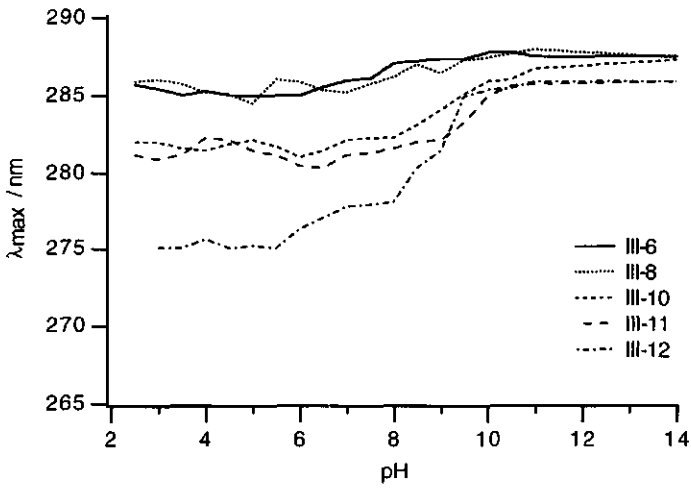

Figure 3.7 **Absorption maxima of III-n as a function of pH.**

Upon comparing Figures 3.6 and 3.7 it is apparent that polyelectrolytes **II-n** show at larger blue shift at the same pH than polyelectrolytes **III-n**, and the pH where the absorption maximum starts to shift is higher for polyelectrolytes **II-n**. The differences between these two series of polyelectrolytes can be ascribed to the presence of the sulfonic acid moieties which render the polyelectrolytes **III-n** slightly more charged than polyelectrolytes **II-n** at equal pH. The hydrophobic interactions within the polyelectrolyte will be less dominating for **III-n** as compared to **II-n**, due to the sulfonic acid moieties which induce more electrostatic repulsion on the backbone.

Temperature dependence Temperature is known to have an important effect on the aggregational state of biopolymers like proteins and DNA. For polyelectrolytes **II-n** and **III-n** the effect of temperature on their aggregation has been studied. As can be seen from Figure 3.8 a shift in absorption maximum of polyelectrolytes **II-12** and **III-12** is observed upon increasing the temperature. Shifts in absorption maxima up to 4 nm are observed for the shorter spacers. The shift in absorption maximum can be explained by loss of Van der Waals interactions between the hydrophobic side chains and loss of $\pi-\pi$ stacking interactions between the chromophores. Both factors result from the increase in water solubility of the polyelectrolytes upon increasing temperature. For polyelectrolytes **II-n** the transitions occur between 50 and 60 °C, for **III-n** between 35 and 42 °C. The spacer length hardly affects these transition temperatures. The lower transition temperatures of **III-n** can be explained by the increased charge density of **III-n** as compared to **II-n** at roughly similar pH values. This results in a lower temperature required to obtain a more open chain conformation for polyelectrolytes **III-n** and improves the solubility of this polyelectrolyte in water. The same reasoning explains the fact that the absorption maxima of **III-n** start to shift to higher wavelengths at a lower pH than **II-n**. When the pH is increased the aggregates become more open and the temperature range where the transitions take place broadens with a small reduction of the mean transition temperature.

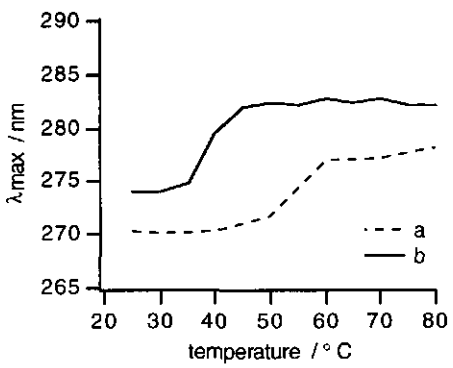

Figure 3.8 **Absorption maxima of II-12 at pH 4.8 (a) and III-12 at pH 4.0 (b) as function of temperature.**

After heating the original UV spectra are restored when the samples are cooled at 25 °C for about 10 minutes. The heating and cooling cycle could be repeated several times yielding identical UV spectra. The expansion of the polymer coils due to temperature increase is thus highly reversible. In literature only a few synthetic polymers have been reported to change their conformation due to both pH and temperature effect, thus mimicking protein behaviour.[23]

3.2.3 Dynamic light scattering

Dynamic light scattering studies (DLS) were performed as a function of pH to study the aqueous polyelectrolyte solutions.[24] The standard autocorrelation method allowed determination of the diffusion coefficients (D_0) for the polyelectrolytes in water. The hydrodynamic radius (R_H) of the polyelectrolyte coils can be determined from D_0 using the Stokes-Einstein equation, assuming the formation of spherical particles.[25] Diffusion

coefficients and hydrodynamic radii for polyelectrolytes **II-n**, **III-n** and the corresponding polyelectrolytes without the chromophores are shown in Table 3.1. The absolute values of the hydrodynamic radii clearly show that we are not dealing with the isolated polyelectrolyte chains but with aggregates consisting of many chains. A highly entangled, spaghetti-like spherical structure of the polyelectrolyte aggregates is proposed. The values of R_H are reproducible with a standard deviation of ±10 %.

Table 3.1 **Diffusion coefficients D_0 ($*10^8$ cm^2 s^{-1}) and hydrodynamic radii R_H (nm) for the polyelectrolytes in water as a function of pH.**

compound	pH	D_0	R_H
C4 acid	7.2	2.1	112
	10.5	2.3	105
C6 acid	7.4	3.8	61
	10.6	2.6	92
C12 acid	7.5	4.4	54
	10.6	3.1	78
C6 sulfonate	4.0	4.5	57
	8.0	3.4	77
	11.1	3.1	84
C12 sulfonate	4.3	7.0	38
	8.1	7.0	38
	11.0	7.7	34
II-6	7.9	8.6	29
	10.4	7.1	35
II-12	7.4	7.7	32
	10.5	4.9	50
III-6	4.3	7.6	34
	7.9	14.8	18
	11.0	9.8	27
III-12	4.3	6.3	41
	8.1	11.7	22
	10.9	19.1	14

For **Cn acids** smaller radii are observed upon increasing the length of the side chains. The longer side chains favour stronger hydrophobic interactions, resulting in smaller radii. An increase in pH causes an increase in charge density on the polyelectrolyte backbone, resulting in increasing electrostatic repulsion between the carboxylic acid groups. Therefore, the tendency of the polyelectrolyte to adopt the random coil conformation can at high pH become

more important than the hydrophobic interactions between the polyelectrolyte side chains, resulting in an increase in aggregate size. As can be seen from Table 3.1, the hydrodynamic radii increase significantly upon increasing pH, except for **C4 acid**. It is known from literature that **C4 acid** has its conformational transition at a degree of dissociation (α) of 0.3, pH $\approx$ 3.1.[26] So it is already in its extended conformation at the lowest pH studied here, and no increase in radius is expected for this compound.

C6 acid also has a conformational transition which starts around $\alpha \approx 0.45$, corresponding to pH $\approx$ 3.5.[26] For **C4 acid** the transition is known to be cooperative, *i.e.* the conformation abruptly changes from the compact to the random coil, whereas for **C6 acid** the transition is less cooperative and proceeds gradually upon increasing pH.[27,28] Probably the conformational transition of **C6 acid** is not complete at pH 7.4 and the increase in R_H can thus be explained by the conformational change of this polymer. According to literature **C12 acid** remains in its compact coil structure upon increasing pH.[29-32] The increase in size observed by DLS is probably due to swelling of the spaghetti-like structure because of the increase in charge density on the polyelectrolyte backbone.

For **C6 sulfonate** the hydrodynamic radius also increases upon increasing pH which can be ascribed to the tendency of the polyelectrolyte to expand upon increasing the charge density on the backbone. Furthermore, this polyelectrolyte is expected to have a conformational transition between pH 4 and 11, just like **C6 acid**. **C12 sulfonate** is a more hydrophobic polyelectrolyte and therefore expected to remain in a compact coil conformation at all pH values studied. An increase in size was expected upon increasing the pH, due to the increase in charge density on the polyelectrolyte backbone which would swell the aggregates. However, the size does not change significantly upon increasing the pH.

The aggregates of **Cn sulfonate** are smaller than the ones formed by **Cn acid**. This can be explained by the improved water solubility of **Cn sulfonate** as compared to **Cn acid**. When preparing the polyelectrolyte solutions the untangling of the polyelectrolyte chains of **Cn sulfonate** may be easier than for **Cn acid** resulting in a smaller aggregate size.

The introduction of chromophores on the polyelectrolyte side chains results in a decrease in aggregate radius. In all chromophore labelled polyelectrolytes the hydrophobic character has increased as compared to the non-labelled polyelectrolytes and, in addition, favourable π–π stacking interactions between the chromophores exist (see paragraph 3.2). For the chromophore labelled polyelectrolytes the π–π stacking interactions also have to be disrupted to be able to adopt the random coil conformation. The radius increase observed for **II-6** and **II-12** upon increasing pH is in agreement with the loss of chromophore stacking as is shown by UV experiments.[33] However, an increase in spacer length does not always lead to smaller particle radii for the labelled polymers, as was expected due to increased hydrophobic interactions. The increase in spacer length gives the chromophores more freedom to have

favourable intra- and intermolecular π–π stacking interactions with each other. Possibly these intermolecular interactions are favoured upon increasing spacer length leading to larger aggregates for **II-12** as compared to **II-6**.

For the polyelectrolytes with sulfonic acid moieties the introduction of chromophores also results in a decrease of the aggregate size. However, upon increasing pH or decreasing spacer length, polyelectrolytes **III-n** do not show the increase in aggregate size as is observed for the other polyelectrolytes. For **III-12** the decrease in R_H upon increasing pH might be explained by the breakdown of the aggregates due to increased electrostatic repulsion. Upon going from pH 4.3 to pH 7.9 the aggregates of **III-6** also decrease in size, possibly due to similar electrostatic repulsion within the aggregates. The size increase at higher pH agrees with the observations made for the other polyelectrolytes.

3.3 Conclusions

The behaviour of polyelectrolytes **II-n** and **III-n** in aqueous solution as a function of the degree of dissociation has been studied by titration, DLS and UV experiments using an intrinsic probe. Polyelectrolytes **II-n**, with maleic acid units along the backbone, show a limited solubility in water. These polyelectrolytes are only soluble above pH 7.0. When one of the carboxylic acid groups within a repeating unit is replaced by a sulfonic acid containing moiety the polyelectrolytes become water soluble down to pH 4.0.

The pK_a^{app} values of polyelectrolytes **II-n**, pK_1^{app} = 3.3 and pK_2^{app} = 6.5, agree well with values reported in literature for analogous polyelectrolytes. Due to the strength of the sulfonic acid moieties, the presence of potassium counterions and precipitation of polyelectrolytes **III-n** at pH < 4.0, it was not possible to determine the pK_a^{app} values of these polyelectrolytes with sufficient accuracy.

The observed blue shift of the UV absorption maximum of **II-n** below pH 8 and **III-n** below pH 6 reveals the presence of ordered microdomains, in which the (cyanobiphenylyl)oxy chromophores form H-aggregates. At pH values above 8 and 6 for **II-n** and **III-n** respectively, the polyelectrolytes show a transition from the compact globular conformation to a more open chain conformation due to the increase in electrostatic repulsion on the polyelectrolyte backbone. An increase in spacer length results in a larger blue shift and the pH value at which the transition starts increases. Polyelectrolytes **II-12** and **III-12** are the most hydrophobic polyelectrolytes within their series. The strongest π–π stacking interactions between the (cyanobiphenylyl)oxy units is observed for these polyelectrolytes because of their hydrophobicity and the fact that they have the most flexible spacer.

UV measurements reveal a temperature induced conformational transition for both series of polyelectrolytes. For polyelectrolytes **III-n** the transition temperature is lower than for **II-n**.

Both the lower pH and the lower temperature necessary to induce a conformational transition of **III-n** as compared to **II-n** can be explained by the higher charge density of **III-n** at comparable pH due to the presence of sulfonic acid moieties, which renders polyelectrolytes **III-n** more water soluble.

Dynamic light scattering data show that polyelectrolytes **Cn acid**, **Cn sulfonate**, **II-n** and **III-n** all form large aggregates in which the polyelectrolyte chains are highly entangled. Upon increasing the polyelectrolyte charge density, the aggregates generally swell due to increased electrostatic repulsion on the polymeric backbones. An increase in spacer length increases the hydrophobic interactions between the side chains and results in a decrease in aggregate size. The attachment of chromophores to the polyelectrolyte side chains results in smaller radii due to increase in polyelectrolyte hydrophobicity and favourable π–π stacking interactions between the chromophores.

3.4 Experimental

3.4.1 Materials

The synthesis of polymers **II-n** and **III-n** have been described in Chapter 2. The poly(maleic acid-*co*-*n*-alkyl vinyl ether)s **Cn acid** were synthesised following a literature procedure.[8] Polymers **Cn sulfonate** were synthesised according to the procedure followed for polymers **III-n** as described in Chapter 2.

Cn acid: ^{1}H NMR (DMSO-d_6, δ, ppm): 0.8 (3H, CH_3), 1.1-1.5 (2n-4H, $(CH_2)_{n-2}$), 1.5-2.1 (2H, CH_2 backbone), 2.4-3.0 (2H, CHCOOH), 3.0-4.0 (3H, $CHOCH_2$), 12.2 (2H, COOH). FTIR (KBr): ν_{OH} 3500-2500, ν_{CH} 2922, 2862, $\nu_{C=O}$ 1726 cm^{-1}. **C4 acid**: Anal. Calcd for $C_{10}H_{16}O_5$ (1 H_2O, M_w/ru 234.24): C 51.27, H 7.75. Found: C 51.72, H 7.31. **C6 acid**: Anal. Calcd for $C_{12}H_{20}O_5$ (1 H_2O, M_w/ru 264.10): C 54.57, H 8.47. Found: C 54.50, H 7.96. **C12 acid**: Anal. Calcd for $C_{18}H_{32}O_5$ (1 H_2O, M_w/ru 346.45): C 62.41, H 9.89. Found: C 62.44, H 9.42.

Cn sulfonate: ^{1}H NMR (DMSO-d_6/ TFA δ, ppm): 0.8 (3H, CH_3), 1.2 (2n-4H, $(CH_2)_{n-2}$), 2.7 (4H, CHCO and CH_2S), 3.4 (5H, CH_2NH, CH_2O and CHO). FTIR (KBr): ν_{NH} 3600-3100, ν_{CH} 2926, 2873, ν_{CONH} 1654, ν_{RCOO^-} 1580, 1395, ν_{CH2} 1470 cm^{-1}. **C6 sulfonate**: Anal. Calcd for $C_{14}H_{23}O_7NSK$ (0.8 KCl, 2.5 H_2O, 0.1 taurine, M_w/ru 505.69): C 33.72, H 5.72, N 3.04, S 6.97, K 13.92. Found: C 33.72, H 5.48, N 3.21, S 6.70, K 14.30. **C12 sulfonate**: Anal. Calcd for $C_{20}H_{35}O_7NSK_2$ (1 KOH, M_w/ru 567.86): C 42.30, H 6.39, N 2.47, S 5.65, K 20.66. Found: C 42.55, H 6.90, N 2.11, S 5.32, K 21.33.

3.5.2 Methods

For the titration experiments, solutions of **II-n** were prepared by addition of a solution of the appropriate amount of dry polymer in 2 mL of THF to a 5 mM KCl solution in ultra pure water at pH 12 (KOH). Subsequently, the THF was removed by stirring under a nitrogen flow. The solutions of **Cn sulfonate** and **III-n** were prepared by dissolving the appropriate amount of dry polymer in a 5 mM KCl solution in ultra pure water at pH 12. The final polymer concentration, C_p, was $1*10^{-3}$ mol of acidic groups per liter. Titrations of the polymer samples were performed with a 0.1 M HCl solution in a thermostatted vessel at 24.5 ± 0.5 °C. Potentiometric titrations were carried out with the computer controlled titration system, Autolab® (ECO Chemie), with a pH combination electrode of type S507A (Beckman). A dynamic titration method was used in which the titration parameters were adjusted during the measurement to obtain a large number of data points around the equivalence points. The pK_a

values were determined from the titration curves consisting of about 600 data points according to known literature procedure.[6]

Dynamic light scattering (DLS) measurements were performed at a scattering angle of 90° using a Lexel Model 85 argon laser as light source (λ = 514 nm). The DLS data were interpreted by cumulants analysis[24,34], using the Statscat program from ALV5000. In the data analysis the formation of spherical aggregates was assumed. The mean hydrodynamic radius, R_H, was calculated from the second cumulant using the Stokes-Einstein relation.

The polyelectrolyte solutions of **Cn acid** and **II-n** for DLS measurements were prepared by addition of a solution of 5.0 mg of dry polymer in 2 mL of THF to water at pH 12 (final volume of 10 mL). Subsequently, the THF was removed by stirring under a nitrogen flow. The solutions of **Cn sulfonate** and **III-n** were prepared by dissolving 5.0 mg of dry polymer in 10 mL of water at pH 12. The freshly prepared solutions were filtered through 0.45 µm RC55 filters (Schleicher & Schuell) to remove dust particles prior to measuring.[35] The stability of the formed aggregates was studied by measuring the same samples again after 14 days. Partial precipitation of the polyelectrolytes was observed, even at high pH, and the microdomain radii were reduced by about 10 %.

The pH dependent UV spectra of polymers **II-n** were recorded on a Beckman DU-7 spectrophotometer. The pH dependent UV spectra of polymers **III-n** and all temperature dependent spectra were recorded on a Perkin-Elmer Lambda 18 UV-VIS spectrophotometer. The polymer concentrations were $5*10^{-5}$ M in monomeric units ($\varepsilon \approx$ 13000 L mol^{-1} cm^{-1}). For the pH dependent measurements, performed at 25 ± 0.1 °C, the polyelectrolytes were dissolved at pH 7, and spectra were recorded after addition of aliquots of diluted HCl or NaOH. The temperature dependent spectra were recorded 5 minutes after the thermostat had reached the appropriate temperature.

3.5 References

1 Laschewsky, A. *Advances in Polymer Science: Polysoaps/ Stabilizers/ Nitrogen-15 NMR*, Springer-Verlag: Berlin; **1995**, *124*, 3.

2 Anton, P.; Köberle, P.; Laschewsky, A. *Makromol. Chem.* **1993**, *194*, 1.

3 Dubin, P. L. *Microdomains in Polymer Solution*, Plenum Press: New York; 1985, v.

4 Borisov, O. V.; Halperin, A. *Langmuir* **1995**, *11*, 2911.

5 Goddard, E. D. *J. Am. Oil Chem. Soc.* **1994**, *71*, 1.

6 Chang, R. *Physical Chemistry with Applications to Biological Systems*, 2nd ed., Macmillan Publishing Co., Inc.: New York, 1981; p. 337.

7 See *e.g.* Ohno, N. *Polymer J.* **1981**, *13*, 719; Kitano, T.; Kawaguchi, S.; Anazawa, N.; Minakata, A. *Macromolecules* **1987**, *20*, 2498.

8 Dubin, P. L.; Strauss, U. P. *J. Phys. Chem.* **1970**, *74*, 2842.

9 Dubin, P. L.; Strauss, U. P. *J. Phys. Chem.* **1973**, *77*, 1427.

10 Dygert, S. L.; Muzii, G.; Saroff, H. A. *J. Phys. Chem.* **1970**, *74*, 2016.

11 Bianchi, E.; Ciferri, A.; Parodi, R.; Rampone, R.; Tealdi, A. *J. Phys. Chem.* **1970**, *74*, 1050.

12 Kawaguchi, S.; Kitano, T.; Ito, K. *Macromolecules* **1991**, *24*, 6030.

13 Reinhardt, S.; Steinert, V.; Werner, K. *Eur. Polym. J.* **1996**, *32*, 935.

14 Strauss, U. P.; Schlesinger, M. S. *J. Phys. Chem.* **1978**, *82*, 571.

15 Nagasawa, M.; Holtzer, A. *J. Am. Chem. Soc.* **1964**, *86*, 538.

16 Around α = 1 the pK_a^{app} values change rapidly due to the logarithmic terms in the equations for pK_1^{app} and pK_2^{app}.

17 Dubin, P. L.; Strauss, U. P. *J. Phys. Chem.* **1967**, *71*, 2757.

18 Villiers, C.; Braud, C. *Nouveau J. Chim.* **1978**, *2*, 33.

19 Everaars, M. D.; Marcelis, A. T. M.; Sudhölter, E. J. R. *Langmuir* **1993**, *9*, 1986.

20 In the UV concentration range, no microcrystals were formed at low pH, indicating that at these concentrations the solubility limit has not been reached.

21 Mc Rae, E. G.; Kasha, M. *J. Chem. Phys.* **1958**, *28*, 721.

22 Kasha, M. *Radiat. Res.* **1963**, *20*, 55.

23 Chen, G.; Hoffman, A. S. *Nature* **1995**, *373*, 49.

24 Candau, S. J. in *Surfactant Solutions: New Methods of Investigation*, Zana, R., ed., Marcel Dekker, Inc.; New York: 1987, Ch. 3.

25 The assumption of the formation of spherical particles is affirmed by small angle neutron scattering (SANS) experiments of poly(1-alkene-*co*-maleic acid)s. These experiments show that copolymers derived from 1-octadecene form cylindrical micelles whereas copolymers derived from the lower 1-alkenes form ellipsoid-shaped micelles. Shih, L.-B.; Mauer, D. H.; Verbrugge, C. J.; Wu, C. F.; Chang, S. L.; Chen, S. H. *Macromolecules* **1988**, *21*, 3235.

26 Calculated from Shimizu, T.; Kwak, J. C. T. *Colloids Surf. A.* **1994**, *82*, 163 and Benrraou, M.; Zana, R.; Varoqui, R.; Pefferkorn, E. *J. Phys. Chem.* **1992**, *96*, 1468, using $pK_I = pH + \log[(1-\alpha)/\alpha]$ and $pK_I = 3.5$.

27 Strauss, U. P.; Barbieri, B. W.; Wong, G. *J. Phys. Chem.* **1979**, *83*, 2840.

28 Barbieri, B. W.; Strauss, U. P. *Macromolecules* **1985**, *18*, 411.

29 Benrraou, M.; Zana, R.; Varoqui, R.; Pefferkorn, E. *J. Phys. Chem.* **1992**, *96*, 1468.

30 Anthony, O.; Zana, R. *Langmuir*, **1996**, *12*, 1967.

31 Binana-Limbele, W.; Zana, R. *Macromolecules* **1990**, *23*, 2731.

32 Anthony, O.; Zana, R. *Macromolecules* **1994**, *27*, 3885.

33 Nieuwkerk, A. C.; Marcelis, A. T. M.; Sudhölter, E. J. R. *Macromolecules* **1995**, *28*, 4986.

34 For more information on the cumulants analysis see *e.g.* Koppel, D. E. *J. Chem. Phys.* **1972**, *57*, 4818.

35 Although the results of different samples of the same compound showed no differences in observed trends, the particle radii varied to some extent (± 10%) with the way the samples were prepared.

Interactions between Hydrophobically Modified Polyelectrolytes and Ammonium Surfactants

Chapter 4

The binding of n-dodecyltrimethylammonium bromide (DTAB) to poly(maleic acid-co-alkyl vinyl ether)s and poly(sulfonyl ethyl maleic monoamide-co-alkyl vinyl ether)s with n-butyl, n-hexyl, n-dodecyl, n-[(4-cyano-4'-biphenylyl)oxy]hexyl and n-[(4-cyano-4'-biphenylyl)oxy]-dodecyl side chains has been investigated by potentiometry using a surfactant selective electrode and surface tension measurements. The binding between DTAB and the polyelectrolytes starts at very low DTAB concentrations and is noncooperative. This is caused by the formation of microdomains by the polyelectrolytes. Although the polyelectrolytes are only weakly surface active when solubilised in water at pH 10, highly surface active complexes are formed in the presence of small amounts of DTAB. The complexes are more hydrophobic than the individual components, resulting in accumulation of the complexes at the air-solution interface.

UV spectroscopy was used to investigate the interactions between the polyelectrolytes and DTAB, n-hexadecyl- and N-(10-(4'-cyanoazobenz-4-oxy)decyl)-N,N,N-trimethylammonium bromide. The shift in the absorption maxima of the chromophores, due to mutual $\pi-\pi$ stacking interactions, was used to obtain information on changes of both polyelectrolytes and surfactants upon addition of surfactants to the polyelectrolytes in aqueous solution. For poly(maleic acid-co-n-butyl vinyl ether) cooperative interaction was found, whereas for the other polyelectrolytes the interaction with surfactants was noncooperative.

4.1 Introduction

Complex water-based fluids containing polymers and surfactants find important practical applications in various areas such as detergency, paints and coatings, cosmetics, adhesives and glues, food and pharmaceutical products and tertiary oil recovery. They also play a key role in many biological systems.[1] For example, they control the functionality and the stability of cell membranes. The interactions between model synthetic or natural polymers and surfactants were studied extensively over the past 30 years.[2-7] It has been generally recognised that detailed knowledge of the interaction between a particular polymer and a surfactant is very important to the application of such a polymer/surfactant system.

Recently, solid polymer-surfactant complexes have also gained a lot of interest due to their application as building blocks for self-organising materials, like switchable biological membranes, non-linear optically-active (NLO) films or conductive polymers and blends.[8-10] These solid complexes are generally prepared from aqueous solution containing polyelectrolytes and surfactants by ion exchange, neutralisation, chemical change, redox reactions or quaternisation. Polymer-surfactant complexes have thus proven to be of enduring interest because of the self-organisation of macromolecules and low molecular weight amphiphiles into higher ordered structures.

A variety of experimental techniques have been utilised to study the nature of polymer-surfactant interactions, including viscosity, surface tension and conductivity measurements, dialysis, fluorescence spectroscopy, NMR, and neutron and light scattering techniques.[3] These studies give information about the influence of hydrophobic and electrostatic effects on polymer-surfactant interactions and on surfactant aggregation mediated by the polymer.

For many polyanion-cationic surfactant systems, it has been found that the interaction strength increases with surfactant chain length and polyanion hydrophobicity and that binding is a cooperative process.[11-13] This cooperativity indicates that the surfactants bind to the polyelectrolytes in the form of micelle-like aggregates.[14] However, for hydrophobically modified polyelectrolytes the interaction increases in strength upon increasing polyelectrolyte or surfactant hydrophobicity, whereas the cooperativity of interaction decreases.[15,16] These polyelectrolytes can form micelle-like aggregates, so-called microdomains, to which individual surfactant molecules bind. The change in cooperativity has been explained in terms of the free energy differences between binding of an oncoming surfactant next to an already bound surfactant molecule and binding to a site where it interacts with the polymers side chains. At low polyelectrolyte hydrophobicity binding next to an already bound surfactant molecule has a more negative free energy than separate binding, whereas at high polyelectrolyte hydrophobicity the binding to polyelectrolyte microdomains has a more favourable free energy.[17,18]

This chapter describes the interactions of poly(maleic acid-*co*-alkyl vinyl ether)s **Cn acid** and **II-n**, and poly(sulfonyl ethyl maleic acid monoamide-*co*-alkyl vinyl ether)s **Cn sulfonate** and **III-n** with dodecyltrimethylammonium bromide (DTAB) as studied by use of a surfactant selective electrode and surface tension measurements. The objective was to gain more insight into the effects of varying charge density and/or hydrophobicity on the interactions between hydrophobically modified polyelectrolytes and surfactants. The interactions are also studied by use of surfactants and poly(maleic acid-*co*-alkyl vinyl ether)s or poly(sulfonyl ethyl maleic acid monoamide-*co*-alkyl vinyl ether)s in which chromophores are present in the polyelectrolyte or in the surfactant or in both components. UV spectroscopy is used to monitor the interactions in aqueous solution at various pH values.

4.2 Results and Discussion

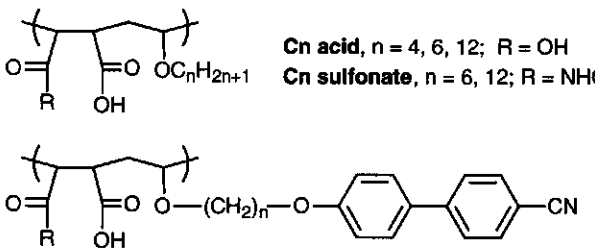

Scheme 4.1 **Polyelectrolytes used in this Chapter.**

4.2.1 Potentiometry

Direct binding studies of surfactants to a variety of polyelectrolytes have been carried out by a large number of research groups. The interaction between polymers and surfactants are usually presented in the form of binding isotherms which give a quantitative measure of the extent of interaction. The technique most often used in these studies is potentiometry using a surfactant selective electrode. The concentration of free, non bonded surfactant is measured by this electrode. The advantage of surfactant selective electrodes in binding studies include excellent sensitivity and reproducibility, small required sample volume, ease of measurement, and electrode tolerance to excess electrolyte.[19,20] A disadvantage is the proportionality of the potential difference E with the logarithm of the concentration which makes it difficult to determine the concentration with the same accuracy in the entire concentration range.

The observed potentiometric curves for the solution mixtures under study deviate from the calibration curve because of surfactant adsorption to the polyelectrolyte. From Figure 4.1 it can be seen that binding of DTAB starts already at very low concentrations. At any C_S,

corresponding to an emf value E, the concentration of free surfactant, C_s^f, is obtained from the calibration curve, at the same E value. Using these values the binding isotherm can be constructed using

$$\beta = C_s^b / C_p = \left(C_s - C_s^f\right) / C_p$$

In this equation, C_s^b is the concentration of surfactant bound to the polymer, C_s is the total surfactant concentration, C_s^f is the free surfactant concentration, and C_p is the concentration of polymeric binding sites.[21-23] This means that for all polyelectrolytes under present study C_p equals twice the concentration of polyelectrolyte repeating units, because one unit contains two possible binding sites. With this definition, $\beta = 1$ corresponds to one bound surfactant per carboxylic acid group in case of polymers **II-n**. It should be noted that at high C_s, the error in β can be large because the calibration plot and the E *vs.* log C_s plot in the presence of polymer are fairly close. A small systematic shift in the calibration plot, by for example 1 mV, can give rise to a systematic trend, *i.e.* an increase or decrease of β upon increasing C_s, at high C_s. For all polyelectrolyte-DTAB systems studied precipitation of the formed complexes started at a DTAB concentration of about 0.5 mM, a ratio of one DTAB molecule per repeating unit. This precipitation at high C_s might interfere with the electrode response. For these reasons, the results at high C_s are not discussed.

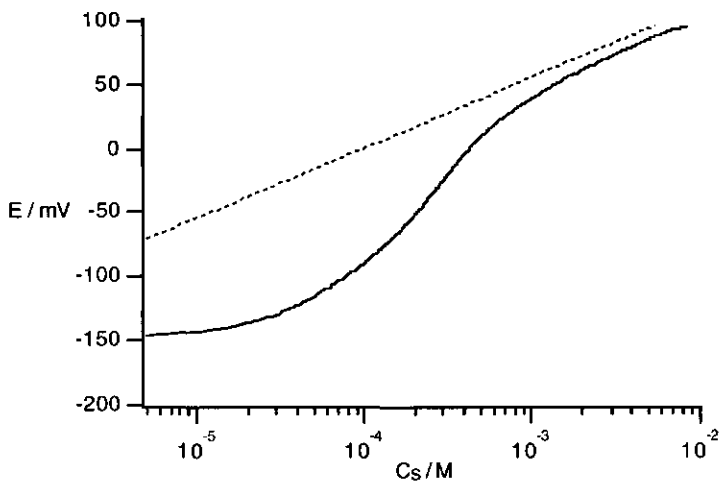

Figure 4.1 **Electrode response to the DTAB concentration C_S in a 1 mM II-6 solution (binding sites L^{-1}) at pH 8.3 in 5 mM KBr at 25 °C. The dotted line represents the electrode response in the absence of polymer (calibration plot).**

The binding isotherms of DTAB with various polyelectrolytes are shown in Figures 4.2 - 4.4. For all polyelectrolytes a slow and continuous increase in β with C_s^f is observed, indicating noncooperative binding.[24] Cooperative binding is indicated by a sudden increase in β in a very narrow concentration range, and may be compared to the formation of micelles at their critical micelle concentration. No abrupt start of surfactant binding to the polyelectrolytes, also known as the critical aggregation concentration (cac), is observed. Zana *et al.* also reported the absence of a cac for the interaction between poly(maleic acid-*co*-*n*-alkyl vinyl ether)s, **Cn acid**, and DTAB and DTAC, which was attributed to the presence of microdomains formed by the polyelectrolyte.[15,16,18] For the polyelectrolyte-DTAB systems studied, the surfactant molecules partition between the aqueous phase and the hydrophobic microdomains formed by the polyelectrolytes (see Chapter 3). The noncooperative behaviour can thus be ascribed to the hydrophobicity of the polyelectrolytes.

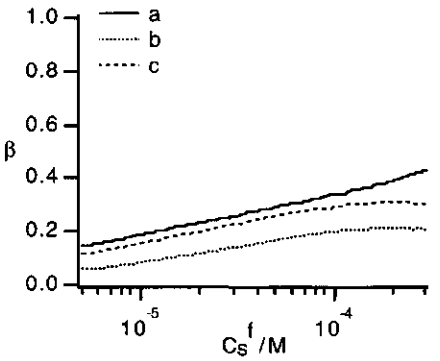

Figure 4.2 **Binding isotherms of DTAB to II-6 at pH 8.3 (a) and pH 11.9 (b), and to II-12 at pH 11.8 (c).**

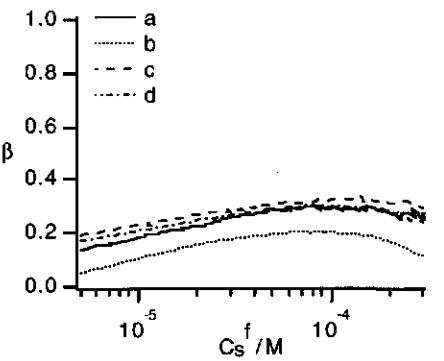

Figure 4.3 **Binding isotherms of DTAB to C6 sulfonate at pH 7.9 (a) and pH 12.0 (b), and to C12 sulfonate at pH 7.9 (c) and pH 11.9 (d).**

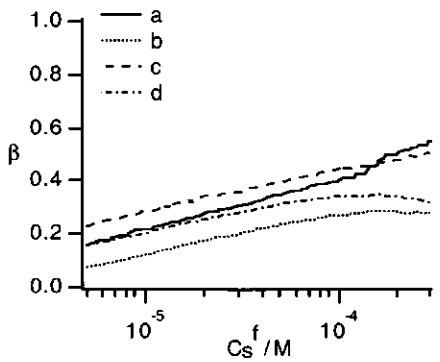

Figure 4.4 **Binding isotherms of DTAB to III-6 at pH 8.4 (a) and pH 11.9 (b), and to III-12 at pH 7.7 (c) and pH 11.9 (d).**

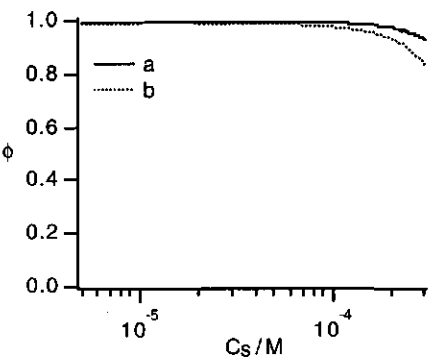

Figure 4.5 **Variation of the fraction of bound surfactant with the total DTAB concentration for III-12 at pH 7.7 (a) and 11.9 (b).**

The polyelectrolyte charge density, which is modified by changing the pH, and the side chain length have small effects on the binding isotherm. Upon increasing the side chain length of the polyelectrolyte or decreasing its charge density, β increases indicating stronger interaction between the polyelectrolyte and DTAB. Both trends can be explained by the overall increase in hydrophobicity of the polyelectrolytes which causes the formation of more compact microdomains. The shape of the curve remains the same upon increasing the side chain length or decreasing the charge density of the polyelectrolyte which indicates similarity in the cooperativity of surfactant binding for all systems studied. The specific ionic nature of the polyelectrolyte binding site hardly influences the binding isotherms.

Most of the surfactant molecules are bound to the polyelectrolytes in the surfactant concentration range investigated. For instance, for **II-12** at $C_s^f = 5*10^{-6}$ M, $\beta = 0.11$, indicating that $C_s^b = 1.1*10^{-4}$ M and that 96% of the surfactants is bound to **II-12**. Likewise, at $C_s^f = 1*10^{-4}$ M ($\beta = 0.29$), $C_s^b = 2.9*10^{-4}$ M and 74% of the surfactants is bound. Similar data hold for the other polymers, and under the experimental conditions used C_s^b is very close to C_s.

Figure 4.5 displays the variations of the fraction of bound surfactant $\phi = C_s^b/C_s$ with C_s for polymer **III-12** at various pH values. Only when $C_s \approx C_p$, ϕ starts to deviate from 1, illustrating the very strong binding of DTAB to the hydrophobic polymer. Similar results are obtained for the other polymers.

Kwak and co-workers have published a large number of binding isotherms for the interaction between cationic surfactants and both synthetic and naturally occurring linear anionic polymers in dilute aqueous solution.[11,13,14,20] They have found strong and highly cooperative surfactant binding which depends on the concentration of added salt, flexibility of the polymer, and the specific nature of the polymer ionic groups. For linear polyelectrolytes interacting with surfactant molecules it is thought that the surfactant molecules form micellar aggregates surrounded by the polyelectrolyte which replaces the surfactant counterions.

For poly(maleic acid-*co*-alkyl vinyl ether)s, **Cn acids**, Zana *et al.* observed cooperative surfactant binding for the short side chains ($n \leq 4$), whereas noncooperative binding is observed for side chains containing more than 4 carbon atoms.[15,16,18] Similar results are reported by Kwak and co-workers for various hydrophobically modified maleic acid copolymers with cationic surfactants.[25-27] The decrease in cooperativity is thought to be due to the formation of microdomains by the polyelectrolytes. When microdomains are present surfactant molecules will preferentially bind to these microdomains, releasing their counterions into solution. Such binding is highly favoured from the energetic point of view because it allows both hydrophobic interactions between bound surfactant alkyl chains and polyelectrolyte side chains constituting the microdomains, and electrostatic interactions between the polyelectrolyte and the oppositely charged surfactant headgroups. The absence of

cooperativity in binding comes from the fact that once a first surfactant molecule is incorporated into a microdomain, a next surfactant molecule will preferably incorporate into another microdomain for entropic reasons. Furthermore, binding of a surfactant molecule will reduce the overall charge of a microdomain resulting in a weakening of the electrostatic attraction between the microdomain and surfactant molecules.

Polyelectrolytes **II-n** and **III-n** form microdomains in aqueous solution as was already discussed in Chapter 3. For **Cn sulfonates** no direct evidence of microdomain formation is available, but the corresponding maleic acid copolymers (**Cn acids**, n = 6, 12) are known to form microdomains in water.[17,28,29] Furthermore, no cooperative binding of DTAB is observed for **Cn sulfonates** between pH 5 and 12 in water implying the formation of microdomains to which the surfactant molecules bind individually. The absence of a cac and the noncooperative binding of DTAB to the studied polyelectrolytes can be ascribed to the hydrophobicity of these polyelectrolytes which causes the formation of microdomains in water.

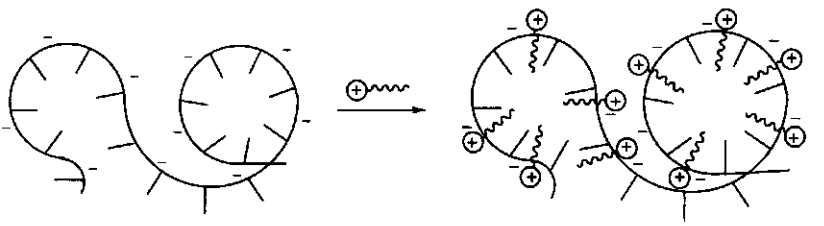

Figure 4.6 **Schematic representation of the interaction between hydrophobically modified polyelectrolytes and oppositely charged surfactants.**

The binding between polyelectrolyte and surfactant is known to increase in strength upon increasing polyelectrolyte and/or surfactant hydrophobicity. The increase in strength results from the additional hydrophobic interactions between the polyelectrolyte side chains and surfactant alkyl chains. For the polyelectrolytes under present investigation the binding constant cannot be determined quantitatively, but the strong binding is clear from the fact that almost all added surfactant binds to the polyelectrolytes, even at very low C_s.

A schematic representation of the interaction between hydrophobically modified polyelectrolytes and oppositely charged surfactant is shown in Figure 4.6. The polyelectrolyte forms microdomains in water to which the surfactant molecules bind with their charged headgroups in close proximity to the charged groups on the polyelectrolyte. The formation of mixed micelles is proposed in which the surfactant counterions are expelled from the aggregate surface, and the surfactant alkyl chains swell the microdomains.[16]

4.2.2 Surface tension measurements

Surface tension measurements afford a simple and informative method to study mixtures of two components, of which one is highly surface active and the other relatively inactive. Many researchers have investigated the interaction between polymers and surfactants in aqueous solution using surface tensiometry.[3,30-34] Generally, the addition of surfactant to an aqueous polymer solution results in a stronger decrease of the surface tension as compared to the addition of the surfactant to pure water. If the polymer itself is not surface active the lowering in surface tension can only be ascribed to interactions between the polymer and surfactant.

In Figure 4.7 the surface tension of pure water and of aqueous solutions of **II-12** and **III-12** are displayed as a function of the DTAB concentration.[35] A DuNoüy ring was used to measure the surface tension. In pure water a gradual decrease in surface tension is observed until the cmc of DTAB, 15.4 mM at 20 °C, is reached. At this point micellar aggregates are formed and no further decrease in surface tension is anticipated because all extra DTAB will form micelles and the free DTAB concentration remains constant. The slight increase in surface tension, observed upon increasing the DTAB concentration above the cmc, is due to impurity of the surfactant.[36] Repeated recrystallisation of DTAB did not yield better results.

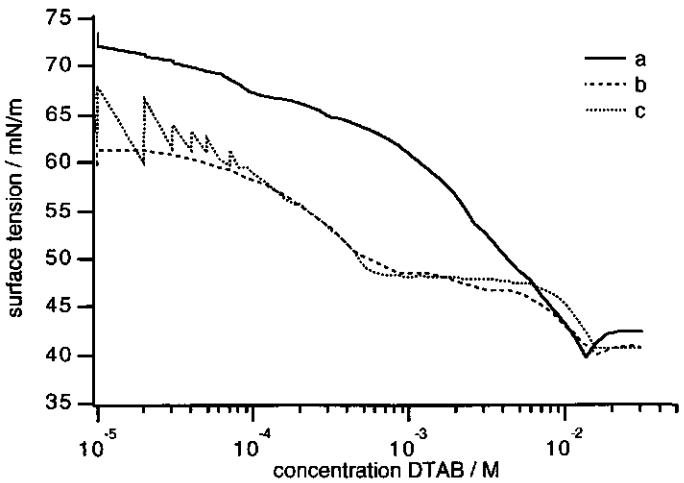

Figure 4.7 **Surface tension of DTAB in pure water (a) and in the presence of II-12 (b), and III-12 (c). Polymer concentration $1*10^{-3}$ mol binding sites L^{-1}, pH 9.9, 20 ± 0.1 °C.**

When DTAB is added to a solution containing polyelectrolyte a synergistic lowering of the surface tension is observed, even after the first addition of DTAB (concentration $1*10^{-5}$ mol L^{-1}, corresponding to a surfactant:binding site ratio of 1:100). Polymers **II-12** and **III-12** are relatively inactive at the air/water interface at this low polymer concentration (see Table 4.1). For several polymers it has been shown that they become more surface active upon increasing

polymer concentration.[37-40] Due to solubility problems at polyelectrolyte concentrations exceeding $1*10^{-2}$ M, the surface activity of the new polyelectrolytes at these higher concentrations was not tested.

Upon increasing the DTAB concentration the surface tension decreases until a plateau is reached. At this point the DTAB concentration roughly equals half the concentration of binding sites. In the plateau the formation of a precipitate is observed due to charge neutralisation of the polyelectrolyte and resulting decreased water solubility. After the plateau the surface tension drops reaching a constant value at high DTAB concentration which results from the formation of free micelles. The formation of free micelles can even be monitored in the presence of polyelectrolytes. Similar changes in the surface tension were observed for the other polyelectrolytes upon increasing the DTAB concentration. The phenomena observed are explained in Figure 4.8, which represents the progressive uptake of surfactant by the polymer.

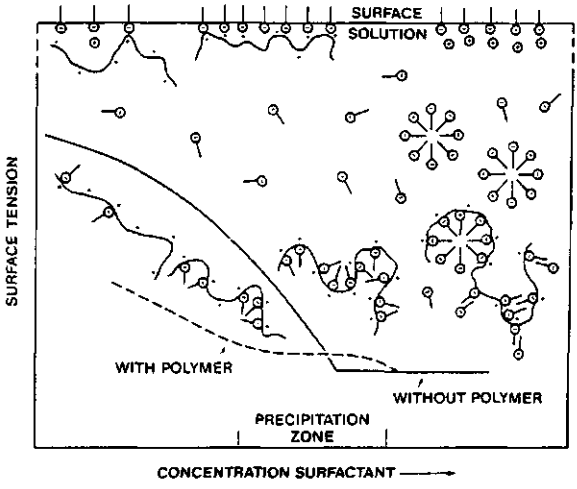

Figure 4.8 **Schematic representation of the conditions in the bulk and at the surface of a solution containing a cationic polymer and anionic surfactant. The full line is the hypothetical surface tension vs. concentration curve of the surfactant alone, the dotted line is that of the mixture with polycation. Simple counterions are depicted only in the surface zone. Taken from reference 3.**

The presence of hydrophobic side chains on the polyelectrolytes, resulting in the formation of hydrophobic microdomains in aqueous solution, does not affect the general features of the polyelectrolyte-surfactant interaction as shown in Figure 4.8. At low DTAB concentration the interaction of DTAB with polyelectrolytes results in a lowering of the surface tension due to the formation of a highly surface active polyelectrolyte-DTAB complex. The hydrophobicity of the formed complex is increased as compared to the individual constituents resulting in a lower solubility in water and favouring accumulation of the complex at the air-solution

64 All experiments were performed far below the critical micelle concentrations of the surfactants. The cmc values at 25 °C are the following: DTAB, 15.4 mM; CTAB, 1 mM; **CNazoC10**, 0.27 mM.

Interactions between Chromophore Labelled Ammonium Surfactants and Hydrophobically Modified Polyelectrolytes

Chapter 5

The interaction of poly(maleic acid-co-alkyl vinyl ether)s and poly(sulfonyl ethyl maleic acid monoamide-co-alkyl vinyl ether)s with and without (cyanobiphenylyl)oxy chromophores with N-(ω-(substituted azobenzoxy)alkyl)-N,N-dimethyl-N-hydroxyethylammonium bromides has been studied by UV spectroscopy. The azobenzene unit is functionalised at the 4'-position with a cyano, methoxy or fluoro substituent and is connected to the surfactant headgroup via a decyl or dodecyl spacer.

Upon addition of surfactants to poly(maleic acid-co-butyl vinyl ether) the absorption maxima (λ_{max}) of the azobenzene chromophores immediately show their maximal blue shift. This indicates cooperative binding of surfactant to this polymer, and the formation of micelle-like aggregates surrounded by polyelectrolyte is assumed. For the interaction of the surfactants with the other polyelectrolytes the λ_{max} values gradually shift to lower values indicating a lower cooperativity of surfactant binding. This is attributed to the formation of microdomains by the polyelectrolytes and the compactness of the microdomains is seen to play an important role in the interaction with the surfactants. For these systems the formation of mixed micelles is assumed.

Upon elongation of the surfactant spacer or changing the endgroup from a cyano to the more hydrophobic fluoro substituent a lower λ_{max} is observed for the chromophores upon initial binding to the polyelectrolytes indicating more cooperative binding.

5.1 Introduction

Spectroscopic techniques like UV/VIS and fluorescence spectroscopy are often used to elucidate the interactions between polymers and surfactants.[1-5] Spectral changes which occur upon the binding of surfactants to polymers, like shifts in absorption maxima, peak widths and peak asymmetry, result from a change in polarity of the microenvironment (solvatochromic shift) or from exciton formation.

Most polymers and surfactants do not possess internal probes to monitor spectroscopic changes, therefore external probes have to be added, like *e.g.* pyrene in fluorescence studies.[2] Another method which is often applied is the modification of polymers or surfactants by covalent bonding of small amounts of probe molecules. A disadvantage of both systems is that the presence of even a modest amount of probe molecules might disturb the interaction between polymers and surfactants.

In the previous chapter the use of UV spectroscopy to study the interaction between polymers and surfactants in which one or both components are labelled with a chromophore has been described. In these systems the chromophores form an intrinsic part of the polymer or surfactant and play a role in determining their physical behaviour.[6,7] Spectral changes observed upon interaction between these polymers and surfactants result from the aggregation or deaggregation of the chromophores.

In this chapter the interaction of the poly(maleic acid-*co*-alkyl vinyl ether)s **Cn acid** and **II-n**, and poly(sulfonyl ethyl maleic acid monoamide-*co*-alkyl vinyl ether)s **Cn sulfonate** and **III-n** with ammonium surfactants is presented. UV spectroscopy is used to monitor the interactions. The ammonium surfactants have a *N,N*-dimethyl-*N*-hydroxyethylammonium headgroup and various azobenzene chromophoric units connected via a decyl or dodecyl spacer. The azobenzene units are functionalised at the 4'-position with a cyano, methoxy or fluoro substituent. Using these various endgroup units the overall dipole moment of the chromophores is altered which may yield additional information on the surfactant polyelectrolyte interaction.

5.2 Results and Discussion

The polyelectrolytes and surfactants used in this Chapter are shown in Scheme 5.1. The synthesis and properties of the surfactants in absence of the polyelectrolytes are described in Chapter 7.

Cn acid - X-Cn-Br In Figure 5.1 the UV absorption spectrum of **F-C12-Br** in pure water is displayed. The concentration of the surfactant molecules used for the measurements

is well below the critical aggregation concentration. For **F-C12-Br** an absorption maximum of 347 nm, associated with a $\pi \rightarrow \pi^*$ transition, is observed for the monomeric species in aqueous solution.

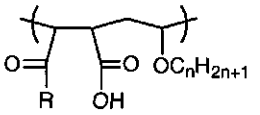

Cn acid, n = 4, 6, 12; R = OH
Cn sulfonate, n = 6, 12; R = $NHCH_2CH_2SO_3^-K^+$

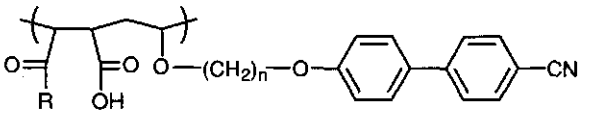

II-n, n = 6, 12; R = OH
III-n, n = 6, 12; R = $NHCH_2CH_2SO_3^-K^+$

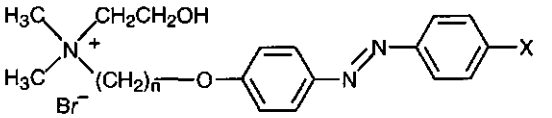

X-Cn-Br X = CN, OMe, F; n = 10, 12

Scheme 5.1 **Polyelectrolytes and surfactants used in this Chapter.**

Upon addition of **F-C12-Br** to an aqueous solution of **C4 acid** the absorption maximum is immediately shifted to 320 nm, a blue shift of 27 nm. According to the molecular exciton model proposed by Kasha[8-10] this shift in absorption maximum results from the parallel aggregation of the fluoroazobenzoxy chromophores (see section 1.2.2). The observed blue shift of the fluoroazobenzoxy units is thus caused by π–π stacking interactions indicating the formation of ordered aggregates consisting of **F-C12-Br** molecules surrounded by the polyelectrolyte.

In Figure 5.2 the absorption maxima of the fluoroazobenzoxy chromophores of **F-C12-Br** at pH 7.8 and 10.9 are displayed as a function of the ratio surfactant to **C4 acid** repeating units. One repeating unit contains two possible binding sites. The fact that the blue shifts are already observed at a 0.1:1 ratio indicates cooperative binding of the surfactants to the polyelectrolyte. This cooperativity suggests that the surfactants bind to the polyelectrolyte in the form of micelle-like aggregates. In section 4.3 the cooperative binding of **CNazoC10** to **C4 acid** was already discussed. Also the dodecyltrimethylammonium cation (DTA^+) is reported to bind cooperatively to **C4 acid** when this polymer has a charge density $\alpha \geq 0.5$.[11,12]

Upon increasing the pH the charge density of the polyelectrolyte is increased resulting in a swelling of the polyelectrolyte due to increased electrostatic repulsion on the backbone. This

affects the interaction with surfactants as can be seen from Figure 5.2. At higher pH **F-C12-Br** still binds cooperatively to the polyelectrolyte, but the blue shift has decreased with 10 nm as compared to the solution at pH 7.8.

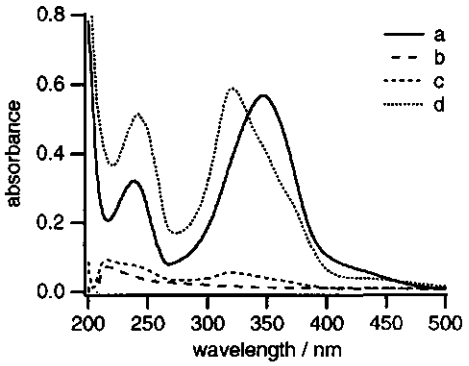

Figure 5.1 **UV absorption spectra of F-C12-Br in pure water (a) and upon addition to C4 acid at pH 7.8. Ratio surfactant to repeating unit 0:1 (b), 0.1:1 (c) and 0.9:1 (d).**

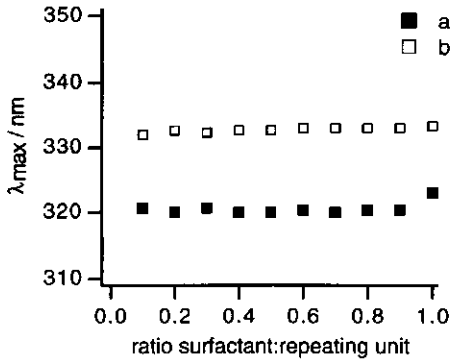

Figure 5.2 **Change in absorption maximum of F-C12-Br upon addition to C4 acid at pH 7.8 (a) and 10.9 (b).**

Besides the mutual orientation of the aggregated chromophores their distance is also a determining factor for the observed shift in λ_{max} and thus for the amount of $\pi-\pi$ stacking interactions. The spectral shift (in wavenumber, $\Delta\nu$) for an aggregate consisting of N monomers with respect to the monomer absorption is given by[13]

$$\Delta\nu = \frac{2}{hc}\frac{N-1}{1}\frac{\mu^2}{r^3}\left(1-3\cos^2\alpha\right)$$

in which μ is the magnitude of the transition dipole moment, r is the centre-to-centre distance between the dipoles and α is the angle between the chromophore long axes and the chromophore centre-to-centre line (see also 1.2.2). The decrease in blue shift upon increasing pH is ascribed to the increased centre-to-centre distance r of the fluoroazobenzoxy chromophores which is forced onto the surfactants by the more extended polyelectrolyte.

The increase in λ_{max} of **F-C12-Br** which can be seen in Figure 5.2 at a 1:1 surfactant to repeating unit ratio is caused by the formation of a polyelectrolyte-surfactant precipitate. An increase in light scattering of the solution is indicative for the formation of this precipitate.

In Table 5.1 the absorption maxima of **X-Cn-Br** in pure water and in the presence of **C4 acid** at various surfactant to repeating unit ratio's are given. For all surfactants an immediate blue shift of the absorption maximum is observed when added to an aqueous solution of **C4 acid**. This implies that all surfactants bind cooperatively to **C4 acid** at both pH values studied. As

was stated before this agrees with reports in literature on cooperative binding of dodecyltrimethylammonium cations to this polyelectrolyte.[11,12]

The alkyl spacer length of the surfactants hardly affects the amount of aggregation of the chromophores. The blue shift of *e.g.* **F-C10-Br** at pH 7.8 is 24 nm, whereas for **F-C12-Br** the shift is 26 nm. As was already clear from Figure 5.2, the conformation of the polyelectrolyte has a large influence on the amount of aggregation of the surfactants. Upon increasing the pH the polyelectrolyte becomes more stretched resulting in a larger distance between the polyelectrolyte binding sites. The distance between the surfactant molecules bound to the polyelectrolyte at higher pH therefore also increases which results in a smaller blue shift of azobenzene chromophores of **CN-Cn-Br** and **F-Cn-Br** at pH 10.9 as compared to pH 7.8.

Table 5.1 **UV absorption maxima (in nm) of X-Cn-Br in pure water and in the presence of C4 acid at various surfactant to repeating unit ratios at pH 7.8 and 10.9.**

		pH 7.8		pH 10.9	
surfactant	**H_2O**	**ratio 0.1:1**	**ratio 0.9:1**	**ratio 0.1:1**	**ratio 0.9:1**
CN-C10-Br	361	339	338	346	349
CN-C12-Br	360	339	338	347	347
MeO-C10-Br	360	339	337	339	340
MeO-C12-Br	358	337	341	338	340
F-C10-Br	349	325	324	331	331
F-C12-Br	347	321	320	332	333

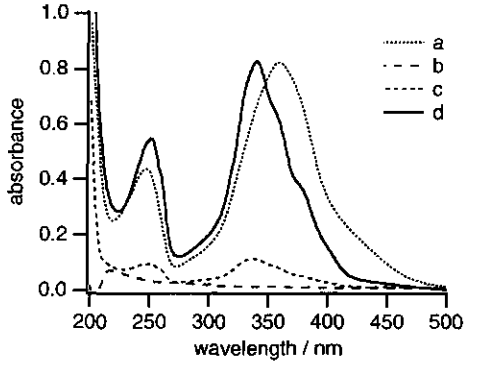

Figure 5.3 **UV absorption spectra of MeO-C12-Br in pure water (a) and upon addition to C4 acid at pH 10.9. Ratio surfactant to repeating unit 0:1 (b) 0.1:1 (c) and 0.9:1 (d).**

When **MeO-Cn-Br** is added to an aqueous solution of **C4 acid** the line width of the absorption peak becomes smaller and some vibrational fine structure (shoulders) appears in the UV spectrum as can be seen in Figure 5.3. Vibrational structure is frequently observed for nonpolar molecules (*e.g.* benzene) in all solvents, whereas the vibrational structure of spectra of polar molecules is generally completely blurred in polar solvents.[14] Both substituents of the methoxyazobenzoxy chromophore of **MeO-Cn-Br** have a similar electron donating capacity which renders the dipole moment of this chromophore essentially zero. In pure water the vibrational fine structure of **MeO-Cn-Br** is blurred but in a nonpolar surrounding, like the inner area of the

C12 acid - X-Cn-Br From literature it is known that **C12 acid** forms microdomains in aqueous solution between pH 1 and 14.[15,16] The compactness of these microdomains depends on the charge density of the polyelectrolytes and thus on the pH of the solution. When **F-C10-Br** is added to **C12 acid** at pH 7.8 a gradual decrease in λ_{max} of the fluoroazobenzoxy chromophores is observed. From Figure 5.6 it can be seen that the absorption maximum is shifted from 350 nm at a 0.1:1 ratio to 327 nm at a 0.9:1 surfactant to repeating unit ratio. The gradual decrease in wavelength of the absorption maximum is seen more clearly in Figure 5.7 which displays λ_{max} as a function of the ratio of the surfactant to polyelectrolyte repeating unit.

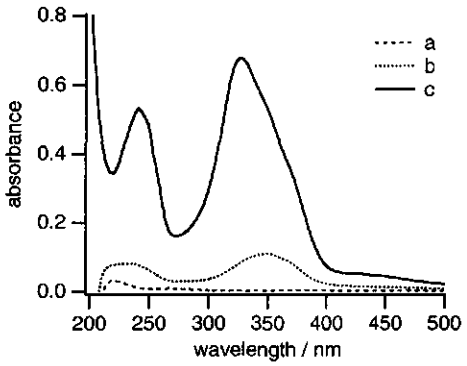

Figure 5.6 **UV absorption spectra of F-C10-Br upon addition to C12 acid at pH 7.8. Ratio surfactant to repeating unit 0:1 (a), 0.1:1 (b) and 0.9:1 (c).**

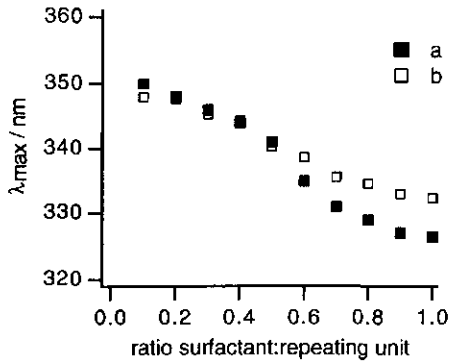

Figure 5.7 **Change in absorption maximum of F-C10-Br upon addition to C12 acid at pH 7.8 (a) and 10.8 (b).**

The gradual decrease in λ_{max} implies a noncooperative binding of the surfactant molecules to the **C12 acid** microdomains. At pH 7.8 $\Delta\lambda_{max}$ is larger than at pH 10.8. This was also observed for surfactant binding to **C4 acid** and **C6 acid** and can be attributed to the smaller distance between the binding sites on the polyelectrolyte backbone at lower pH. This brings the surfactant molecules closer together resulting in stronger interaction between the chromophores.

From Table 5.3 it can be seen that **X-Cn-Br** binds noncooperatively to **C12 acid**. The addition of **F-C12-Br** to **C12 acid** results in an absorption maximum of 335 nm at a 0.1:1 ratio. This is a blue shift of 12 nm as compared to the monomeric surfactant. The blue shift is clearly less than the blue shift observed in the presence of **C4 acid** and **C6 acid** at a 0.1:1 ratio. This indicates a less cooperative binding of **F-C12-Br** to **C12 acid** at pH 7.8. However, at this pH **F-C12-Br** definitely binds more cooperatively to **C12 acid** than the other surfactants. This may be attributed to the more hydrophobic nature of **F-C12-Br** as compared to **F-C10-Br** and **CN-Cn-Br**.

Table 5.3 **UV absorption maxima (in nm) of X-Cn-Br in pure water and in the presence of C12 acid at various surfactant to repeating unit ratios at pH 7.8 and 10.9.**

		pH 7.8		pH 10.9	
surfactant	**H_2O**	**ratio 0.1:1**	**ratio 0.9:1**	**ratio 0.1:1**	**ratio 0.9:1**
CN-C10-Br	361	366	337	363	347
CN-C12-Br	360	356	337	358	347
F-C10-Br	349	350	327	348	333
F-C12-Br	347	335	328	346	332

An increase in alkyl spacer length of the surfactant results in more cooperative surfactant binding to **C12 acid**, as is clear from the lower absorption maxima for **X-C12-Br** than for **X-C10-Br**. This was also observed for surfactant binding to **C6 acid**.

The small red shift of the absorption maximum of **CN-C10-Br** at both pH values results from the dissolution of the surfactant tails into the microdomains formed by the polyelectrolyte. These microdomains provide an apolar environment for the surfactant tails. Generally, the absorption maximum of chromophores is shifted to higher wavelength upon decreasing the polarity of the solvent.

As was already discussed for the binding of **F-C10-Br** to **C12 acid**, an increase in pH results in a decrease of $\Delta\lambda_{max}$, which is the overall change in absorption maximum upon going from a 0.1:1 ratio to a 0.9:1 surfactant to repeating unit ratio. For all surfactants a decrease in $\Delta\lambda_{max}$ is observed upon increasing the pH. The distance between the binding sites on the backbone increases upon increasing pH due to increased electrostatic repulsion between the binding sites. This forces the surfactant molecules to be further apart resulting in an increase in the mutual chromophore distance.

C6 sulfonate - X-Cn-Br The binding of **F-Cn-Br** to **C6 sulfonate** is presented in Figures 5.9 and 5.10. The absorption maximum of **F-C10-Br** in pure water is 349 nm. As can be seen in Figure 5.9 the absorption maximum of this surfactant is already blue shifted at a 0.1:1 surfactant to repeating unit ratio resulting from aggregation of the fluoroazobenzoxy chromophores. A further decrease of the absorption maximum with increasing surfactant concentration is observed.

The pH of the solution hardly affects the cooperativity of binding but the pH does affect the solubility of the formed polyelectrolyte-surfactant complex. The increase in λ_{max} which can be seen in Figure 5.9 at a surfactant to repeating unit ratio beyond 0.5:1, results from precipitation of the formed complex. Precipitation starts at a lower surfactant to repeating unit ratio when the pH of the solution is lowered. The charge density on the polyelectrolyte backbone is reduced upon decreasing the pH, resulting in an reduced hydrophilicity of the

An increase in spacer length of the surfactant results in a small increase in cooperativity of binding, which is clear from the lowering of the absorption maximum by about 10 nm after the first addition of surfactant. For **CN-C12-Br** at pH 7.8 an absorption maximum of 352 nm is observed at a 0.1:1 surfactant to repeating unit ratio. This indicates that some of the cyanoazobenzoxy chromophores are aggregated parallel with respect to each other. The absorption maximum gradually decreases to 340 nm at a 0.9:1 ratio.

The overall $\Delta\lambda_{max}$ of the fluoroazobenzoxy and cyanoazobenzoxy substituted surfactants is similar. The presence of a fluoro endgroup instead of a cyano endgroup only results in a lower absolute absorption maximum which can be attributed to the decrease in polarity of the surfactant chromophore upon replacing a cyano group by a fluoro atom.

At pH 7.8 all surfactants show comparable binding to **C12 acid** and **C12 sulfonate**. A gradual decrease in absorption maximum starting from the same wavelength at a 0.1:1 ratio is observed. At pH 10.9 the surfactants with a C10 spacer also show similar binding to **C12 acid** and **C12 sulfonate**. However, at this pH **X-C12-Br** bind less cooperatively to **C12 acid** than to **C12 sulfonate**. The microdomains formed by **C12 acid** are expected to be more compact than those formed by **C12 sulfonate**. This results in a more difficult penetration of the microdomains of **C12 acid** by the surfactant molecules. Therefore a lower cooperativity is observed for **C12 acid** than for **C12 sulfonate**.

II-6 - X-Cn-Br In Chapter 3 the formation of microdomains by polyelectrolytes **II-n** and **III-n** was discussed. By determining the λ_{max} of their pendant chromophores it was shown that both series of polymers form microdomains in aqueous solution at the pH values investigated. In the previous section it is shown that the compactness of these microdomains plays an important role in the interaction with surfactants.

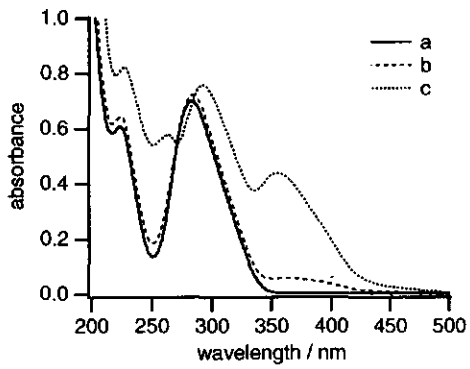

Figure 5.17 **UV absorption spectra of II-6 upon addition of CN-C12-Br at pH 7.6. Ratio surfactant to repeating unit 0:1 (a), 0.1:1 (b) and 1:1 (c).**

As was already shown in section 4.3 the use of different chromophores on a polyelectrolyte and surfactant can provide valuable information on the interactions between these components. The absorption maximum of the (cyanobiphenylyl)oxy chromophores of **II-6** at pH 7.6 is 280 nm. The polyelectrolyte forms microdomains at this pH. From Figure 5.17 the gradual loss of $\pi - \pi$ stacking interactions between the (cyanobiphenylyl)oxy chromophores upon titration with **CN-**

C12-Br can be seen.[17] Simultaneously, the cyanoazobenzoxy chromophores seem to aggregate as can be seen from the blue shift of the absorption maximum of these chromophores.

Figures 5.18 and 5.19 display the shifts in absorption maxima more clearly. The aggregation between the (cyanobiphenylyl)oxy units of the polyelectrolyte is lost upon interaction with **CN-C12-Br**. The surfactant molecules penetrate between the polyelectrolyte side chains disrupting the $\pi-\pi$ stacking interactions. The cyanoazobenzoxy chromophores of the surfactant initially show a red shift as compared to the absorption maximum of the monomeric compound. This solvatochromic shift is due to the burial of individual surfactant molecules in the apolar polyelectrolyte microdomains.

Upon increasing the surfactant concentration the absorption maximum shifts to lower wavelength. The surfactant molecules start to aggregate resulting in a decrease in the absorption maximum due to $\pi-\pi$ stacking interactions between the cyanoazobenzoxy chromophores. It should be noted that both solvation of the surfactant in the apolar polyelectrolyte microdomains and aggregation of the cyanoazobenzoxy chromophores determine the overall absorption maximum of these chromophores.

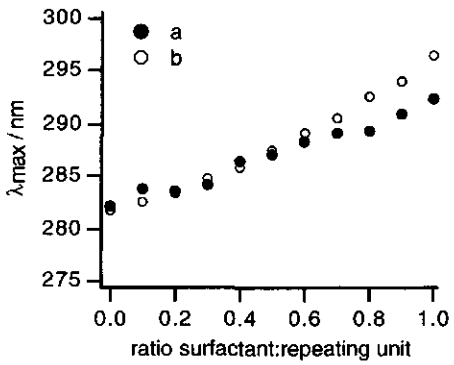

Figure 5.18 **Change in absorption maximum of the (cyanobiphenylyl)oxy chromophores of II-6 upon titration with CN-C12-Br at pH 7.6 (a) and 10.6 (b).**

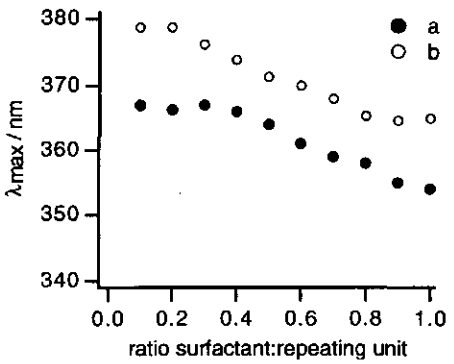

Figure 5.19 **Change in absorption maximum of the cyanoazobenzoxy chromophores of CN-C12-Br upon addition to II-6 at pH 7.6 (a) and 10.6 (b).**

In Table 5.4 the absorption maxima of the (cyanobiphenylyl)oxy chromophores of **II-6** and the azobenzene chromophores of **X-Cn-Br** are displayed at various surfactant to repeating unit ratio's and two pH values.

For all **II-6-X-Cn-Br** systems an increase in the absorption maximum of the (cyanobiphenylyl)oxy chromophores is observed. This is caused by a gradual loss of the (cyanobiphenylyl)oxy stacking interactions. Simultaneously, the absorption maximum of the azobenzene chromophores is seen to decrease. Initially, at a 0.1:1 surfactant to polyelectrolyte

repeating unit ratio, all azobenzene surfactants show a red shift of their absorption maxima which is caused by a burial of the surfactant molecules into the apolar microdomains formed by the polyelectrolyte. These so-called solvatochromic shifts are larger at higher pH due to the more open microdomain structure which makes them more penetrable.

At low pH the absorption maxima of **CN-C10-Br** and **CN-C12-Br** at a 1:1 surfactant to repeating unit ratio are 356 and 354 nm respectively. This indicates some aggregation between the chromophores as their maxima are shifted about 5 nm as compared to the absorption maxima of the monomeric species. The aggregation between the (cyanobiphenylyl)oxy chromophores of the polyelectrolyte is almost completely lost. This indicates the formation of mixed micelle-like aggregates in which the cyanoazobenzene surfactants are somewhat clustered.

Table 5.4 **UV absorption maxima (in nm) of the (cyanobiphenylyl)oxy chromophores of II-6 (CB) and the azobenzene chromophores of X-Cn-Br (AB) at various surfactant to polymer repeating unit ratios and at various pH.**

		CB		AB	
surfactant	**pH**	**ratio 0.1:1**	**ratio 1:1**	**ratio 0.1:1**	**ratio 1:1**
CN-C10-Br	7.8	282	289	373	356
	10.7	283	296	379	360
CN-C12-Br	7.6	283	292	367	354
	10.6	283	296	379	365
F-C10-Br	7.8	282	284	355	350
	10.7	282	293	356	351
F-C12-Br	7.6	284	287	351	348
	10.3	284	293	355	353

For **F-C10-Br** and **F-C12-Br** at pH ~ 7.7 the final absorption maxima are 350 and 348 nm respectively. This indicates that the surfactants are monomerically dispersed in the polyelectrolyte microdomains. The aggregation between the polyelectrolyte chromophores is only partially lost. As for the previously discussed system, mixed micelle-like aggregates are formed but in this case the (cyanobiphenylyl)oxy chromophores still show some aggregation.

At pH ~ 10.6 the aggregation of the (cyanobiphenylyl)oxy chromophores is disrupted by all surfactants. The azobenzene chromophores all display their monomeric absorption maxima at a 1:1 ratio. Again this indicates the formation of mixed micelles, but in these systems the polyelectrolyte side chains and surfactant molecules are both randomly distributed within the mixed micelles.

The alkyl spacer length hardly influences the interaction between surfactants and **II-6**. The surfactant endgroup only shows some influence at pH ~ 7.7, mainly on the aggregational state

of the surfactants themselves. The fluoro substituted surfactants show a smaller tendency to aggregate as compared to the cyanoazobenzoxy carrying surfactants.

II-12 - X-Cn-Br In Table 5.5 the UV absorption maxima of the (cyanobiphenylyl)oxy units of **II-12** and the azobenzene chromophores of **X-Cn-Br** are presented. For these systems a gradual shift in absorption maximum for both the (cyanobiphenylyl)oxy and azobenzene units is found, indicative for noncooperative binding. As was also seen for **II-6**, the loss in $\pi - \pi$ stacking interactions between the (cyanobiphenylyl)oxy chromophores is higher at higher pH. This is due to the more open microdomain structure at the higher pH which makes the penetration with surfactants more favourable.

Table 5.5 **UV absorption maxima (in nm) of the (cyanobiphenylyl)oxy chromophores of II-12 (CB) and the azobenzene chromophores of X-Cn-Br (AB) at various surfactant to polymer repeating unit ratios and at various pH.**

		CB		AB	
surfactant	**pH**	**ratio 0.1:1**	**ratio 1:1**	**ratio 0.1:1**	**ratio 1:1**
CN-C10-Br	7.5	278	283	368	353
	10.7	281	290	373	364
CN-C12-Br	7.7	281	287	361	351
	10.7	281	291	372	362
F-C10-Br	7.5	278	287	352	347
	10.7	281	292	355	350
F-C12-Br	7.7	282	287		
	10.4	281	289	352	348

As for **II-6-X-Cn-Br** the formation of mixed micelle-like aggregates is anticipated for **II-12** upon addition of surfactants. The absorption maxima of the **CN-Cn-Br** chromophores at a 1:1 ratio at pH ~ 7.6 are blue shifted as compared to the monomerically dispersed chromophores. This indicates some clustering of the surfactant molecules. Also the polyelectrolyte chromophores are still partly aggregated. The formation of mixed micelles is again anticipated but in contrast to the situation with **II-6** both the surfactants and the polyelectrolyte side chains show some clustering within these micelles. For **F-Cn-Br** at pH ~ 7.6 the chromophores are monomerically dispersed in the mixed micelles. The absorption maxima of the polyelectrolyte chromophores indicate that these chromophores are clustered. At pH ~ 10.7 the azobenzene chromophores all show the absorption maxima of the monomeric species. Also the (cyanobiphenylyl)oxy stacking interactions are lost upon interaction with the surfactants. Similar to **II-6** in the presence of surfactants **X-Cn-Br** at pH

~ 10.7 the formation of mixed micelle like aggregates with randomly dispersed surfactant molecules and polyelectrolyte side chains is proposed.
The surfactant spacer length hardly influences the interaction with **II-12**. The surfactant endgroup does show a small influence. This may be attributed to the difference in polarity of the chromophore of the surfactants.

III-n - X-Cn-Br The shifts in absorption maxima of **III-6** upon titration with **X-Cn-Br** are shown in Table 5.6. A small, gradual increase in the λ_{max} of the (cyanobiphenylyl)oxy units is observed indicating noncooperative interaction between the polyelectrolyte microdomains and surfactant molecules. The cyanoazobenzoxy carrying surfactants are initially solvated within the microdomains formed by the polyelectrolyte resulting in a small red shift of the absorption maxima. Increasing the surfactant concentration results in the decrease of the absorption maxima of these surfactants due to chromophore aggregation. Based on the observed changes in the absorption spectra the formation of mixed micelles is proposed for all **III-6-X-Cn-Br** systems.

Table 5.6 **UV absorption maxima (in nm) of the (cyanobiphenylyl)oxy chromophores of III-6 (CB) and the azobenzene chromophores of X-Cn-Br (AB) at various surfactant to polymer repeating unit ratios and at various pH.**

		CB		AB	
surfactant	**pH**	**ratio 0.1:1**	**ratio 1:1**	**ratio 0.1:1**	**ratio 1:1**
CN-C10-Br	4.0	287	289	370	354
	7.6	286	290	370	359
	11.0	290	293	366	352
CN-C12-Br	4.0	287	293	366	354
	7.2	286	290	360	355
	11.0	288	293	363	353
F-C10-Br	4.1	285	287		
	7.6	285	288		
	11.1	286	292		
F-C12-Br	4.0	285	291		
	7.3	284	287		
	11.1	285	292		

An increase in surfactant spacer length only shows an effect at pH 4.0 when the most compact microdomains are present. The solvatochromic shift of the cyanoazobenzoxy chromophores is slightly larger for the shorter chained surfactants which might be attributed to stronger interactions between the chromophores for the surfactants with a dodecyl spacer. A delicate

balance between solvation in apolar microdomains and π–π stacking interactions determines the absorption maximum. The stronger interactions between the **CN-C12-Br** as compared to **CN-C10-Br** was discussed before.

The fluoroazobenzoxy carrying surfactants show a smaller influence on the (cyanobiphenylyl)oxy destacking of the polyelectrolyte apparently resulting from weaker interactions between these surfactants and the polyelectrolyte microdomains. The absorption maxima of the fluoroazobenzoxy chromophores could however not be determined because their absorption peaks partly overlap with the (cyanobiphenylyl)oxy absorption peaks.

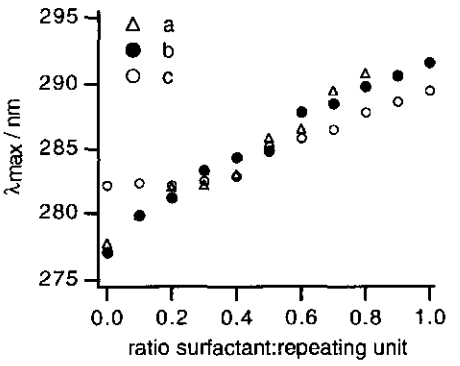

Figure 5.20 **Change in absorption maximum of III-12 upon titration with F-C10-Br at pH 4.0 (a), 7.7 (b) and 11.1 (c).**

For **III-12** only the interaction with **F-Cn-Br** was investigated. In Figure 5.20 the absorption maxima of the (cyanobiphenylyl)oxy chromophores of ***III-12*** upon titration with **F-C10-Br** is shown. The overall decrease in (cyanobiphenylyl)oxy stacking interactions at pH 4.0 and 7.7 is the same whereas at pH 11.1 the $\Delta\lambda_{max}$ is smaller. A similar trend is observed when **F-C12-Br** is added to **III-12** at various pH values. As for the previously discussed polyelectrolyte-surfactant systems, the formation of mixed micelle-like aggregates is proposed.

5.3 Conclusions

The binding of surfactants to polyelectrolytes is seen to depend on the side chain length and charge density of the polyelectrolytes which determines the conformation and compactness of the microdomains formed in aqueous solution. Furthermore, the spacer length of the surfactant and the endgroup of their chromophore play a role in the interaction. There exists a delicate balance between all these factors.

The conformation of the polyelectrolyte is very important for the interactions with surfactants. The short chained polyelectrolyte **C4 acid** is in its extended conformation at pH > 3.1 and no microdomains are formed at the pH values used. Upon addition of azobenzene labelled surfactants to **C4 acid** the λ_{max} of the surfactants immediately show their maximal blue shift. This indicates cooperative binding of surfactants to **C4 acid**. The surfactant molecules form micelle-like aggregates which are surrounded by the polyelectrolyte chains.

6.1 Introduction

With the increasing interest in ultra thin organic films for applications as electronic and electro-optical devices and as models for biological membranes, the Langmuir-Blodgett (LB) technique has received considerable attention.[1-5] One of the advantages of using the Langmuir-Blodgett technique is that films of desired structures with thicknesses controlled at the molecular level can be obtained. Initially, research primarily focused on mono- and multilayers of low-molecular weight molecules. However, these films suffer from thermal and mechanical instability and are sensitive towards environmental attack. Due to their superior stability, LB films of polymers are nowadays studied for their application in optical and electronic devices. Because of their distinct hydrophilic and hydrophobic parts necessary for monolayer formation on a subphase, amphiphilic polymers are a class of polymers frequently used to prepare mono- and multilayers.[6-9] Copolymers of maleic anhydride and α-olefins or alkyl vinyl ethers display good homogeneity and stability of the monolayer. Furthermore, the fluidity and mobility of their LB films can be tuned by use of different side chains.[3]
In the previous chapters the "spontaneous" self-assembly of the poly(maleic acid-*co*-(*n*-[(4-cyano-4'-biphenyl)oxy]alkyl vinyl ether)s **II-n** in aqueous solution in the absence and presence of surfactants has been described. In this chapter the Langmuir technique is used to obtain "artificial" self-assembled structures of polymers **I-n** and **II-n**. The influence of various metal ions and surfactants on the monolayer formation of **II-n** is presented. The transfer of the amphiphilic polymers **II-n** onto various hydrophilic substrates is also described. The LB films were studied with UV spectroscopy and second harmonic generation.

6.2 Results and Discussion

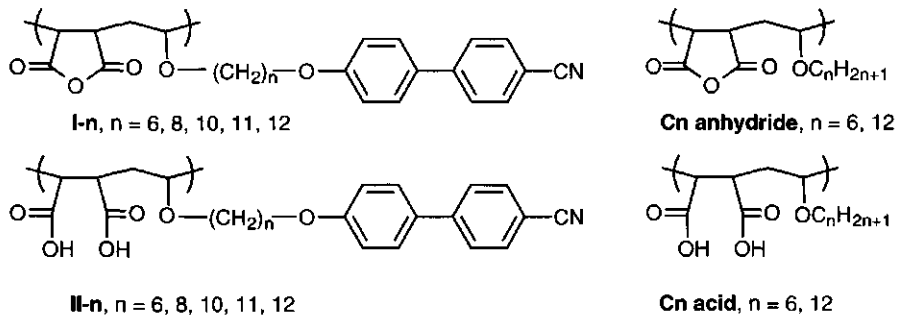

Scheme 6.1 **Structures of the polymers used in this Chapter.**

6.2.1 Polymers I-n

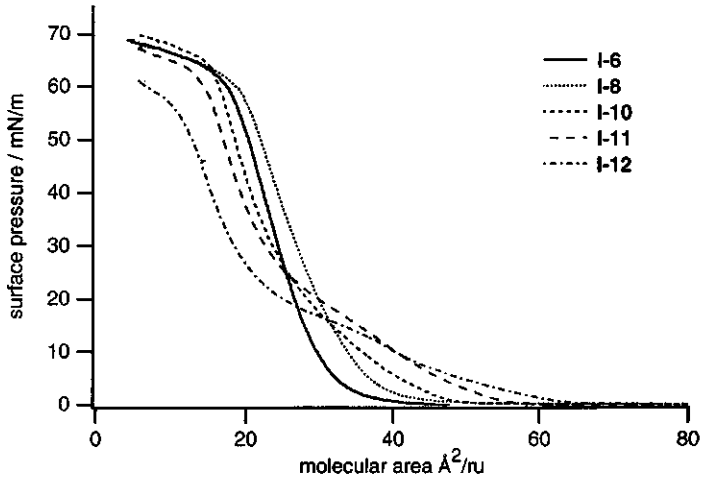

Figure 6.1 **Surface pressure-area isotherms of polymers I-n at 20 °C.**

In Figure 6.1 the π–A isotherms for the polymers **I-n** are displayed. The polymers have lift-off areas between 36 and 65 Å^2 per repeating unit, *i.e.* per each alternating pair of monomer units in the backbone. At the lift-off area the polymers start to interact and it thus gives information on the initial orientation of the polymers on the subphase. In Table 6.1 the lift-off areas for polymers **I-n** are presented. For comparison the values for two polymers without the (cyanobiphenylyl)oxy chromophores are also presented.

Table 6.1 **Lift-off areas (Å^2/repeating unit) of polymers with a maleic anhydride moiety.**

polymer	lift-off area
C6 anhydride	**36**
C12 anhydride	**32**
I-6	**36**
I-8	**39**
I-10	**45**
I-11	**53**
I-12	**65**

For **C6 anhydride** the lift-off area is 36 Å^2 per repeating unit. The cross-sectional area of a methylene chain is approximately 20 Å^2. The large area occupied by a repeating unit indicates that the polymer backbone is oriented parallel to the water surface with the maleic anhydride units immersed into water and the side chains oriented towards the air. In this way the hydrophilic maleic anhydride moieties can easily interact with the water whereas the lipophilic chains can minimise their contact with water. For a poly(maleic anhydride-*co*-hexadec-1-ene) Davis *et al.*[23] reported a lift-off area of 28 Å^2/ru indicating a slightly smaller polymeric area interaction with the aqueous subphase compared the **Cn**

anhydride polymers connecting their side chain through an ether bond. The ether oxygen connecting the side chain with the backbone thus has favourable interactions with the water subphase. As the length of the alkyl group is increased, the lift-off area is decreasing. This is due to an increase in hydrophobic interactions between the side chains which tends to keep the side chains together.[6,23,24] The isotherms of **Cn anhydride** are relatively steep with collapse pressures of about 55 mN/m, indicating the formation of stable condensed monolayers.

Attaching a chromophore to the side chain has a remarkable effect on the π-A isotherms. For **I-6** the lift-off area is comparable to **C6 anhydride** indicating a similar orientation of the polymers at the subphase. On increasing the spacer length between the chromophore and the backbone the lift-off area is increasing indicating an interaction of the side chains with the aqueous subphase. The molecular area of a (cyanobiphenylyl)oxy unit is approximately 47 $Å^2$.[25,26] The flat orientation of this unit onto the subphase combined with the backbone interaction with the subphase, taken to be 32 $Å^2$ as for **C12 anhydride**, will lead to a lift-off area of about 80 $Å^2$. If the chromophore is oriented with its polar cyano group into the subphase, about 20 $Å^2$ is needed and the overall lift-off area would be 52 $Å^2$.[25] For **I-11** and **I-12** an orientation of the chromophores with the cyano group immersing in the water subphase is suggested. For both **I-11** and **I-12** a completely flat orientation of the chromophores onto the subphase as observed for 4'-*n*-octyl-4-cyanobiphenyl[26] is hampered, but an increase in spacer length seems to provide more orientational freedom for the chromophores to approach this flat orientation. For the shorter spacers free orientation of the chromophores is limited by the spacer length.[27] For these compounds most of the chromophores are oriented randomly into the air. Upon increasing spacer length the isotherms become less steep indicating a larger compressibility due to decreasing order of the monolayer.

The stability of the monolayers on pure water was tested at 14 and 30 mN/m.[23,28] The surface area occupied by the polymers decreased in time, and no stable monolayes could be formed at these pressures. The instability of the monolayers is attributed to the hydrolysis of the maleic anhydride units to the maleic acid moieties. Davis *et al.*[23] have studied the hydrolysis of poly(maleic anhydride-*co*-hexadec-1-ene) on an aqueous subphase at pH 5.6 and 20 °C. They found that the hydrolysis is essentially complete in 24 hours, and suggested this is sufficiently slow to prepare stable monolayers and LB films. To retard the hydrolysis π-A isotherms were recorded on an acidified subphase. On pure water and on the acidified subphase the same isotherms were obtained for **I-n**. This indicates that the conversion of some of the maleic anhydride moieties to maleic acid units at neutral pH does not significantly influence the π-A isotherm. Unfortunately, polymers **I-n** on an aqueous subphase at pH 1 at various pressures also did not give stable monolayers and no LB films could be prepared.[29]

6.2.2 Polymers II-n

The π-A isotherms of polymers **II-n** are shown in Figure 6.2. The lift-off areas of **II-n** and the corresponding maleic acid copolymers without a chromophore are given in Table 6.2. The lift-off areas of **Cn acid** correspond well to the values of 39 and 41 Å^2/ru reported for poly(maleic acid–*co*-hexadec-1-ene)[23] and poly-(maleic acid-*co*-octadecyl vinyl ether)[30] respectively. The lift-off areas for **Cn acid** are much larger that the cross-sectional area of a methylene chain (approximately 20 Å^2). This suggests that the hydrophilic headgroups are rather large and that they therefore include both carboxylic acid groups, *i.e.* both these groups are in contact with the water surface. The isotherms are relatively steep with collapse pressures above 50 mN/m, indicating the formation of condensed layers.

Table 6.2 **Lift-off areas (Å^2/repeating unit) of polymers with a maleic acid moiety.**

polymer	lift-off area
C6 acid	38
C12 acid	38
II-6	65
II-8	69
II-10	75
II-11	85
II-12	89

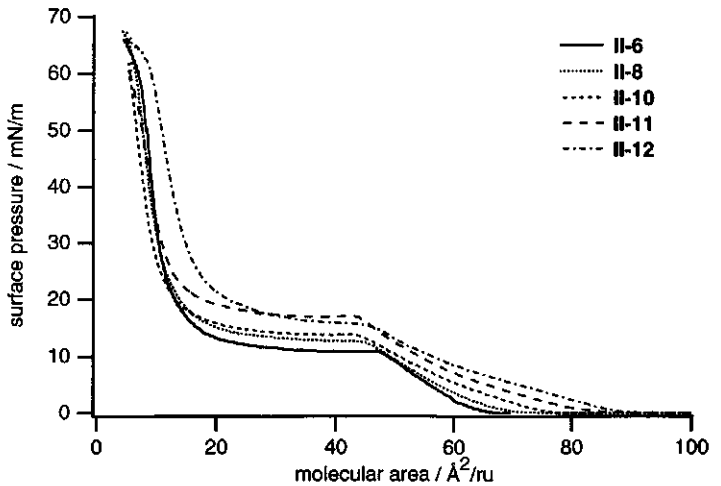

Figure 6.2 **Surface pressure-area isotherms for polymers II-n at 20 °C.**

As compared to **I-n** a clear increase in lift-off area for polymers **II-n** is observed. Upon comparing **Cn acid** with **Cn anhydride** an increase in molecular area is also observed. This increase is due to the increased flexibility of the polymer backbone upon hydrolysis of the maleic anhydride moieties. For polymers **II-n** this increased flexibility, which also affects the liquid crystalline behaviour (2.3.5), allows the chromophores to have more extensive

interactions with the aqueous subphase. Taking the lift-off area of the **Cn acid** as the molecular area necessary to accommodate the polymeric backbone and adding the area for a (cyanobiphenylyl)oxy chromophore a minimum lift-off area of 85 $Å^2$ per repeating unit is necessary to have both backbone-subphase and chromophore-subphase interactions. For **II-11** and **II-12** this condition is probably met, as is clear from the observed lift-off areas. For the shorter spacers the cyano group is immersed into the subphase as is clear form the increase in lift-off area as compared to **Cn acid**, but the side chains hamper the interaction of the rest of the chromophore with water.

Interestingly, all polymers **II-n** show a plateau in their π–A isotherm. The molecular area at the low area side of the π-A isotherm, approximately 15 $Å^2$/ru, is too small to accommodate the monolayer. The molecular area equals about one third of the molecular area at the start of the plateau. This indicates that a triple layer is formed upon compression. Triple layer formation is also observed for some low molecular weight fatty acids[31] and compounds carrying a cyanobiphenyl moiety.[26,32,33]

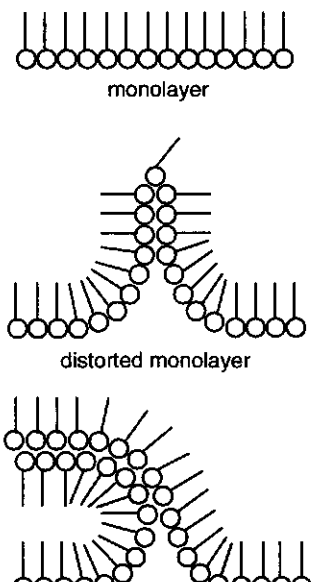

Figure 6.3 **Model for the transformation of a monolayer into a triple layer.**

Due to the strong dipole-dipole attraction 4'-*n*-octyl-4-cyanobiphenyl shows an antiparallel orientation in the bulk smectic A phase. At the water surface the interactions with water are strong enough to break the antiparallel orientation and to create a monolayer. Upon increasing surface pressure the antiparallel orientation is found again in the triple layer which is formed by the cooperative sliding of a bilayer on top of the original monolayer (Figure 6.3). Further experimental evidence for triple layer formation is obtained by BAM and compression-expansion experiments. Compression-expansion cycles indicate a complete reversibility of the π-A isotherm of both **II-6** and **II-12** before the plateau is reached. In the region of the plateau a drop in pressure in the expansion curves is observed. A second compression taken 5 minutes after the first cycle again leads to the same curve. Consecutive compression-expansion cycles to various pressures for polymer **II-6** are shown in Figure 6.4. The polymer layer is compressed to 5, 10, 20, 30, 40, 50 and 60 mN/m respectively. The π–A isotherm upon compression can be seen to be the same after each compression-expansion cycle. This semi-reversibility can be attributed to the ordered structure. The process of sliding a bilayer over a monolayer can

readily be reversed. When the surface pressure drops below the transition pressure the triple layer "unzips" to regenerate the monolayer. The reproducability of the isotherms for successive compressions is indicative for a highly flexible system.

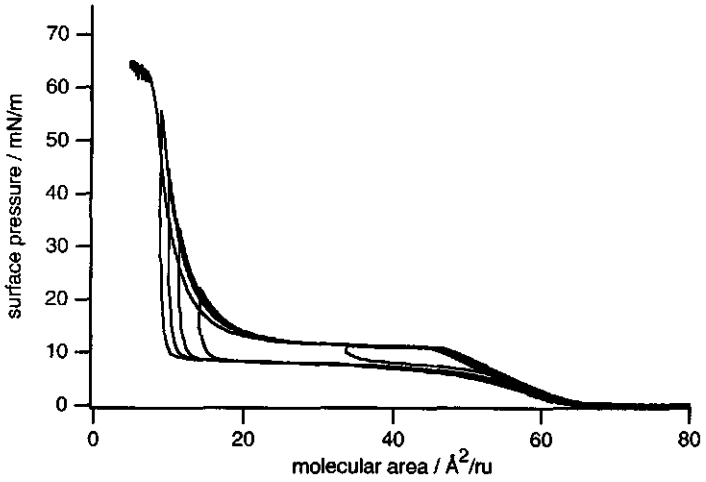

Figure 6.4 **Consecutive compression-expansion cycles for polymer II-6 at 20 °C.**

When the monolayer is compressed to 60 mN/m it collapses. The π–A isotherm taken after collapse shows the general features of the original π–A isotherm, but the lift-off area has decreased by approximately 30 %. This is due to partial dissolution of the polymer into the subphase at high surface pressures.

The monolayer stability of **II-6** and **II-12** was investigated on pure water at 20 °C and surface pressures of 10 and 14 mN/m respectively. The triple layer stability of both polymers was studied at 30 mN/m. Below the plateau pressure, 12 mN/m for **II-6** and 15 mN/m for **II-12**, the monolayer became stable within 40 minutes. Thus the initial area reduction can be attributed to the reorganisation of the monolayer and is not due to collapse or dissolution into the subphase. At 30 mN/m the area kept reducing in time and no stable triple layers were formed even after 5 hours. It is possible that the triple layer was not completely formed and more time is needed to obtain a stable triple layer, or possibly some material is lost by dissolution into the subphase.

Brewster angle microscopy is used to visualise the morphology and domain structures of the monolayers of polymers **II-6** and **II-12** on water. In Figure 6.5 the micrographs are shown for **II-6** at 0 and 12 mN/m. Immediately after spreading the film is homogeneously organised at near zero surface pressure. Upon increasing the surface pressure to the plateau value straight lines are observed probably indicating the formation of a triple layer. At the point where a layer folds a small difference in refractive index may occur which appears as lighter or darker

regions in the image. Increasing pressure showed no other changes. The image became blurred in the plateau region which may be ascribed to the stiffening of the layer or to layers moving on top of each other.

From these results it is concluded that a triple layer is formed upon compression of polymers **II-n** on an aqueous subphase. The $\pi-\pi$ stacking interactions between the (cyanobiphenylyl)oxy moieties cause the side chains to be well-aligned in its monolayer. The highly aligned polymers are favourably oriented for a cooperative transition to a triple layer.

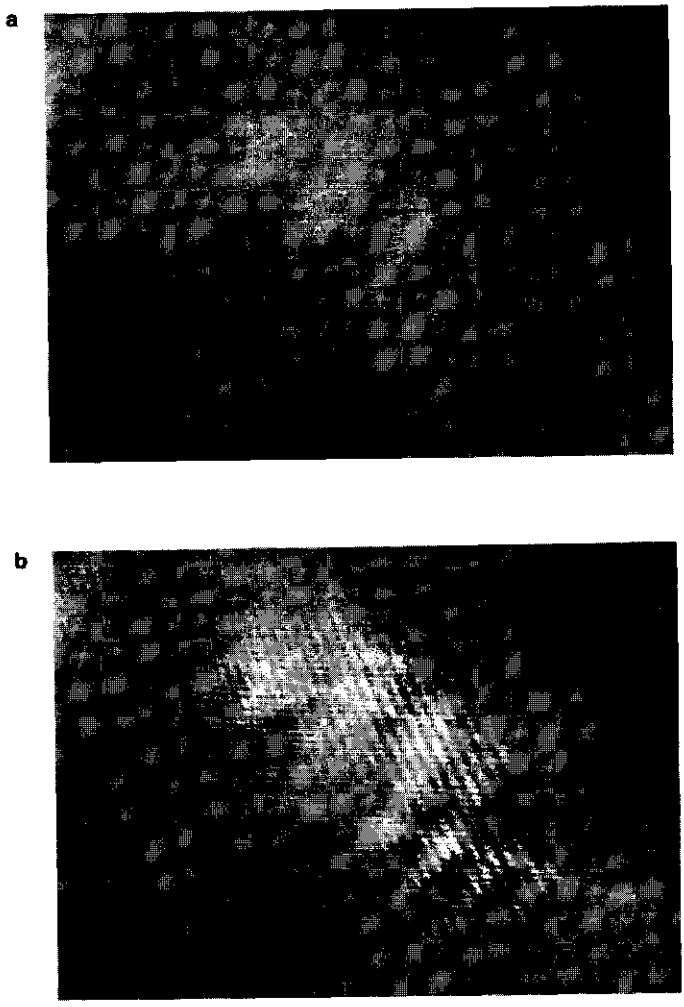

Figure 6.5 **Brewster angle microscope images of polymer II-6 at 0 (a) and 12 mN/m (b). Image size 594 * 920 μm^2.**

The surface pressure at the transition to the plateau region rises by increasing the number of methylene units in the spacer. Higher pressures are necessary for triple layer formation indicating that the increased flexibility gives rise to a stabilisation of the monolayer.

6.2.3 Subphase variation

pH As already mentioned in 6.2.1 the addition of acid can be used to stabilise a monolayer of a maleic anhydride polymer by retarding the hydrolysis to the maleic acid polymer. It is clear that the variation in subphase pH might also influence the monolayer formation of polymers **II-n**. At low pH all carboxylic acid groups will be protonated whereas at high pH deprotonation of these units will lead to an increase in electrostatic repulsion at the air-water interface. At high pH the polymers are known to dissolve in bulk water (see Chapter 3), and this might seriously affect the monolayer formation. The advantage of an acidified subphase is the decrease in polymer solubility, possibly leading to an increased stability of the monolayer.

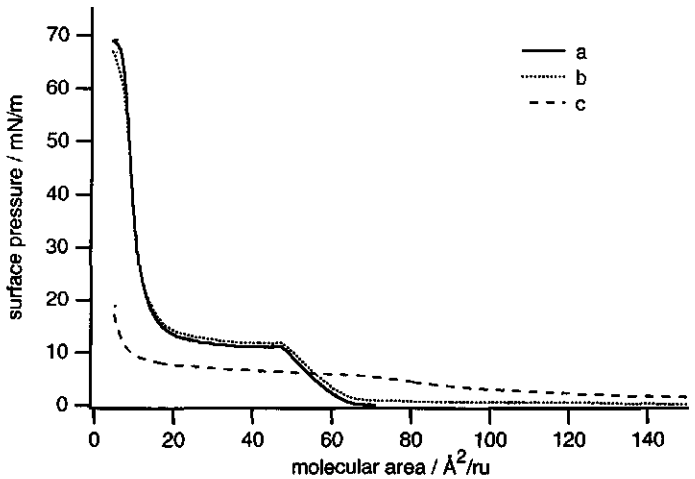

Figure 6.6 **Surface pressure-area isotherms of polymer II-6 on water at pH 1 (a), pH 7 (b) and pH 13 (c).**

In Figure 6.6 the π−A isotherms of **II-6** at various pH values are shown. At pH 1 the polyelectrolytes are not dissociated whereas at pH 7 almost completely ionised polyelectrolytes are expected due to their pK_a^{app} values of 3.5 and 6.6 (Chapter 3). However, essentially the same isotherms are obtained at pH 1 and 7. It has been shown that the apparent pK_a values of acids near interfaces can be several units higher as compared to the bulk solution.[10] Based on this the apparent pK_a values of **II-n** at the interface are expected to be several units higher than in bulk solution, explaining the resemblance in π-A isotherms at pH 1 and 7. At high pH an increase in lift-off area due to increased electrostatic repulsion along

the backbone is observed. However, polymer **II-6** partly dissolves in the subphase which can be seen from the disappearance of the plateau and the low molecular area just before the collapse. Polymer **II-12** also displays the same π–A isotherm at low and neutral pH. At high pH a slight increase in lift-off area and plateau pressure is observed. Due to electrostatic repulsion on the backbone by deprotonation of the carboxylic acid moieties the backbone will be stretched more and each repeating unit of the polymer will occupy a relatively larger area at the surface. The monolayer of **II-12** is slightly more stabilised at pH 13 than at pH 1 and 7, resulting in an increase of the plateau pressure. Overall it thus seems that most carboxylic acid groups are not dissociated at pH 1 and 7, whereas at pH 13 most of the groups are dissociated.

Various counterions For poly(maleic acid-*co*-*n*-octadecyl vinyl ether) Lee *et al.*[30] reported more expanded monolayers in the presence of Na^+, Mg^{2+} and Al^{3+} in the aqueous subphase. The copolymers interact with the metal ions at the interface resulting in a change in the monolayer organisation. Only the presence of divalent Mg^{2+} resulted in the formation of carboxylate ions as studied by FTIR. The effect of various divalent counterions on the monolayer formation of polymers **II-*n*** is described in this section.

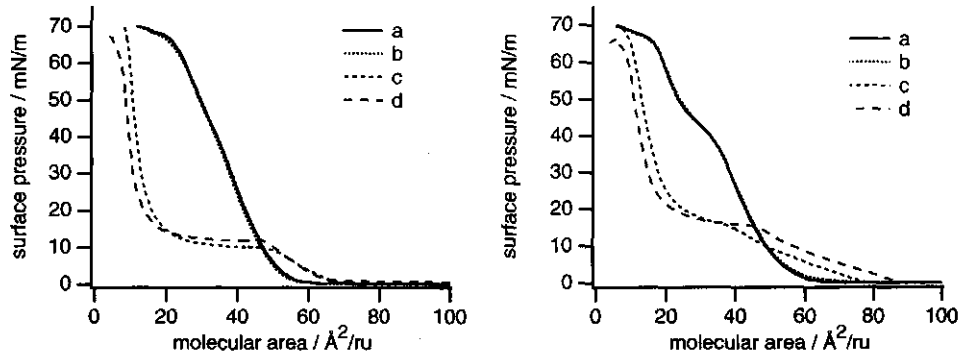

Figure 6.7 **Surface pressure-area isotherms of polymer II-6 (left) and II-12 (right) on 1 mM solutions of $CuCl_2$ (a), $Cu(ClO_4)_2$ (b), $MgCl_2$ (c) and on pure water (d). The pH of the subphase varied between 5.3 and 6.1 (see also reference 34).**

The lift-off area remains the same for **II-6** in the presence of Mg^{2+} indicating that binding of the Mg^{2+} ions to the maleic acid moieties hardly influences the interactions of the backbone with the subphase. It does however, result in a slight destabilisation of the monolayer of **II-6** as observed by the lowering the pressure of the plateau. For **II-12** the presence of Mg^{2+} results in a small decrease in lift-off area and the plateau is seen to disappear almost completely. Increased interactions of the backbone with the subphase apparently hinder the folding of the monolayer into a triple layer.

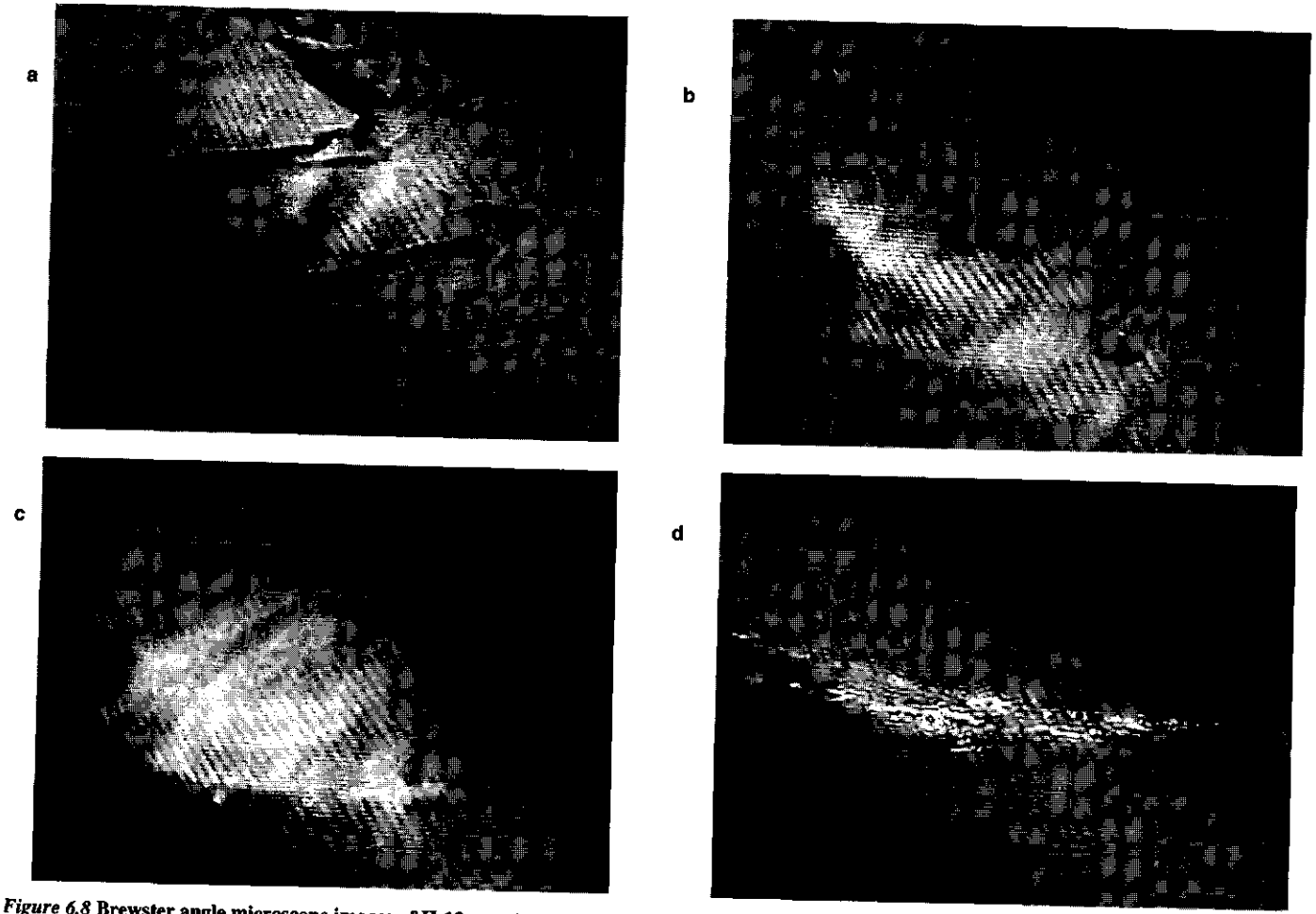

Figure 6.8 **Brewster angle microscope images of II-12 on a 1 mM $CuCl_2$ subphase at 0 (a), 6 (b), 50 (c) and 60 mN/m (d). Image size 594*920 μm^2.**

Use of copper as the double charged counterion results in the complete loss of triple layer formation for both **II-6** and **II-12**. Apparently, Cu^{2+} ions bind more strongly to the maleic acid moieties as compared to Mg^{2+}. Upon binding of Cu^{2+} to the polymers a neutral complex is formed from which the counterions are expelled. The counterion of Cu^{2+} thus has no effect on the π–A isotherms of **II-6** and **II-12**. Comparison of the lift-off areas for **II-6** and **II-12** on a Cu^{2+} subphase indicates the same conformation of both polymeric backbones on the subphase. For **II-12** however, at 40 mN/m a phase transition is observed. This could be the result of a liquid condensed to crystalline phase transition or might result from a conformational ordering of the chromophores. The increased spacer length for **II-12** as compared to **II-6** provides extra freedom for the chromophores to orient themselves at higher pressures.

In Figure 6.8 the BAM images of **II-12** on a $CuCl_2$ subphase are shown. Clearly the formation of islands at the interface directly after deposition can be seen. Upon increasing the surface pressure these islands merge forming a homogeneous monolayer. Above 40 mN/m the formation of some crystalline domains is observed (Figure 6.8c). Apparently, part of the monolayer crystallises at these high pressures. When the pressure exceeds 60 mN/m collapse of the layer is observed.

Surfactants In the search for stable and transferable polymeric monolayers the use of polyelectrolytes has only recently become of interest. Most research has focused on water-soluble polymers present in the subphase in order to stabilise oppositely charged monolayers composed of low-molecular weight compounds[35-38,39] or polymers.[40] The formation of tails and loops by the polymer backbone can only be controlled to a small extend in these systems and the interpretation of the resulting π-A isotherms is complicated. Additionally, the transfer of these monolayers is often difficult due to the tail and loop formation. By spreading the polyelectrolyte on a subphase containing low molecular weight amphiphilic compounds more unfolded states of the polyelectrolyte are reached in which loops and tails are almost completely avoided. The monolayer can be more accurately interpreted and transfer of the monolayer onto a substrate leads to better LB films. Michel and Nitsch[41] have used various polyelectrolytes and surfactants demonstrating that the formation of polyelectrolyte-surfactant complexes is not only governed by simple electrostatic interactions, but also by the compound specific adsorption equilibria and kinetics at the air-water interface.

In literature the addition of surfactants to a subphase is thus merely used to prepare more stable mono- and multilayers for various applications. The addition of surfactants to the subphase can also provide more information on the electrostatic and hydrophobic interactions between hydrophobically modified polyelectrolytes and surfactants. In studying this it is

important to have the polymer in its extended state implying the need to spread the polymer onto a surfactant containing subphase.[42]

When a 1 mM dodecyltrimethylammonium bromide (DTAB) subphase is used a large increase in lift-off area is observed. For **II-12** the lift-off area increases from 89 on pure water to 170 Å^2/repeating unit on the 1 mM DTAB subphase. For **II-6** an increase from 65 to 150 Å^2/repeating unit is observed.[43] The enormous increase in lift-off area is due to both electrostatic and hydrophobic interactions between DTAB and **II-n**. The hydrophobic tail of DTAB penetrates between the side chains of the polymers resulting in an increase in lift-off area. The reference compound without the hydrophobic tail, tetramethylammonium bromide, displays only weak interactions with the maleic acid units resulting in a slightly smaller molecular area for the repeating units. However, this interaction is strong enough to prevent the formation of a triple layer. The plateau in the π-A isotherm has disappeared and instead two transitions in the isotherm are observed which may be related to conformational changes of the polymer upon compression.

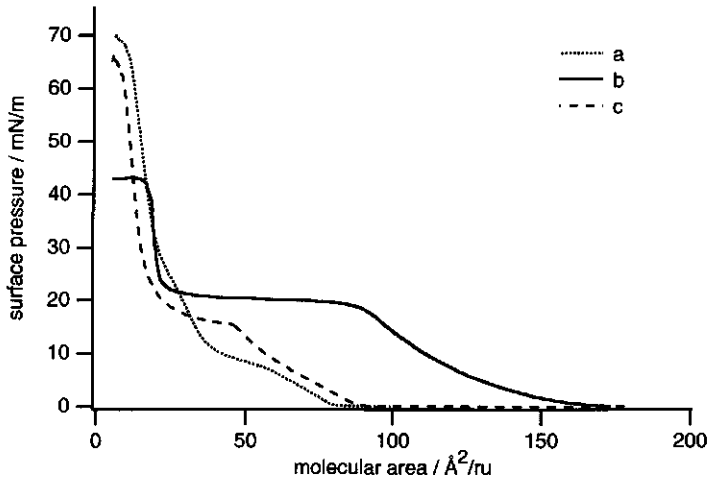

Figure 6.9 **Surface pressure-area isotherm of II-12 on 1 mM $N(CH_3)_4Br$ (a), 1 mM DTAB (b), and pure water (c).**

When polymers **II-n** are spread on a 1 mM DTAB solution a plateau is formed in the π-A isotherm. Again this is due to triple layer formation. The monolayer initially formed in the presence of DTAB is more stable than the one formed on pure water as is clear from the increased surface pressure in the plateau region. The triple layer is less stable as observed from the lowering of the collapse pressure as compared to pure water.

For maleic acid copolymers without the (cyanobiphenylyl)oxy moieties a similar increase in lift-off is observed in the π–A isotherms. For **C6 acid** and **C12 acid** the same lift-off areas are

observed in absence and presence of DTAB, 38 and 130 Å^2/ru respectively. DTAB also interacts with these polymers by electrostatic and hydrophobic interactions. The DTAB tails penetrate between the polymeric side chains increasing the molecular area.

Brewster angle microscopy of **II-6** on a 1 mM DTAB subphase shows the formation of a homogeneous monolayer just after spreading from DMSO/chloroform (Figure 6.10). Upon reducing the area available for **II-6** on pure water lines indicative for triple layer formation are observed in the plateau region. This is also found for this polymer on a subphase containing 1 mM of DTAB. The image also becomes blurred in the plateau region. The collapse of the triple layer clearly started on the lines, which can be imagined as relatively unstable regions in the otherwise uniform layers.

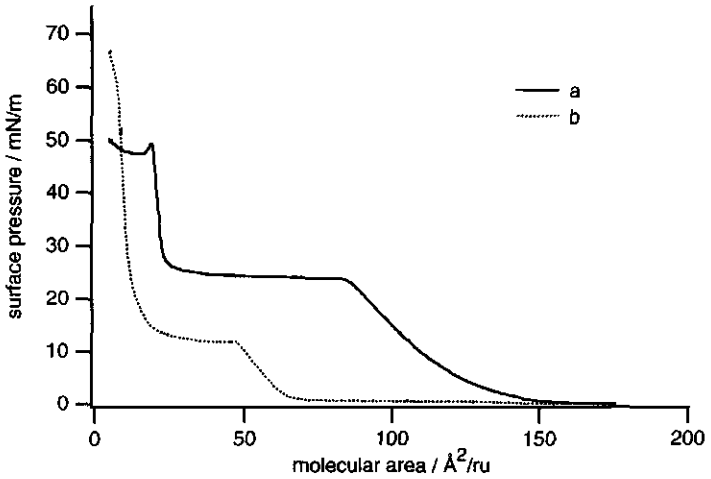

Figure 6.10 **Surface pressure-area isotherms of II-6 on 1 mM DTAB (a) and pure water (b).**

Besides the influence of a positively charged surfactant, the influence of a negatively charged surfactant was also investigated. The UV experiments described in Chapter 4 showed no interaction between polyelectrolytes **II-n** and the negatively charged sodium dodecyl sulfate (SDS). However, when polymers **II-6** and **II-12** are spread on a 1 mM SDS subphase an enormous increase in lift-off area is observed, and a slight tendency to form a triple layer is still apparent (Figure 6.12).

This shows that interaction between the polyelectrolytes **II-n** and a negatively charged surfactant at the interface occurs. In the UV measurements the polymers were dissolved in water and hydrophobic microdomains were formed with a negatively charged surface. Dodecyl sulfate ions do not interact with these microdomains because of electrostatic repulsion and the hydrophobic tails can not penetrate into the hydrophobic microdomains.

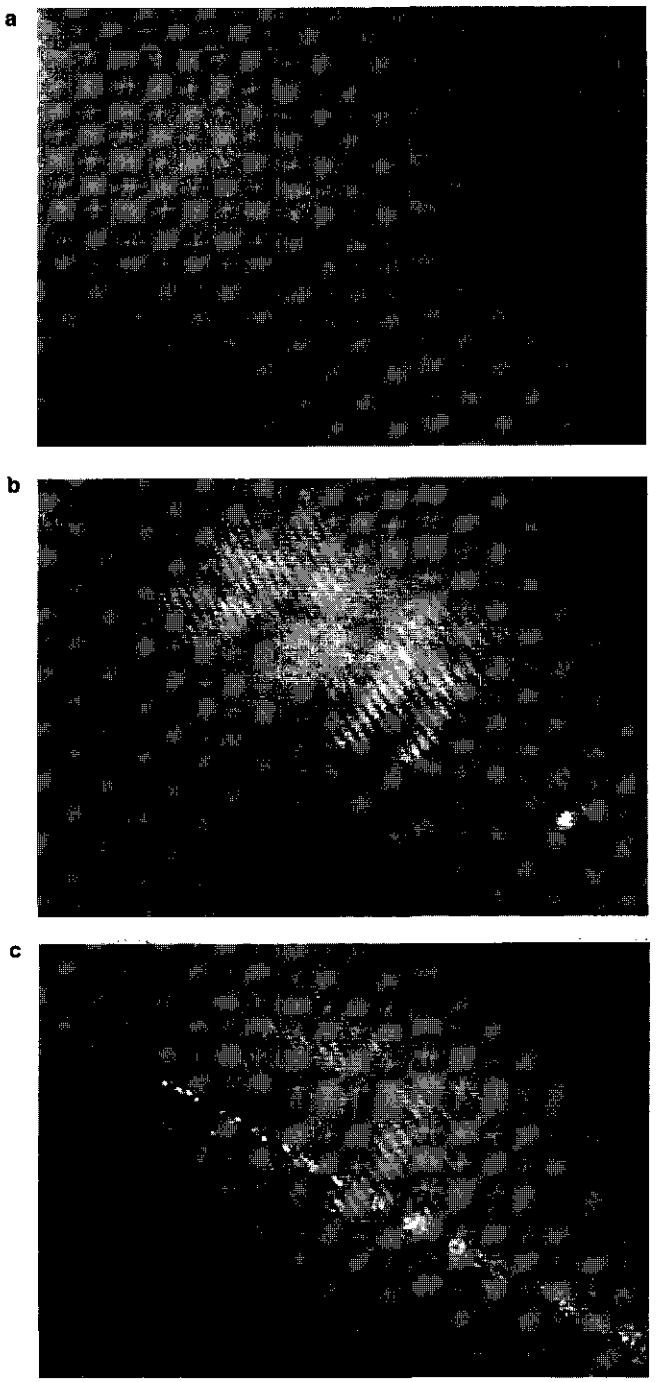

Figure 6.11 **Brewster angle microscope images of II-6 on a 1 mM DTAB subphase at 0 (a), 25 (b) and 50 mN/m (c). Image size 571 * 920 μm^2.**

When SDS is added to the subphase this surface active agent will partly accumulate at the surface. Although the carboxylic acid groups of **II-n** are not completely dissociated at the pH of the subphase (6.5), the acidic groups will tend to shy from the negative charges of the SDS molecules and the polymer will extend. At the same time the hydrophobic tails of SDS tend to aggregate with the hydrophobic side chains of the polymer increasing the molecular area per repeating unit necessary to accommodate the polymer.

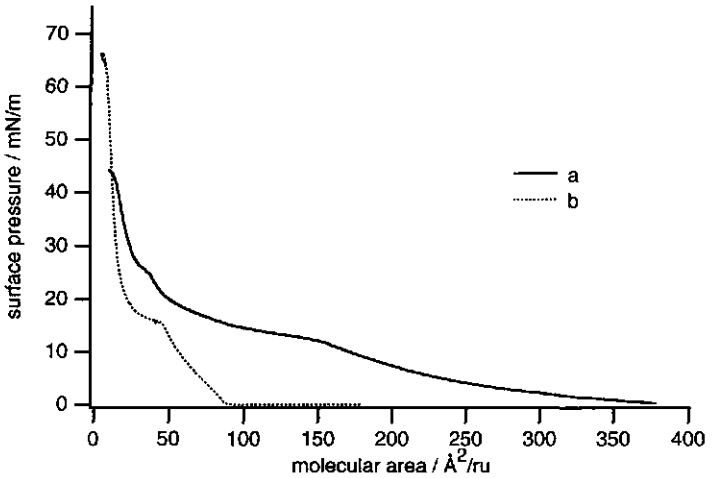

Figure 6.12 **Surface pressure-area isotherms of II-12 on 1 mM SDS (a) and pure water (b).**

6.2.4 Kinetics

The increase in lift-off area upon addition of DTAB to the subphase offers the opportunity to monitor the binding of DTAB to the polymer monolayer using a Langmuir trough. In such an experiment a stable polymeric monolayer is formed followed by the addition of DTAB using a microsyringe. The increase in surface area, due to the binding of DTAB to polymer, is monitored in time. The experimental set-up is shown in Figure 6.13. This type of experiment has also been used to study the binding of dyes to monolayers[44], the recognition properties of cyclodextrin monolayers[45] and binding of antibodies and proteins to lipids.[46]

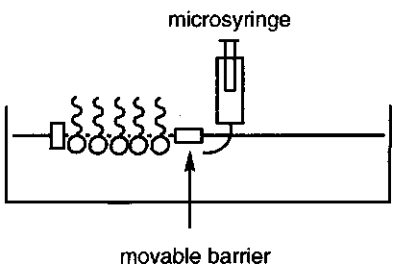

Figure 6.13 **Experimental set-up for measuring the binding of surfactant to polymer.**

A typical curve for the binding of DTAB to **II-12** is shown in Figure 6.14. It can be seen from the curve that the area per repeating unit is doubled, comparable to the molecular area of **II-12** on a DTAB subphase at 10 mN/m. A similar increase in area is observed for **II-6** at 5 mN/m. A tenfold excess of DTAB to the number of carboxylic acid groups is needed to start binding of DTAB to the monolayer. This means that DTAB has to be added at a concentration above the cmc, so micelles are injected underneath the monolayer. The DTAB micelles are added to a large volume of water and immediately break up after injection. Up to a fifty fold excess of DTAB the experiment can be performed, but at a higher excess of DTAB the area increase is too fast for the movement of the barrier. This can be seen from the increase in surface pressure above 10 mN/m when DTAB is present in a more than 50-fold excess. As the rate of area increase increases with the DTAB concentration diffusion of DTAB monomers to the monolayer is thought to be the main factor determining the rate of binding.

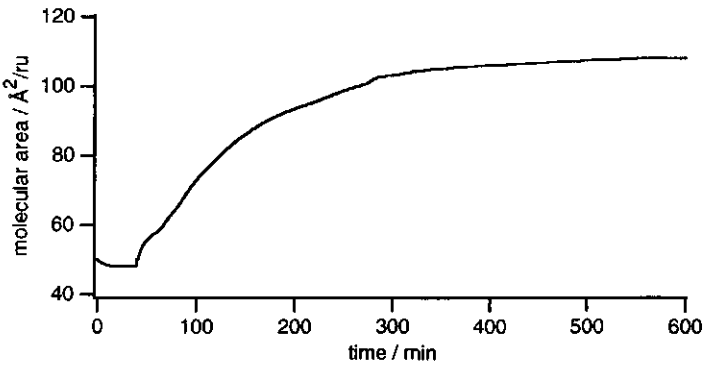

Figure 6.14 **Effect of the addition of DTAB to a monolayer of polymer II-12 at 10 mN/m.**

6.2.5 Monolayer transfer

A stable monolayer at the air-water interface is a prerequisite for obtaining Langmuir-Blodgett films. The monolayer stability of **II-6** at 10 mN/m was studied at 20 °C. Figure 6.15 shows the spontaneous area loss in the monolayer of **II-6** on pure water which occurs just after the start of the experiment. The monolayer becomes stable after about 40 minutes. The initial area reduction can be attributed to a reorganisation of the monolayer and is not due to collapse of the layer or dissolution of the polymer into the subphase. When the monolayer was stable, transfer onto hydrophilic quartz was started. The arrow indicates the start of the transfer cycles. Dipping was started downwards and no material was transferred onto the hydrophilic substrate. Upon receding the substrate monolayer material was transferred as indicated by the decrease in area. The barrier did not move during the waiting cycle prior to the subsequent dipping, which indicates a fast stabilisation of the monolayer after the substrate has been pulled out.

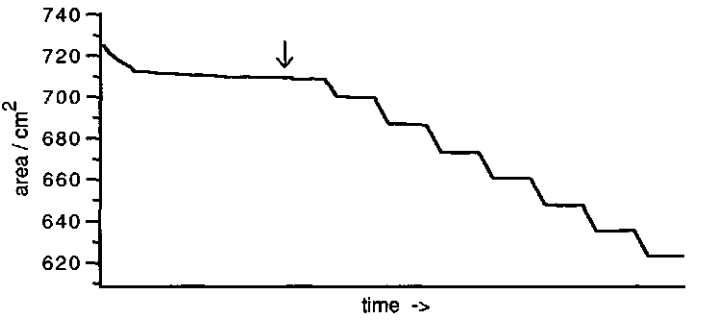

Figure 6.15 **Isobaric measurement of a II-6 monolayer at 10 mN/m and 20 °C. The arrow indicates the start of the transfer cycles.**

Material was only transferred on upward movement of the substrate indicating Z-type transfer. Z-type transfer onto hydrophilic quartz is also found for polymer **II-12**. Up to at least 40 layers could be deposited for this compound. The multilayer transferred onto quartz was studied by UV spectroscopy to obtain information on the ordering within the layers. For **II-12** the absorbance maximum of the deposited layers was 286 nm, a blue shift of about 10 nm as compared to the monomeric spectrum of a (cyanobiphenylyl)oxy moiety in THF (295 nm) or water (292 nm). According to the exciton model developed by Kasha[47,48], a blue shift of the absorption maximum in solution results from chromophore aggregation with the dipole moments along the long axes parallel to each other. The shift in absorption maximum observed for **II-12** indicates some chromophore aggregation, thus ordering, within the deposited layers. Furthermore, the shift was not dependent on the angle of the incoming UV light, indicating the same amount of ordering in all directions. The formation of small ordered domains in which the chromophores are ordered to some extent is assumed for **II-12**.

For **II-6** the absorption maximum was found around 294 nm, similar to the value found for the monomeric chromophores in solution. No chromophore aggregation is thus observed. For the multilayers of **II-6** a dependence of the maximum absorbance on the angle of the incoming UV light was observed. Possibly the chromophores have a preferred orientation with respect to the substrate.[27]

Stable monolayers of **II-6** and **II-12** could also be obtained on 1 mM $CuCl_2$ at 30 mN/m and on 1 mM of DTAB at 14 mN/m. Successful (Z-type) transfer was only obtained from DTAB. Transfer onto hydrophilic glass also gave Z-type transfer. Second harmonic generation (SHG) measurements were performed for multilayers of **II-6** and **II-12** which were transferred from pure water and from a subphase containing 1 mM of DTAB. Unfortunately, no or very small SHG signals were measured indicating that there is no non-centrosymmetric order within the transferred layers.[22]

Surface pressure-area isotherms can be obtained for **Cn anhydride, I-n, Cn acid** and **II-n** on various aqueous subphases. The lift-off areas of **I-11** and **I-12** suggest an orientation of the (cyanobiphenylyl)oxy chromophores with the cyano groups immersing into the subphase. For the polymers **I-n** with shorter side chains most of the chromophores are oriented into the air. Although π-A isotherms can be monitored for the maleic anhydride copolymers **I-n**, their sensitivity towards hydrolysis makes them useless for the preparation of stable monolayers and LB films.

Polymers **II-n** have a more flexible backbone which results in an almost flat orientation of the (cyanobiphenylyl)oxy chromophores of **II-11** and **II-12** on pure water. For the shorter spacers this orientation is hampered but the cyano groups are believed to be in contact with the subphase. Upon reducing the area available per repeating unit a plateau is formed in the π-A isotherms of **II-n** which indicates the formation of a triple layer by these polymers. This is confirmed by the semi-reversibility of the compression-expansion cycles of **II-6** and **II-12** and Brewster angle microscopy.

When Cu^{2+} ions are added to the subphase the triple layer formation is prevented by the strong complexation of Cu^{2+} with the maleic acid moieties. The addition of both cationic and anionic surfactant ions leads to an enormous increase in lift-off area due to electrostatic and hydrophobic interactions between the two species. The increase in lift-off area upon surfactant-polymer interaction is shown to be useful in studying the binding of surfactants to polymers.

At low pressure, the maleic acid polymers **II-n** form stable monolayers which can be transferred to hydrophilic substrates in a Z-type fashion. DTAB stabilises the monolayers of **II-n** and the formed complex can be transferred in a Z-type fashion. However, Second Harmonic Generation measurements show that there is no non-centrosymmetric order within the deposited layers.

6.4 Experimental

6.4.1 Materials

The synthesis and characterisation of the polymers has been described in chapters 2 and 3. Sodium dodecyl sulfate (Merck), $MgCl_2$ (Merck), $CuCl_2$ (Acros), $Cu(ClO_4)_2$ (Acros) and $N(CH_3)_4Br$ (Aldrich) were used as received. Dodecyltrimethylammonium bromide (Kodak) was recrystallised twice from ethanol.

6.4.2 Methods

The surface pressure-area isotherms were recorded on a Lauda FW2 Filmwaage, which was thermostatted at 20 °C. The water used for the subphase was purified by filtration through a Seralpur Pro C90 purification system. The polymers were spread from chloroform/DMSO solutions (85/15 v/v) (1 mg/ml) onto the aqueous subphase

by use of a Hamilton syringe. After spreading, the monolayer was allowed to equilibrate for 5 minutes before compression started. A compression rate of 20 cm^2/min was used.

Monolayers were transferred onto hydrophilic glass and quartz at a constant surface pressure of 10 mN/m for **II-6** and 10 or 14 mN/m for **II-12**. The vertical dipping rate was 3 mm/min. Before use the substrates were thoroughly cleaned by sonication in a DECON-soap solution for 15 min. After extensive rinsing with ultra pure water and ethanol, the substrates were dried by purging with a stream of nitrogen.

The Brewster angle microscope was home built. Technical details on the assembly of this microscope are published.[13]

The SHG measurements were performed according to Ashwell *et al.*[49] In their procedure the measured SHG signals are compared to the value of $1*10^{-4}$ found for a hemicyanine dye.

6.7 References

1 Kajiyama, T.; Oishi, Y.; Uchida, M.; Takashima, Y. *Langmuir* **1993**, *9*, 1978.
2 Tieke, B. *Adv. Mater.* **1991**, *3*, 532.
3 Embs, F.; Funhoff, D.; Laschewsky, A.; Licht, U.; Ohst, H.; Prass, W.; Ringsdorf, H.; Wegner, G.; Wehrmann, R. *Adv. Mater.* **1991**, *3*, 25.
4 Swalen, J. D.; Allara, D. L.; Andrade, J. D.; Chandross, E. A.; Garoff, S.; Israelachvili, J.; McCarthy, T. J.; Murray, R.; Pease, R. F.; Rabolt, J. F.; Wynne, K. J.; Yu, H. *Langmuir* **1987**, *3*, 932.
5 Petty, M. C.; Wood, S. *Int. Laboratory* **1997**, *27*, 8.
6 Noordegraaf, M. A.; Kuiper, G. J.; Marcelis, A. T. M.; Sudhölter, E. J. R. *Macromol. Chem. Phys.* **1997**, *198*, 3681.
7 Hodge, P.; Khoshdel, E.; Tredgold, R. H.; Vickers, A. J.; Winter, C. S. *Brit. Polym. J.* **1985**, *17*, 368.
8 Davis, F.; Hodge, P.; Towns, C. R.; Ali-Adib, Z. *Macromolecules* **1991**, *24*, 5695.
9 Tebbe, H.; Ackern, F. van; Tieke, B. *Macromol. Chem. Phys.* **1995**, *196*, 1475.
10 Clint, J. H. *Surfactant Aggregation*, Blackie: Glasgow and London; 1992, Ch. 3.
11 Oishi, Y.; Takashima, Y; Suehiro, K.; Kajiyama, T. *Langmuir* **1997**, *13*, 2527.
12 Everaars, M. D. *Ammonium Amphiphiles Carrying Mesogenic Units - Synthesis, Properties, Applications*, Ph. D. Thesis; Wageningen Agricultural University, 1997.
13 Cohen Stuart, M. A.; Wegh, R. A. J.; Kroon, J. M.; Sudhölter, E. J. R. *Langmuir* **1996**, *12*, 2863.
14 Mul, M. N. G. de; Mann Jr., J. A. *Langmuir* **1994**, *10*, 2311.
15 Popovitz-Biro, R.; Hill, K.; Shavit, E.; Hung, D. J.; Lahav, M.; Leiserowitz, L.; Sagiv, J.; Hsiung, H.; Meredith, G. R.; Vanherzeele, H. *J. Am. Chem. Soc.* **1990**, *112*, 2498.
16 Ashwell, G. J.; Jackson, P. D.; Crossland, W. A. *Nature* **1994**, *368*, 438.
17 Ledoux, I.; Josse, D.; Vidakovic, P.; Zyss, J.; Hann, R. A.; Gordon, P. F.; Bothwell, B. D.; Gupta, S. K.; Allen, S.; Robin, P.; Chastaing, E.; Dubois, J. C. *Europhys. Lett.* **1987**, *3*, 803.
18 Carr, N.; Goodwin, M. J.; McRoberts, A. M.; Gray, G. W.; Marsden, R.; Scrowstoon, R. M. *Makromol. Chem., Rapid Commun.* **1987**, *8*, 487.
19 Ringsdorf, H.; Schlarb, B.; Venzmer, J. *Angew. Chem.* **1988**, *27*, 113.
20 Senoh, T.; Sanui, K.; Ogata, N. *Chem. Lett.* **1990**, 1849.
21 Burland, D. M.; Miller, R. D.; Walsh, C. A. *Chem. Rev.* **1994**, *94*, 31.
22 Aktsipetrov, O. A.; Akhmediev, N. N.; Baranova, I. M.; Mishina, E. D.; Novak, V. R. *Sov. Phys. JEPT* **1985**, *62*, 524.
23 Davis, F.; Hodge, P.; Towns, C. R.; Ali-Adib, Z. *Macromolecules* **1991**, *24*, 5695.
24 Miyashita, T.; Suwa, T. *Thin Solid Films* **1996**, *284-285*, 330.
25 Calculated using data from Mul, M. N. G. de; Mann Jr., J. A. *Langmuir* **1994**, *10*, 2311.
26 Limiting molecular area for 4'-*n*-octyl-4-cyanobiphenyl on water is 47 $Å^2$. Taken from Xue, J.; Jung, C. S.; Kim, M. W. *Phys. Rev. Lett.* **1992**, *69*, 474.
27 This is also observed for surfactant molecules carrying two cyanobiphenyl chromophores via flexible spacers. Reference 12, Ch. 10; Everaars, M. D.; Marcelis, A. T. M.; Sudhölter, E. J. R. *Thin Solid Films* **1994**, *242*, 78.
28 Kang, Y. S.; Risbud, S.; Rabolt, J.; Stroeve, P. *Langmuir* **1996**, *12*, 4345.
29 Freshly prepared solutions of polymers **I-n** in DMSO/chloroform should be used because of hydrolyses of these polymers by the water present in DMSO.
30 Lee, B.-J.; Choi, G.; Kwon, Y.-S. *Thin Solid Films* **1996**, *284-285*, 564.

31 McFate, C.; Ward, D.; Olmsted III, J. *Langmuir* **1993**, *9*, 1036.
32 Biensan, C.; Desbat, B.; Turlet, J. M. *Thin Solid Films* **1996**, *284-285*, 293.
33 Schröter, J. A.; Plehnert, R.; Tschierske, C.; Katholy, S.; Janietz, D.; Penacorada, F.; Brehmer, L. *Langmuir* **1997**, *13*, 796.
34 The various subphases all had pH values between 5.3 and 6.1. In this range the pH is not expected to have an effect on the polymer conformation at the interface (see also 6.2.3).
35 Pugelli, M.; Gabrielli, G. *Colloid Polym. Sci.* **1983**, *261*, 82.
36 Shimomura, M.; Kunitake, T. *Thin Solid Films* **1985**, *132*, 243.
37 Chi, L. F.; Johnston, R. R.; Ringsdorf, H. *Langmuir* **1991**, *7*, 2323.
38 Tachibana, H.; Azumi, R.; Tanake, M.; Matsumoto, M.; Sako, S.; Sakai, H.; Abe, M.; Kondo, Y.; Yoshino, N. *Thin Solid Films* **1996**, *284-285*, 73.
39 Meijere, K. de; Brezesinski, G.; Möhwald, H. *Macromolecules* **1997**, *30*, 2337.
40 Lee, B.-L.; Kunitake, T. *Langmuir* **1994**, *10*, 557.
41 Michel, T.; Nitsch, W. *Thin Solid Films* **1994**, *242*, 234.
42 For polymers **II-n** this is experimentally also the only method which can be used because of the low solubility of the polymers in pure water.
43 For only DTAB no change in surface pressure could be monitored indicating that DTAB does not form a (stable) monolayer.
44 Okazaki, C.; Kuniyoshi, S.; Kudo, K.; Tanaka, K. *Jpn. J. Appl. Phys.* **1990**, *29*, 2506.
45 Tanaka, M.; Azumi, R.; Tachibana, H.; Nakamura, T.; Kawabata, Y.; Matsumoto, M.; Miyasaka, T.; Tagaki, W.; Nakahara, H.; Fukuda, K. *Thin Solid Films* **1994**, *244*, 832.
46 Ahlers, M.; Müller, .W.; Reichert, A.; Ringsdorf, H.; Venzmer, J. *Angew. Chem. Int. Ed. Engl.* **1990**, *29*, 1269.
47 McRae, E. G.; Kasha, M. *J. Chem. Phys.* **1958**, *28*, 721.
48 Kasha, M.; Rawls, H. R.; Ashraf El-Bayoumi, M. *Pure Appl. Chem.* **1965**, *11*, 371.
49 Ashwell, G. J.; Jefferies, G.; Hamilton, D. G.; Lynch, D. E.; Roberts, M. P. S.; Bahra, G. S.; Brown, C. R. *Nature* **1995**, *375*, 385.

Ion Pair Amphiphiles from Sodium Dodecyl Sulfate and Ammonium Amphiphiles Carrying Functionalised Azobenzene Units

Chapter 7

New ammonium amphiphiles having a N,N-dimethyl-N-hydroxyethylammonium headgroup and various azobenzene units connected by a decyl or dodecyl spacer have been synthesised. The azobenzene unit is functionalised at the 4'-position with a cyano, methoxy or fluoro substituent. For the cyano substituted amphotropes and the fluoro compound with a dodecyl spacer a smectic A phase is formed as was observed by polarisation microscopy and differential scanning calorimetry. Complexation with sodium dodecyl sulfate, SDS, in a 1:1 molar ratio induces the formation of smectic phases for the compounds with a decyl spacer. The compounds with a dodecyl spacer showed rather complex behaviour attributed to different crystal morphologies.

The ammonium amphotropes form aggregates in water when heated above their Krafft temperature. However, these aggregates are not stable and crystallise upon cooling. The ion pair amphiphiles with SDS form vesicles in water as observed by optical and electron microscopy. The observed blue shift in the UV absorption maximum of the amphotropes upon addition of SDS indicates π–π stacking between the azobenzene chromophores resulting from aggregation.

7.1 Introduction

Since the early 1980s a new class of compounds in which the structural features of amphiphiles and thermotropic liquid crystals are combined has become a focus of interest. These so-called amphotropes are composed of a polar headgroup, one or more hydrophobic tails and a mesogenic unit incorporated in the hydrophobic part. The mesogenic unit, usually consisting of a rigid aromatic group, has the capability to induce thermotropic liquid crystalline phases.[1] Lyotropic phases, caused by a polar headgroup in combination with one or more hydrophobic tails, are observed when these compounds are dispersed in water.

Kunitake *et al.*[2-9] were the first to study the lyotropic behaviour of single-chained amphotropes of the type head-spacer-mesogen-tail. The synthesis and physical properties of many amphotropic monomers and polymers have been investigated since then.[10,11] Differences in aggregate morphology are observed depending on both methylene spacer length and mesogenic unit.[12] Temperature dependent critical aggregation concentration (cac) measurements have shown that the aggregate stability is determined by hydrophobic interactions and additional favourable enthalpic interactions, which are attributed to mutual π–π stacking interactions between the mesogens in the aggregate. In comparison to stilbene and biphenyl mesogenic units azobenzene mesogens were found to have the strongest π–π stacking interaction and they form the most stable aggregates.[12]

A series of novel single-chained *N,N*-dimethyl-*N*-hydroxyethylammonium amphiphiles carrying functionalised azobenzene units connected to the headgroup via a variable methylene spacer is synthesised. The thermotropic phase behaviour is studied by optical microscopy and differential scanning calorimetry. Critical aggregation concentrations in water have been measured, and the aggregate morphology is studied.

Finally, ion pair amphiphiles (IPA's) were prepared from the ammonium amphotropes with sodium dodecyl sulfate (SDS) as the second component. The ionic coupling of an amphotrope to an oppositely charged amphiphile often results in the formation or stabilisation of a liquid crystalline phase.[13] Furthermore, ion pair amphiphiles have been proposed as interesting materials for both theoretical investigations and practical device applications.[13,14] The thermotropic and lyotropic behaviour of the ion pair amphiphiles was investigated by differential scanning calorimetry, optical and electron microscopy, and UV spectroscopy.

7.2 Results and Discussion

7.2.1 Ammonium amphotropes

The synthesis of the compounds is outlined in Scheme 7.1. *N,N*-dimethyl-*N*-hydroxyethyl-ammonium was chosen as headgroup because, by lowering the Krafft temperature, it better

stabilises aqueous dispersions of amphiphiles as compared to a trimethylammonium headgroup.[5] The composition and purity of the compounds was checked by 200 MHz ^{1}H-NMR, thin layer chromatography and elemental analyses.

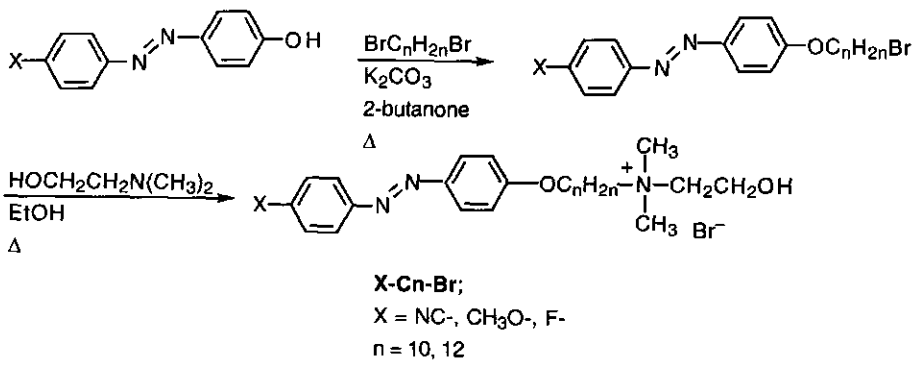

X-Cn-Br;
X = NC-, CH_3O-, F-
n = 10, 12

Scheme 7.1 **Synthetic pathway to the amphotropes.**

The thermal behaviour of the compounds was studied by differential scanning calorimetry (DSC) and polarisation microscopy. Both techniques displayed the same phase transition temperatures. Phase transition temperatures and enthalpies, taken from the second heating scans, are given in Table 7.1.

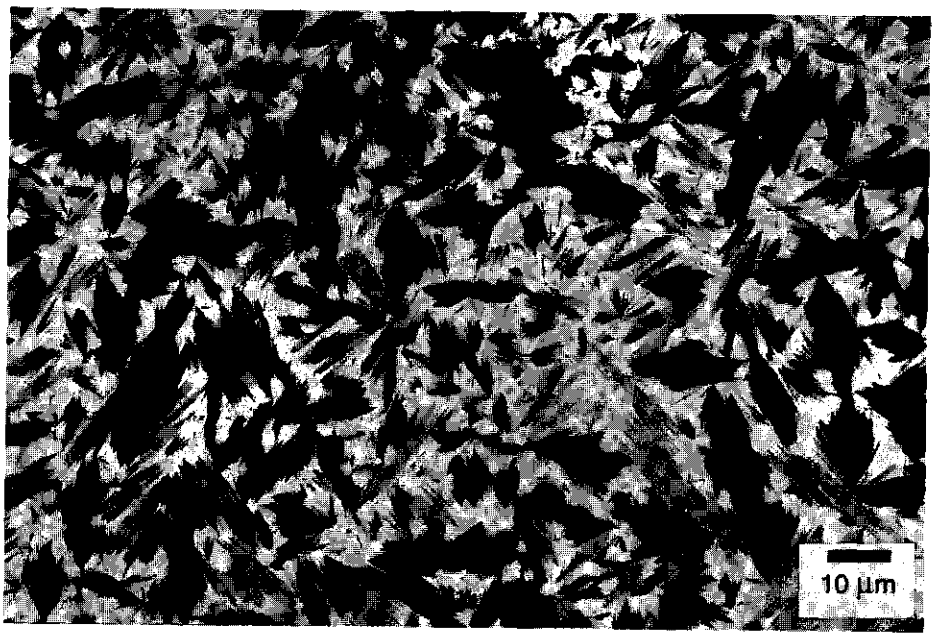

Figure 7.1 **Texture of the smectic A phase of CN-C12-Br as viewed between crossed polarizers.**

For compounds **F-C12-Br**, **CN-C10-Br** and **CN-C12-Br** a fan-shaped focal-conic texture typical of a smectic A phase is found (Figure 7.1). In addition, regions of homeotropic texture are observed, which indicate that the director is oriented perpendicular to the glass slides. The tendency of ionically functionalised liquid crystals to align perpendicularly to the substrate has already been observed by other research groups.[15,16]

The homeotropic alignment can be disrupted by shearing the sample between the two glass slides. No liquid crystalline phases are observed for **F-C10-Br**, **MeO-C10-Br** and **MeO-C12-Br**. For these compounds different crystal morphologies, exhibiting different crystal-crystal transitions and melting temperatures, are observed.

Table 7.1 **Phase transition temperatures (°C) and corresponding enthalpy changes (ΔH in kJ/mol) taken from the second heating scans of compounds X-Cn-Br.**

compound	transition temperature [a]	ΔH
F-C10-Br	159 (C_1 - C_2)	21.6
	180 (C_2 - I)	21.2
F-C12-Br	170 (C_1 - S_A)	40.2
	186 (S_A - I)	4.1
CN-C10-Br	145 (C_1 - S_A)	34.1
	201 (S_A - I)	4.4
CN-C12-Br	147 (C_1 - S_A)	35.1
	194 (S_A - I)	4.4
MeO-C10-Br	149 (C_1 - C_2)	16.0
	196 (C_2 - I)	24.7
MeO-C12-Br	169 (C_1 - C_2)	18.7
	192 (C_2 - I)	13.2
	197 (C_3 - I)	8.4

a) C_1, C_2, C_3 are different crystal morphologies having different melting temperatures [11], S_A is smectic A, I is isotropic.

The dipole moment of the azobenzene mesogen, which is varied by use of different terminal units, displays a large influence on the thermotropic phase behaviour of **X-Cn-Br**. The alkoxy spacer at the 4-position of the mesogen is an electron donating group. An electron withdrawing substituent, like cyano, at the 4'-position gives rise to a mesogen with a large overall dipole moment. Surfactants carrying this mesogen form ordered smectic A phases which is ascribed to the tendency of mesogens with a high dipole moment to form antiparallel dimers due to favourable dipolar interactions.[1,17,18]

MeO-Cn-Br has no overall dipole moment, which hampers the formation of liquid crystalline phases. For **F-Cn-Br** the thermotropic behaviour depends on the spacer length. For **F-C12-Br**

a smectic A phase is formed. The dodecyl spacer apparently allows the fluoroazobenzoxy mesogens to organise, whereas the decyl spacer is too short and interferes with the organisation of the mesogens.

7.2.2 Ion Pair Amphiphiles

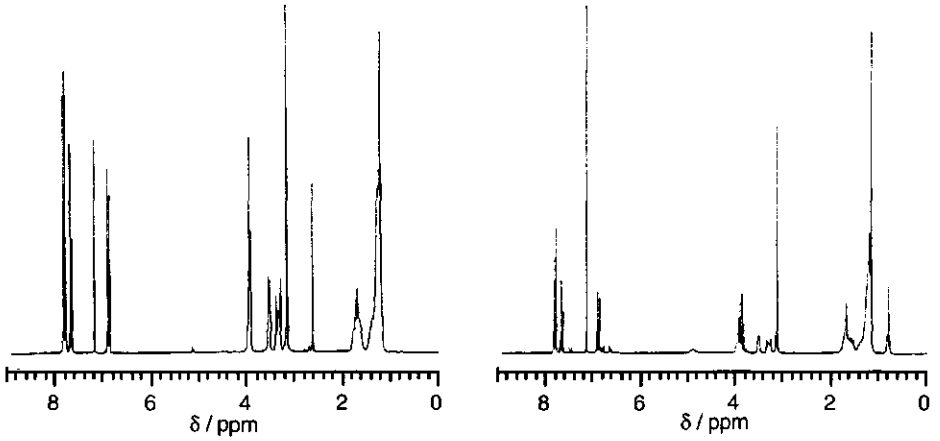

Figure 7.2 **^{1}H NMR spectra of CN-C_{12}-Br (left) and CN-C_{12}-DS (right).**

Solid complexes of the ammonium amphotropes and SDS were prepared by mixing equimolar solutions of both components in dichloromethane followed by extraction with water to remove the sodium and bromide counterions. The formation of 1:1 complexes was confirmed by ^{1}H NMR by determination of the ratio of the methyl protons of the ammonium headgroup at 3.2 ppm to the protons of the terminal methyl group of the SDS hydrophobic tail at 0.9 ppm (Figure 7.2).

The thermotropic phase behaviour of the ion pair amphiphiles was investigated by DSC and polarisation microscopy. It was found that the melting temperatures are lowered as compared to the noncomplexed amphotropes (see Table 7.2).

The crystal packing of the ammonium amphotropes is disturbed by the dodecyl sulfate ions (DS^-) resulting in the lowering of the melting temperatures. The DS^- ions also cause the dilution of the mesogens in the sample, thus lowering the isotropisation temperature. There is a delicate balance between these two effects on the thermotropic behaviour of the ammonium amphotropes. For all **X-C10$^+$** complexes with DS^- as counterion smectic A phases are observed. Changing the counterion from Br^- to DS^- induces the formation of S_A phases in both **F-C10-DS** and **MeO-C10-DS**. The melting temperatures of these compounds are lowered more relative to the isotropisation temperature resulting in the formation of mesophases. The mesophase of **CN-C10-DS** is destabilised as compared to the pure

amphotrope. This is clear from the smaller temperature range where the smectic phase is observed. Like for **CN-C10-DS**, a smaller smectic range is observed for **CN-C12-DS**, but the presence of different crystal morphologies makes the data interpretation difficult. Different crystal morphologies are also observed for **F-C12-DS** and **MeO-C12-DS**. The same transitions are observed in both the first and second heating scans.

Table 7.2 **Phase transition temperatures (°C) and corresponding enthalpy changes (ΔH in kJ/mol) taken from the second heating scans of the complexes X-Cn-DS.**

compound	transition temperature [a]	ΔH
F-C10-DS	56 (C_1 - C_2)	3.1
	63 (C_2 - C_3)	3.2
	90 (C_3 - S_A)	31.7
	108 (S_A - I)	2.4
F-C12-DS	92 (C_1 - S_A)	15.1
	117 (S_A - I)	27.2
	130 (C_2 - I)	1.5
CN-C10-DS	103 (C_1 - S_A)	38.4
	114 (S_A - I)	1.8
CN-C12-DS	120 (C_1 - S_A)	23.2
	123 (S_A - I)	1.1
	130 (C_2 - I)	16.2
MeO-C10-DS	80 (C_1 - S_A)	26.4
	124 (S_A - I)	5.2
MeO-C12-DS [b]	128 (C_1 - I)	7.7

a) C_1, C_2, C_3 are different crystal morphologies having different melting temperatures [11], S_A is smectic A, I is isotropic.
b) Complicated thermotropic behaviour probably due to different crystal morphologies of the sample.

7.2.3 Amphotrope aggregation in aqueous solution

All amphotropes are insoluble in water at room temperature. Krafft temperatures, *i.e.* the temperature where the solubility equals the critical aggregation concentration (cac), were determined by heating of an aqueous amphotrope dispersion and inspection by optical microscopy. The temperature where the hydrated crystals melt is taken as the Krafft temperature.

Thermal transition temperatures of aqueous dispersions of the amphotropes as determined by DSC, agree well with the values found by optical microscopy. Results are given in Table 7.3. For the compounds with a dodecyl spacer the Krafft temperatures are higher than for those with the shorter decyl spacers. Similar results have been reported in literature.[19] The Krafft

temperature increases upon going from the cyano to the methoxy to the fluoro substituted compounds. The solubility of the amphotropes is influenced by the headgroup. For *N*-(ω-(cyanoazobenzoxy)alkyl)-*N,N,N*-trimethylammonium bromides Krafft temperatures of 47 and 67 °C are found for the decyl and the dodecyl compound respectively.[20] For **CN-C10-Br** the hydrated crystals melt at 51 °C, so at a slightly higher temperature as compared to the trimethylammonium amphotrope. For **CN-C12-Br** the Krafft temperature is lowered by 11 °C as compared to the amphotrope with a trimethylammonium headgroup. The hydroxyethyl group apparently makes the surfactant more hydrophilic thus facilitating the dissolution in water.

Table 7.3 **Krafft temperatures (°C)[a] and critical aggregation concentrations (M) for X-Cn-Br at 50 °C in water.**

compound	T_{Krafft}	cac
F-C10-Br	60	$1.0 * 10^{-3}$
CN-C10-Br	51	$1.4 * 10^{-3}$
MeO-C10-Br	53	$1.0 * 10^{-3}$
F-C12-Br	71	$1.6 * 10^{-4}$
CN-C12-Br	56	$3.9 * 10^{-4}$
MeO-C12-Br	61	$1.5 * 10^{-4}$

a) Determined by optical microscopy.

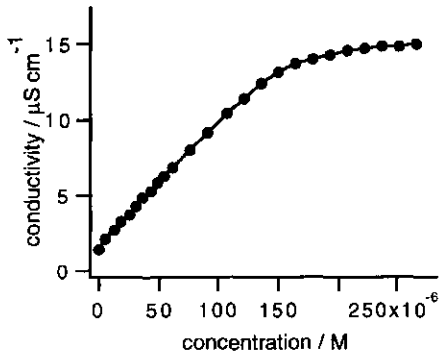

Figure 7.3 **Determination of the cac of MeO-C12-Br by measuring the electrical conductivity of an aqueous solution versus the MeO-C12-Br concentration.**

The critical aggregation concentrations have been determined by conductivity measurements at 50 °C (Figure 7.3). At this temperature the concentrated amphotrope solutions are stable for the duration of the experiment. Results are shown in Table 7.3.

The amphiphiles carrying the longer alkyl chain show a lower cac. This is usually observed for amphiphiles in a homologous series. The 4'-cyanoazobenzoxy containing amphotropes exhibit a higher cac than the other compounds. This can be attributed to their more polar substituent, making them more soluble in water as compared to amphotropes substituted with a methoxy or fluoro group.

To discriminate between the formation of spherical micelles and larger aggregates like rod-like micelles and vesicles ^{1}H NMR line broadening experiments were performed for all amphotropes. Motions of spherical micelles in solution are isotropic on the ^{1}H NMR time scale. In contrast, the motions of the much larger rod-like micelles or vesicles are slower and anisotropic. The line widths at peak half-height of all C-H resonances of surfactants aggregated in rod-like micelles are broad as compared to those of spherical micelles. For octylammonium chloride an increase in line width of 5 Hz is reported upon forming rod-like micelles whereas dodecylammonium chloride shows an increase of 35 Hz.[21,22] For the alkyl chain protons of **X-Cn-Br** the line widths at half height above the cac increased between 15 and 35 Hz as compared to the monomers (Figure 7.4). This indicates that the amphotropes do not form spherical micelles at the cac, but higher ordered aggregates like rod-like micelles or vesicles.[21,22]

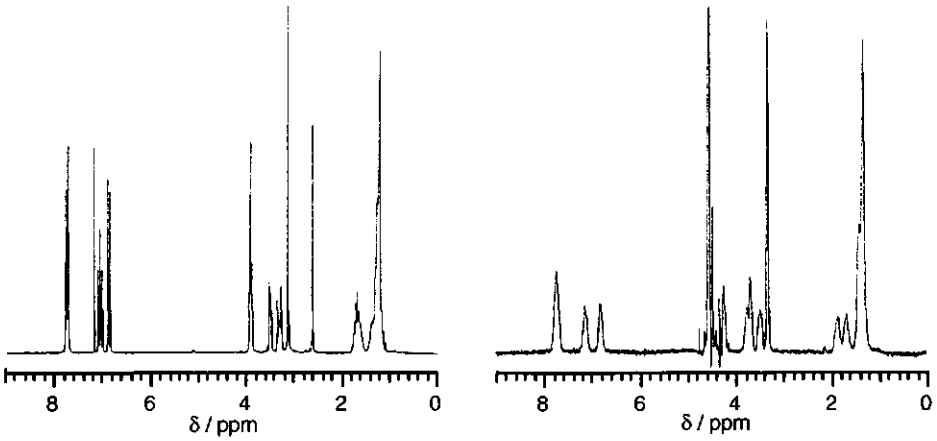

Figure 7.4 **200 MHz ^{1}H NMR spectra of F-C12-Br as monomers in $CDCl_3$ /CD_3OD at 25 °C (left) and above the cac in D_2O at 70 °C (right).**

Optical microscopy of the solid amphotropes in contact with water shows the formation of myelin structures upon heating. At 70 °C the formation of giant vesicles is observed for compounds **CN-Cn-Br** and **MeO-Cn-Br**.[5,23] These vesicle solutions are not stable and crystallise upon cooling. Sonication does not increase the vesicle stability.

The transition temperatures of sonicated 1% (w/w) amphotrope solutions in water, as determined by DSC, correspond to the crystal to aggregate transitions. These transition temperatures correspond to the Krafft temperatures as observed by optical microscopy. Although **F-Cn-Br** also forms myelin structures, no giant vesicles of these compounds are observed by optical microscopy.

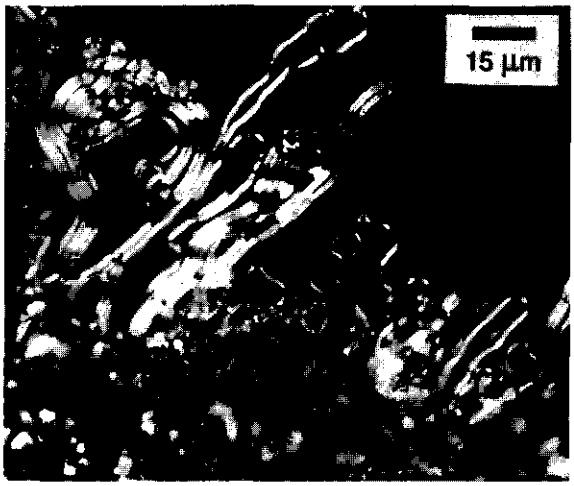

Figure 7.5 **Myelin formation of CN-C10-Br upon heating to 53 °C as viewed under the optical microscope.**

7.2.4 Formation of ion pair amphiphiles in aqueous solution

Several studies have been performed on IPA's in aqueous solution, *e.g.* IPA's of alkyltrimethylammonium bromides with sodium dodecyl sulfate or fatty acids.[17,24-28] Some single-chained amphotropes were reported to form ion pair amphiphiles which formed giant vesicles as was observed by light microscopy.[12]

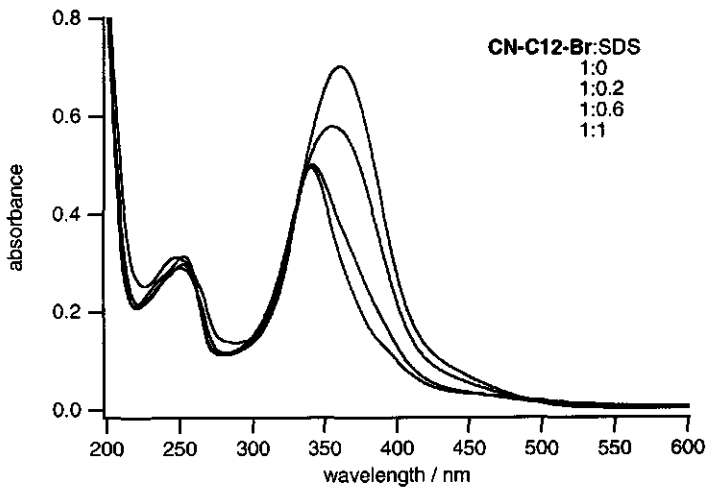

Figure 7.6 **UV absorption spectra of an aqueous solution of CN-C12-Br upon addition of SDS at 25 °C. [CN-C12-Br] = 3.2 * 10^{-6} M.**

The formation of ion pair amphiphiles of the synthesised ammonium amphotropes with SDS has been investigated by UV spectroscopy. Figure 7.6 displays the spectral changes observed upon addition of SDS to an aqueous solution of **CN-C12-Br**.

At UV concentrations no surfactant aggregates are present in water. The spectrum of **CN-C12-Br** without SDS thus shows the monomerically dispersed compound with an absorption maximum at 360 nm. Upon addition of SDS a shift of the absorption maximum to lower wavelength accompanied with a decrease in absorbance is observed. This blue shift indicates the formation of ordered structures in which the azobenzene units have favourable mutual π–π stacking interactions. According to the molecular exciton model of McRae and Kasha, the blue shift of the absorption maximum is indicative of linear chromophore aggregation in which the transition dipole moments are parallel to each other and ordered perpendicular to the stacking direction (the so-called H-aggregate).[30]

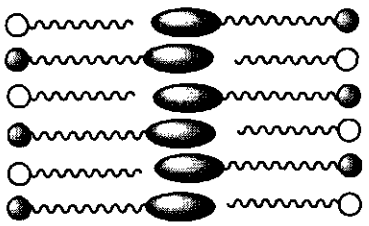

Figure 7.7 **Proposed structure of the bilayer complexes of Ion Pair Amphiphiles.**

The maximum blue shift is observed at an amphotrope:SDS molar ratio of 1:1. The ion pair amphiphiles probably form bilayer aggregates in which the ammonium and sulfate headgroups alternate. This is schematically shown in Figure 7.7. The packing of the mesogenic units is presumably antiparallel in this aggregate and gives rise to strong π–π stacking interactions in the bilayer. The absorption maxima of the monomeric ammonium amphotropes in water and of their IPA's with SDS are given in Table 7.4.

Table 7.4 **Absorption maxima (in nm) for the aqueous solutions of X-Cn-Br and their ion pair complexes with SDS at a molar ratio of 1:1.**

compound	monomer	IPA
F-C10-Br	349	327
CN-C10-Br	361	335
MeO-C10-Br	360	337
F-C12-Br	347	317
CN-C12-Br	360	340
MeO-C12-Br	358	333

Upon standing for 48 hours the UV spectra of solutions of the 1:1 complexes of all compounds with SDS show an increase in light scattering which is indicative for the onset of precipitation. Upon increasing the amount of SDS, at SDS concentrations below its cmc, a

small decrease in blue shift (2-4 nm) is observed for all mixed vesicles. This is due to the dissolution of the extra SDS molecules in the vesicles causing a small loss in chromophore stacking. At SDS concentrations far above its cmc, at ratio's of amphotrope:SDS up to 1:200, differences in behaviour between the ammonium amphotropes are observed. The aggregates of SDS with surfactants with a dodecyl spacer and **MeO-C10-Br** show a negligible decrease in the blue shift at these high SDS concentrations. The aggregates are rather stable and hardly dissolve in the SDS micelles.

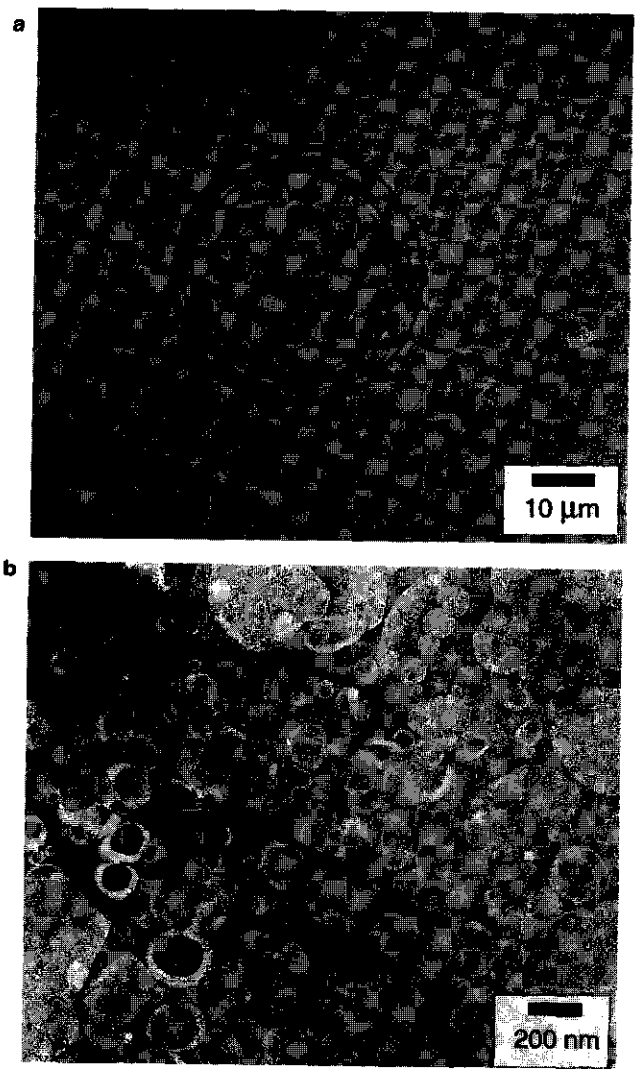

Figure 7.8 **(a) Optical micrograph of the giant vesicles formed upon heating of MeO-C12-Br in a SDS solution. (b) Electron micrograph of vesicles of a sonicated MeO-C12-Br-SDS mixture.**

IPA's from mesogen carrying alkyltrimethylammonium amphotropes with SDS also form stable aggregates which do not dissolve in the SDS micelles formed at high SDS concentrations.[12] The **F-C10-Br**-SDS vesicles show an absorption maximum at 337 nm at high SDS concentrations. The **F-C10-Br**-SDS vesicles partially dissolve in the SDS micelles resulting in a partial loss in stacking interactions between the chromophores and a smaller blue shift as compared to the IPA. The UV spectrum of the **CN-C10-Br**-SDS vesicle solution displays the monomerically dispersed cyanoazobenzoxy chromophores upon increasing the amount of SDS, due to the dissolution of the mixed vesicles in the SDS micelles. Probably the cac of **CN-C10-Br**-SDS is higher than the cac's of the other IPA's. This results in the destabilisation of the formed aggregates as compared to the aggregates formed from the other IPA's, resulting in the breakdown of the **CN-C10-Br**-SDS vesicles.

When crystals of the ammonium amphotropes are hydrated in an SDS solution at 70 °C the formation of giant vesicles is observed by optical microscopy. In the absence of SDS the ammonium amphotropes also form giant vesicles but these are less stable. The giant vesicles formed by **MeO-C12-Br** in an aqueous SDS solution are shown in Figure 7.8a. The electron micrograph of a sonicated 1:1 complex of **MeO-C12-Br** and SDS shows the presence of small vesicles (Figure 7.8b).

The sonicated 1% (w/w) solutions of **CN-C10-Br**, **CN-C12-Br**, **MeO-C10-Br** and **MeO-C12-Br** with SDS (in a 1:1 molar ratio) are stable for at least 24 hours. Vesicles consisting of double chained amphiphiles and biological bilayers have a gel-to-liquid crystalline phase transition (T_c) due to the melting of the hydrophobic chains in the inner part of the bilayer. We tried to measure a gel-to-liquid crystalline phase transition for the IPA vesicles by DSC. However, no T_c's are observed between 0 and 70 °C. The transition temperatures may lie outside the measured range or maybe the amount of ordering in the gel phase is too low. It has been suggested before that a phase transition is only observed by DSC when the difference in ordering between the two phases is large.[29]

Aggregates formed from **F-Cn-Br**-SDS upon sonication were less stable than the ones formed by **CN-Cn-Br** and **MeO-Cn-Br** as indicated by the fast precipitation after preparation. DSC of these sonicated **F-Cn-Br**-SDS solutions show transition temperatures below the Krafft temperatures of the pure **F-Cn-Br** amphiphiles. The complexation with SDS probably enhances the solubilisation of the ammonium amphiphiles and thus a lowering of the Krafft temperatures is observed.

7.3 Conclusions

A series of novel ammonium amphotropes has been synthesised and their thermotropic and lyotropic behaviour was investigated. Compounds **CN-C10-Br**, **CN-C12-Br** and **F-C12-Br**

display a smectic A liquid crystalline phase. Upon complexation with SDS the melting and isotropisation temperatures of all compounds are lowered and smectic A phases are observed for **F-C10-DS**, **CN-C10-DS**, **MeO-C10-DS**, **F-C12-DS** and **CN-C12-DS**. The highest critical aggregation concentrations are found for the most hydrophilic compounds, **CN-Cn-Br**. By optical microscopy the formation of myelin structures for all amphotropes is observed upon heating with water. Subsequently, giant vesicles are formed from **CN-C10-Br**, **MeO-C10-Br**, **CN-C12-Br** and **MeO-C12-Br**. These vesicles are not stable and at room temperature crystallisation occurs.

Giant vesicles are also observed upon heating solid samples in the presence of aqueous SDS. Excess of SDS completely solubilises the **CN-C10-Br**-SDS mixed vesicles, whereas for **F-C10-Br**-SDS partial dissolution of the mixed vesicles into the SDS micelles is observed. For **MeO-C10-Br**-SDS, **CN-C12-Br**-SDS, **MeO-C12-Br**-SDS and **F-C12-Br**-SDS negligible dissolution is observed. These vesicles are found to be rather stable. Stacking of the mesogenic units in the mixed vesicles into H-type aggregates is clearly demonstrated by the observed blue shift in the optical absorption spectrum.

7.4 Experimental

7.4.1 Materials

Sodium dodecyl sulfate (Merck) and *N,N*-dimethylethanolamine (Aldrich) were used as obtained.

4'-Cyano-4-hydroxyazobenzene, 4'-fluoro-4-hydroxyazobenzene and 4-hydroxy-4'-methoxyazobenzene were prepared by reaction of the diazonium salts of 4-aminobenzonitril, 4-fluoroaniline and 4-methoxyaniline with phenol.[31] The 1-bromo-ω-(substituted azobenzoxy)alkanes were prepared as described before.[12]

***N*-(ω-(Substituted azobenzoxy)alkyl)-*N,N*-dimethyl-*N*-hydroxyethylammonium bromide (X-Cn-Br)**

A solution of 3.4 mmol of the appropriate bromide in 35 mL of ethanol and 10 mmol of N,N-dimethylethanolamine was refluxed for 24 hours. The precipitate was filtered off and washed thoroughly with diethylether. The yields varied from 86 to 97 %.

F-C10-Br: ^{1}H NMR ($CDCl_3/CD_3OD$, TMS, δ, ppm): 1.2-1.5 (m, 12 H, $(CH_2)_6$), 1.7 (m, 4 H, CH_2CH_2O and CH_2CH_2N), 3.2 (s, 6 H, $N(CH_3)_2$), 3.4 (m, 2 H, NCH_2), 3.6 (m, 2 H, NCH_2CH_2OH), 4.0 (t, 4 H, 2 OCH_2), 6.9 (d, 2 H, *o* to alkoxy), 7.1 (dd, 2 H, *o* to fluoro), 7.8 (m, 4 H, *o* to azo). Anal. Calcd for $C_{26}H_{39}BrFN_3O_2$ (M_W 524.51): C 59.53, H 7.49, N 8.01. Found: C 59.41, H 7.41, N 8.01.

CN-C10-Br: ^{1}H NMR ($CDCl_3/CD_3OD$, TMS, δ, ppm): 1.2-1.5 (m, 12 H, $(CH_2)_6$), 1.8 (m, 4 H, CH_2CH_2O and CH_2CH_2N), 3.2 (s, 6 H, $N(CH_3)_2$), 3.4 (m, 2 H, NCH_2), 3.6 (m, 2 H, NCH_2CH_2OH), 4.0 (t, 4 H, 2 OCH_2), 7.0 (d, 2 H, *o* to alkoxy), 7.7 (d, 2 H, *o* to cyano), 7.9 (d, 4 H, *o* to azo). Anal. Calcd for $C_{27}H_{39}BrN_4O_2$ (M_W 531.53): C 61.01, H 7.40, N 10.54. Found: C 60.86, H 7.49, N 10.56.

MeO-C10-Br: ^{1}H NMR ($CDCl_3/CD_3OD$, TMS, δ, ppm): 1.2-1.5 (m, 12 H, $(CH_2)_6$), 1.7 (m, 4 H, CH_2CH_2O and CH_2CH_2N), 3.2 (s, 6 H, $N(CH_3)_2$), 3.4 (m, 2 H, NCH_2), 3.6 (m, 2 H, NCH_2CH_2OH), 3.8 (s, 3 H, CH_3O), 4.0 (t, 4 H, 2 OCH_2), 7.0 (dd, 4 H, *o* to alkoxy), 7.8 (dd, 4 H, *o* to azo). Anal. Calcd for $C_{27}H_{42}BrN_3O_3$ (M_W 536.55): C 60.44, H 7.89, N 7.83. Found: C 60.28, H 7.95, N 7.81.

F-C12-Br: ^{1}H NMR ($CDCl_3/CD_3OD$, TMS, δ, ppm): 1.2-1.5 (m, 16 H, $(CH_2)_8$), 1.7 (m, 4 H, CH_2CH_2O and CH_2CH_2N), 3.2 (s, 6 H, $N(CH_3)_2$), 3.4 (m, 2 H, NCH_2), 3.6 (m, 2 H, NCH_2CH_2OH), 4.0 (t, 4 H, 2 OCH_2), 6.9 (d, 2 H, *o* to alkoxy), 7.1 (dd, 2 H, *o* to fluoro), 7.8 (m, 4 H, *o* to azo). Anal. Calcd for $C_{28}H_{43}BrFN_3O_2$ (M_w 552.56): C 60.86, H 7.84, N 7.61. Found: C 60.72, H 7.94, N 7.61.

CN-C12-Br: ^{1}H NMR ($CDCl_3/CD_3OD$, TMS, δ, ppm): 1.2-1.5 (m, 16 H, $(CH_2)_8$), 1.7 (m, 4 H, CH_2CH_2O and CH_2CH_2N), 3.2 (s, 6 H, $N(CH_3)_2$), 3.4 (m, 2 H, NCH_2), 3.6 (m, 2 H, NCH_2CH_2OH), 4.0 (t, 4 H, 2 OCH_2), 7.0 (d, 2 H, *o* to alkoxy), 7.8 (d, 2 H, *o* to cyano), 7.9 (d, 4 H, *o* to azo). Anal. Calcd for $C_{29}H_{43}BrN_4O_2$ (M_w 559.58): C 62.24, H 7.75, N 10.01. Found: C 62.09, H 7.82, N 10.00.

MeO-C12-Br: ^{1}H NMR ($CDCl_3/CD_3OD$, TMS, δ, ppm): 1.2-1.5 (m, 16 H, $(CH_2)_8$), 1.7 (m, 4 H, CH_2CH_2O and CH_2CH_2N), 3.2 (s, 6 H, $N(CH_3)_2$), 3.4 (m, 2 H, NCH_2), 3.6 (m, 2 H, NCH_2CH_2OH), 3.8 (s, 3 H, CH_3O), 4.0 (t, 4 H, 2 OCH_2), 7.0 (dd, 4 H, *o* to alkoxy), 7.8 (dd, 4 H, *o* to azo). Anal. Calcd for $C_{29}H_{46}BrN_3O_3$ (M_w 564.60): C 61.69, H 8.21, N 7.44. Found: C 61.50, H 8.24, N 7.38.

X-Cn-DS complexes were prepared by mixing equimolar amounts of both components in CH_2Cl_2 and washing with water to remove the NaBr. After drying over $MgSO_4$ the solvent was evaporated under reduced pressure. The formation of the 1:1 complexes was confirmed by ^{1}H NMR.

7.4.2 Methods

^{1}H NMR (200 MHz) spectra were recorded on a Bruker AC200 spectrometer. The line broadening experiments were performed with 4 mM solutions of **X-Cn-Br** in D_2O at 70 °C. A Perkin-Elmer DSC-7 differential scanning calorimeter was used to determine the thermal phase transition enthalpies and temperatures, which are reported as the maxima of their endothermic peaks of the second heating scans. In all cases, heating and cooling rates were 10 °C/min. The sample solutions for DSC measurements consisted of a 1% (w/w) **X-C_n-Br** or **X-C_n-Br**-SDS (1:1) dispersion in water prepared by sonication. Polarisation microscopy was performed using an Olympus BH-2 microscope equipped with a Mettler FP82HT hot stage and a FP80HT temperature controller. The Krafft temperatures were determined by heating a concentrated amphotrope solution between glass slides. The temperature where the crystals melted upon heating was taken as the Krafft temperature.

Electron microscopy (JEOL 1200 EX II electron microscope) was carried out for samples that were negatively stained with a 1% aqueous uranyl acetate solution.

Critical aggregation concentrations were determined by measuring the specific conductivity of an amphiphile solution as a function of the concentration. A Philips Digital Conductivity meter PW 9527 with a Philips PW9550/60 electrode (cell constant 0.82 cm^{-1}) was used. The measuring compartment was thermostatted at 50 ± 0.5 °C with a Haake FE 2 Thermostat.

UV spectra were recorded on a Perkin Elmer Lambda 18 UV/VIS spectrophotometer at 25 °C. All amphiphiles were dissolved in ultra pure water (Seralpur Pro 90C) and the spectra were recorded after the addition of aliquots of an SDS solution.

7.5 References

1 Tschierske, C. *Prog. Polym. Sci.* **1996**, *21*, 775.
2 Nishimi, T.; Ishikawa, Y.; Ando, R.; Kunitake, T. *Recl. Trav. Chim. Pays-Bas* **1994**, *113*, 201.
3 Okahata, Y.; Kunitake, T. *Ber. Bunsenges. Phys. Chem.* **1980**, *84*, 550.
4 Shimomura, Y.; Kunitake, T. *J. Am. Chem. Soc.* **1982**, *104*, 1757.
5 Shimomura, Y.; Ando, R.; Kunitake, T. *Ber. Bunsenges. Phys. Chem.* **1983**, *87*, 1134.
6 Nishimi, T.; Ishikawa, Y.; Kunitake, T.; Sekita, M.; Xu, G.; Okuyama, K. *Chem. Lett.* **1993**, 295.
7 Kunitake, T. *Angew. Chem.* **1992**, *104*, 692.
8 Kimizuka, N.; Kunitake, T. *Chem. Lett.* **1988**, 827.
9 Shimomura, Y.; Kunitake, T. *Chem. Lett.* **1981**, 1001.

10 Adams, J.; Rettig, W.; Duran, R. S.; Naciri, J.; Shashidnar, R. J. *J. Phys. Chem.* **1993**, *97*, 2021.
11 Menzel, H.; Weichart, B.; Schmidt, A.; Paul, S.; Knoll, W.; Stumpe, J.; Fisher, T. *Langmuir* **1994**, *10*, 1926.
12 Everaars, M. D.; Marcelis, A. T. M.; Kuijpers, A. J.; Laverdure, E.; Koronova, J.; Koudijs, A.; Sudhölter, E. J. R. *Langmuir* **1995**, *11*, 3705.
13 See *e.g.* Bazuin, C. G.; Tork , A. *Macromolecules* **1995**, *28*, 8877; Bazuin, C. G.; Brandys, F. A.; Eve, T. M.; Plant , M. *Macromolecular Symp.* **1994**, *84*, 183; Moon, J. H.; Choi, J. U.; Kim, J. H.; Chung, H.; Hahn, J. H.; Kim, S. B.; Park, J. W. *J. Mater. Chem.* **1996**, *6*, 365.
14 Nishimi, T.; Tachikawa, M.; Maeda, T.; Ishikawa, Y.; Kunitake, T. *Chem. Lett.* **1994**, 331.
15 Gohy, J. F.; Vanhoorne, P.; Jérôme, R. *Macromolecules* **1996**, *29*, 3376.
16 Ujiie, S.; Iimura, K. *Macromolecules* **1992**, *25*, 3174.
17 Shimomura, M.; Aiba, S.; Tajima, N.; Inoue, N.; Okuyama, K. *Langmuir* **1995**, *11*, 969.
18 Schleek, T.; Imrie, C. T.; Rice, D. M.; Karasz, F. E.; Attard, G. S. *J. Pol. Sci. Part A.: Pol. Chem.* **1993**, *31*, 1859.
19 Moroi, Y. *Micelles, Theoretical and Applied Aspects,* Plenum Press: New York; 1992, p. 124.
20 Everaars, M. D.; Kuijpers, A. J. Wageningen Agricultural University. Personal communication.
21 Kalyanasundaram, K.; Grätzel, M.; Thomas, J. K. *J. Am. Chem. Soc.* **1975**, *97*, 3915.
22 Nery, H.; Marchal, J. P.; Canet, D.; Cases, J. M. *J. Colloid Interface Sci.* **1980**, *77*, 174.
23 Kunitake, T. *MRS Bulletin* **1995**, 22.
24 Herrington, K. L.; Kaler, E. W.; Muller, D. D.; Zasadzinski, J. A.; Chiruvolu, S. *J. Phys. Chem.* **1993**, *97*, 13792.
25 Filipovic-Vincekovic, N.; Skrtic, D.; Tomasic, V. *Ber. Bunsenges. Phys. Chem.* **1991**, *95*, 1646.
26 Chung, Y.; Regen, S. L.; Fukuda, H.; Hirano, H. *Langmuir* **1992**, *8*, 2843.
27 Fukuda, H.; Kawata, K.; Okuda, H.; Regen, S. L. *J. Am. Chem. Soc.* **1990**, *112*, 1635.
28 Kaler, E. W.; Murthy, A. K.; Rodriquez, B. E.; Zasadzinski, J. A. *Science* **1989**, *245*, 1371.
29 McRae, E. G.; Kasha, M. *Physical Processes in Radiation Biology,* Academic Press: New York; 1964, p. 23.
30 Okahata, Y. ; Ando, R.; Kunitake, T. *Ber. Bunsenges. Phys. Chem.* **1981**, *85*, 789.
31 Vogel, A. I. *Textbook of Practical Organic Chemistry*, Longman Scientific & Technical: Harlow; 1989, p. 949.

Summary

Hydrophobically modified polyelectrolytes can form micelle-like aggregates, so-called microdomains, in aqueous solution. The hydrophobic side chains constitute the apolar inner part of these microdomains and the hydrophilic groups on the polyelectrolyte backbone are at the surface of the microdomains. The microdomain formation is mainly determined by the polyelectrolyte charge density, which can be varied by changing the pH of the solution, and the length of the hydrophobic side chains. The flexibility of the backbone and the structure of the side chains are also important.

From literature it is known that the interaction between hydrophobically modified polyelectrolytes, also called polysoaps, and surfactants strongly depends on the charge density on the polyelectrolyte and the length of the hydrophobic side chains. These factors also determine the microdomain formation. The interaction between surfactants and polyelectrolytes in aqueous solution is thus highly dependent on the presence of microdomains. The research described in this thesis was aimed at determining the effects of charge density and hydrophobicity of polyelectrolytes on the interaction with surfactants.

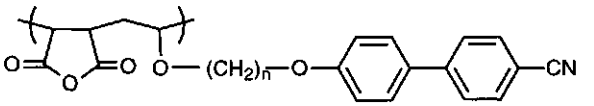

I-n, n = 6, 8, 10, 11, 12

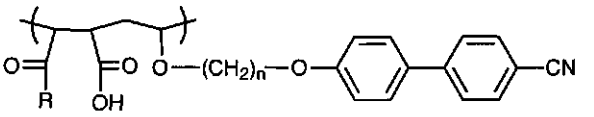

II-n, R = OH; n = 6, 8, 10, 11, 12
III-n, R = $NHCH_2CH_2SO_3^-K^+$; n = 6, 8, 10, 11, 12

Copolymers from maleic anhydride and alkyl vinyl ethers (**I-n**) have been synthesised by radical polymerisation. These polymers were hydrolysed to polyelectrolytes **II-n**. By reaction of **I-n** with 2-aminoethanesulfonic acid polyelectrolytes **III-n** were obtained. The alkyl vinyl ethers are substituted with rigid aromatic units, (cyanobiphenylyl)oxy units, which can induce the formation of liquid crystalline phases. Polymers **I-n** and **II-n** indeed form these phases. The isotropisation temperature of **II-n** is higher than for **I-n** due to the more flexible backbone of **II-n**. The enthalpy gain associated with the formation of the liquid crystalline phase increases with increasing spacer length and is larger for **II-n** than for **I-n** at comparable spacer length (Chapter 2).

The (cyanobiphenylyl)oxy units can also be used as chromophores. By the use of spectroscopic techniques one can study the microdomain formation of the polyelectrolytes

and the interaction with surfactants. The UV spectra of the polyelectrolytes depend on the pH of the solution, thus on the charge density of the polyelectrolyte, and on the hydrophobicity of the side chain. When the chromophores aggregate a blue shift of the absorption maximum of the (cyanobiphenylyl)oxy chromophores as compared to the monomeric absorption maximum is observed. So-called $\pi-\pi$ stacking interactions between parallel oriented aggregated chromophores are responsible for the blue shift. The extent of the blue shift is indicative for the conformation of the polyelectrolyte. UV measurements show that microdomains are formed by the polyelectrolytes **II-n** and **III-n** at $2 < pH < 13$, and that more compact microdomains are formed at lower pH.

Dynamic light scattering experiments confirm the formation of large aggregates in which the polyelectrolyte chains are highly entangled. Generally, the aggregates swell upon increasing the charge density, due to increased electrostatic repulsion on the polyelectrolyte backbone, and upon decreasing the side chain length (Chapter 3).

Oppositely charged surfactant molecules bind strongly to polyelectrolytes **II-n** and **III-n** in aqueous solution. Measurements using a dodecyltrimethylammonium (DTA^+) selective electrode shows that DTA^+ binds strongly and noncooperatively to both labelled and non-labelled polyelectrolytes. The surfactant molecules bind individually to the microdomains formed by a polyelectrolyte, indicating the formation of mixed micellar aggregates.

Surface tension measurements also show the very strong binding between the polyelectrolytes and DTAB which results in a synergistic lowering of the surface tension. The hydrophilicity of the polyelectrolytes is lowered in the presence of DTAB which results in a decrease in water solubility and an increase in the amount of polyelectrolyte-DTA^+ complex at the air-solution interface (Chapter 4).

By UV spectroscopy it is shown that within the microdomains the (cyanobiphenylyl)oxy chromophores are aggregated which results in a blue shift of the absorption maximum. Upon addition of surfactant molecules the blue shift decreases because the surfactant molecules penetrate between the hydrophobic side chains of the polyelectrolyte. The decrease in blue shift depends on the charge of the surfactant headgroup and on its hydrophobicity. The negatively charged sodium dodecyl sulfate (SDS) shows no influence on the wavelength of the absorption maximum and does not penetrate the microdomains. A non-ionic surfactant like polyoxyethylene(4)lauryl ether (Brij 30) interacts with the polyelectrolytes by purely hydrophobic interactions which results in a small decrease of the blue shift of the (cyanobiphenylyl)oxy chromophores. In addition to the results from the DTA^+ selective electrode and the surface tension measurements, the UV measurements also show the very strong interaction between polyelectrolytes and oppositely charged surfactants. Addition of a cationically charged surfactant causes the largest decrease in blue shift, thus the largest destacking of the (cyanobiphenylyl)oxy chromophores. The hydrophobicity of the surfactant

is also of importance as is clear from the larger decrease in blue shift observed for the addition of hexadecyltrimethylammonium bromide as compared to dodecyltrimethylammonium bromide. Upon increasing the surfactant concentration the blue shifts decrease gradually indicating noncooperative binding between the surfactants and hydrophobically modified polyelectrolytes. This agrees with the results obtained from measurements with the DTA^+ selective electrode (Chapter 4).

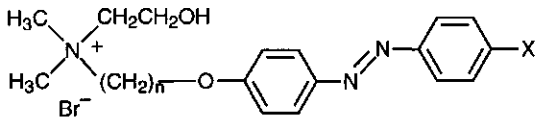

X-Cn-Br X = CN, OMe, F; n = 10, 12

The addition of surfactant molecules which are labelled with a chromophore to a polyelectrolyte solution yields extra information on the interactions. Therefore new surfactants carrying azobenzene chromophores, **X-Cn-Br**, were synthesised. The azobenzene units are substituted at the 4'-position with a cyano, methoxy or fluoro group. Initially, the interaction between these surfactants and nonlabelled polyelectrolytes was studied. The addition of **X-Cn-Br** to poly(maleic acid-*co*-*n*-butyl vinyl ether) results immediately in a maximum blue shift of the absorption maximum of the azobenzene groups. This indicates that the surfactants bind cooperatively to poly(maleic acid-*co*-*n*-butyl vinyl ether) allowing direct stacking between the azobenzene units. At the pH values used, poly(maleic acid-*co*-*n*-butyl vinyl ether) is in its extended conformation. When surfactant is added, the surfactant molecules form micelle-like aggregates surrounded by polyelectrolyte, and the counterions are disposed into solution. Upon increasing the side chain length of the polyelectrolyte the cooperativity decreases as is clear from the fact that the maximum blue shift is not immediately attained. The cooperativity also decreases upon decreasing the charge density on the polyelectrolyte. Both changes induce the formation of microdomains by the polyelectrolyte. When surfactants bind to these microdomains, mixed micelles are formed in which the surfactants sometimes cluster.

By labelling both polyelectrolyte and surfactant, the effects of interaction between polyelectrolytes and surfactants on the surfactant aggregation and on the disruption of the polyelectrolyte microdomains can be monitored. The measurements show that both the polyelectrolyte charge density and the length of the side chains influence the amount of interaction. These factors not only influence the electrostatic and hydrophobic attraction of surfactants to the polyelectrolytes, but they also determine the compactness of the microdomains. The spacer length of the surfactants and their terminal group seem to influence mainly the interaction between surfactant molecules (Chapter 4 and 5).

By use of the Langmuir technique the behaviour of polyelectrolytes **I-n** and **II-n** at the air-water interface is studied. Immediately after spreading both polymers form homogeneous layers on the subphase. The lift-off area per repeating unit indicates that the cyano groups of the chromophores of **I-11** and **I-12** are immersed into the subphase. For **I-6**, **I-8** and **I-10** the side chains are oriented randomly into the air. Polyelectrolytes **II-n** have a more flexible backbone than **I-n** which allows the (cyanobiphenylyl)oxy chromophores of **II-11** and **II-12** to assume a flat orientation on the subphase. This flat orientation is hindered for the shorter chained polyelectrolytes, but the cyano groups of **II-6**, **II-8** and **II-10** are thought to interact with the subphase. Polymers **II-n** all show a plateau in their π-A isotherms. In this plateau a triple layer is formed by folding a polymeric double layer onto a monolayer. At a molecular area of one third of the onset of the plateau the pressure starts to rise again, after which the triple layer collapses. The triple layer formation is confirmed by the semi-reversibility of compression-expansion experiments and Brewster angle microscopy.

The addition of both positively and negatively charged surfactants results in an increase in the lift-off area of **II-n**. This results from electrostatic interactions between the polyelectrolyte backbone and the surfactant headgroups, and hydrophobic interactions between the surfactant tails and polyelectrolyte side chains.

Monolayers of polyelectrolytes **II-n** can be transferred from pure water and from a 1 mM DTAB solution onto hydrophilic quartz or glass in a Z-type fashion. However, both UV spectroscopy and Second Harmonic Generation measurements show there is no overall order within the transferred layers (Chapter 6).

Besides the addition of the azobenzene substituted surfactants to solutions containing polyelectrolytes, their thermotropic and lyotropic phase behaviour in the absence and presence of SDS is also studied. The terminal substituent on the azobenzene chromophores and the counterion, bromide or dodecyl sulfate, influence the physical properties. Smectic A phases are found for **CN-Cn-Br**, **F-C12-Br**, **CN-Cn-DS**, **MeO-C10-DS** and **F-Cn-DS**. The formation of myelin structures of **CN-Cn-Br** and **MeO-Cn-Br** in water is seen by optical microscopy. These myelins transform into giant vesicles which are, however, not very stable and crystallise at room temperature. Vesicles formed in the presence of SDS, from so-called ion pair amphiphiles, are more stable due to the electrostatic and hydrophobic interactions. UV spectra of the ion pair amphiphiles display a blue shift of the azobenzene chromophores as compared to the monomeric chromophores, which indicates that the chromophores are parallelly aggregated within these mixed vesicles (Chapter 7).

Samenvatting

Polyelektrolyten met hydrofobe zijketens kunnen in water micel-achtige aggregaten vormen, de zogenaamde microdomeinen. De zijketens bevinden zich in het apolaire gedeelte van deze microdomeinen en de hydrofiele groepen van de hoofdketen zitten aan het oppervlak van het aggregaat. De microdomeinvorming hangt voornamelijk af van de ladingsdichtheid op de hoofdketen, die gevarieerd kan worden door de pH van de oplossing te veranderen, en de lengte van de zijketens. Ook de flexibiliteit van de hoofdketen en de ruimtelijke struktuur van de hydrofobe zijketens spelen een rol.

Uit literatuurstudie is gebleken dat de interactie van hydrofoob gemodificeerde polyelektrolyten, ook wel polyzepen genoemd, met surfactanten sterk afhankelijk is van de lading op het polyelektrolyt en de lengte van de hydrofobe zijketens. Deze faktoren spelen ook een belangrijke rol bij het vormen van microdomeinen. Er kan dus gezegd worden dat de interactie tussen surfactanten en polyelektrolyten sterk afhankelijk is van de mate van microdomeinvorming. De doelstelling van het onderzoek zoals beschreven in dit proefschrift was het bepalen van het effekt van ladingsdichtheid en hydrofobiciteit van polyelektrolyten op de interactie met surfactanten.

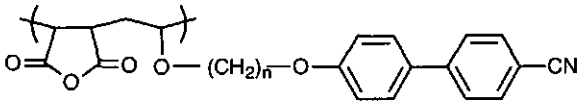

I-n, n = 6, 8, 10, 11, 12

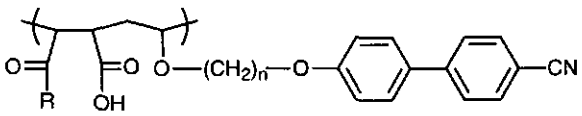

II-n, R = OH; n = 6, 8, 10, 11, 12
III-n, R = $NHCH_2CH_2SO_3^-K^+$; n = 6, 8, 10, 11, 12

Door middel van radikaalpolymerisatie uitgaande van maleïnezuuranhydride en alkylvinylethers zijn de polymeren **I-n** gesynthetiseerd. Vervolgens zijn de polymeren gehydrolyseerd tot de polyelektrolyten **II-n**. De reaktie van polymeren **I-n** met 2-aminoethaansulfonzuur leverde polyelektrolyten **III-n**. Aan de alkylvinylethers zijn rigide aromatische eenheden, (cyanobifenylyl)oxy groepen, gekoppeld die de vorming van vloeibaar kristallijne fasen kunnen induceren. De polymeren **I-n** en **II-n** vormen zulke fasen. De isotropisatietemperatuur is hoger voor de polymeren **II-n** welke een meer flexibele hoofdketen hebben dan polymeren **I-n**. De enthalpieverandering neemt toe met verlengen van de alkylspacer en is bij vergelijkbare ketenlengte groter voor **II-n** dan voor **I-n** (Hoofdstuk 2).

beïnvloedt. Deze faktoren hebben direkte invloed op de elektrostatische en hydrofobe aantrekking van de surfactanten tot de polyelektrolyten, maar bepalen ook de compactheid van de microdomeinen. De spacerlengte van de surfactanten en hun eindgroep lijken vooral de interactie tussen de surfactantmoleculen te beïnvloeden (Hoofdstukken 4 en 5).

Met de Langmuir techniek is het gedrag van de polymeren **I-n** en **II-n** aan het water-lucht grensvlak onderzocht. Beide soorten polymeren vormen direct na spreiding mooie homogene lagen op de subfase. Uit het benodigde oppervlak per repeterende eenheid kan worden afgeleid dat de (cyanobifenylyl)oxy chromoforen van de polymeren **I-11** en **I-12** met de cyaan groep in het water te liggen terwijl de zijketens van **I-6**, **I-8** en **I-10** zich willekeurig in de lucht richten. Polymeren **II-n** hebben een flexibelere hoofdketen dan **I-n** waardoor de (cyanobifenylyl)oxy groepen meer interactie met het water kunnen hebben en platter op de subfase liggen. Voor **II-6**, **II-8** en **II-10** verhindert de spacer de platte oriëntatie en steken waarschijnlijk alleen de cyano groepen in de subfase. Polymeren **II-n** vertonen allemaal een plateau in hun π-A isotherm. In dit plateau wordt een drielaag gevormd waarbij een polymere dubbellaag over de monolaag heenvouwt. Op een derde van het oppervlak waar het plateau begint loopt de druk verder op waarna de drielaag ineenstort. Compressie-expansie experimenten en Brewsterhoek microscopie bevestigen de vorming van de drielagen.

Het toevoegen van zowel positief als negatief geladen surfactanten aan de subfase zorgt voor een enorme toename in het benodigde oppervlak van **II-n** per repeterende eenheid. Dit is het gevolg van elektrostatische interacties tussen de polymere hoofdketen en surfactant kopgroepen en hydrofobe interacties tussen de polymere zijketens en de alkylstaarten van het surfactant.

De monolagen van de polymeren **II-n** kunnen via Z-type transfer worden overgebracht op hydrofiele substraten als glas en kwarts. Zowel UV spectroscopy als niet-lineair optische metingen van deze getransfereerde lagen tonen echter aan dat er geen macroscopische ordening optreedt in deze lagen (Hoofdstuk 6).

Van de nieuwe ammonium surfactanten met eindstandige azobenzeengroepen zijn ook de vloeibaar kristallijne eigenschappen en het aggregatiegedrag in water bestudeerd. De azobenzeen eindgroep en het tegenion, bromide of dodecyl sulfate, beïnvloeden deze eigenschappen. Smectische fasen worden gevonden voor **CN-Cn-Br**, **F-C12-Br**, **CN-Cn-DS**, **MeO-C10-DS** en **F-Cn-DS**. Optische microscopie toont de vorming van myeline structuren voor **CN-Cn-Br** en **MeO-Cn-Br** in water gevolgd door de vorming van reuzenvesikels. Deze zijn echter niet stabiel en kristalliseren uit bij kamertemperatuur. De vesikels gevormd in aanwezigheid van SDS zijn stabieler als gevolg van gunstige elektrostatische en hydrofobe interacties tussen beide componenten. De blauwverschuiving van het absorptiemaximum van de azobenzeen chromoforen toont aan dat er parallelle aggregatie van de chromoforen optreedt in deze gemengde vesikels (Hoofdstuk 7).

Curriculum Vitae

Armanda Cinderella Nieuwkerk werd geboren op 4 maart 1969 te Rotterdam. In 1987 behaalde zij het VWO diploma aan het Nienoord College te Leek. In datzelfde jaar werd begonnen met de studie Scheikunde aan de Rijksuniversiteit Groningen. Als afstudeerrichting werd gekozen voor Fysisch Organische Chemie onder leiding van prof. dr. J. B. F. N. Engberts. In het kader van een Erasmus-uitwisseling werd, onder leiding van prof. dr. U. Tonellato en dr. P. Tecilla, stage gelopen binnen de groep Organische Chemie aan de Universitá di Padova (Italië). Het doctoraal examen werd behaald in maart 1993. In de periode van 1 juni 1993 tot 1 juni 1997 was zij als onderzoekster in opleiding verbonden aan de vakgroep Organische Chemie van de Landbouwuniversiteit Wageningen. Daar werd het in dit proefschrift beschreven onderzoek uitgevoerd onder leiding van prof. dr. E. J. R. Sudhölter en dr. A. T. M. Marcelis.

List of Publications

A. C. Nieuwkerk, A. T. M. Marcelis, E. J. R. Sudhölter
Polyelectrolytes carrying pendant (cyanobiphenylyl)oxy mesogenic groups. Preparation, characterization, and pH-dependent behavior in aqueous solution.
Macromolecules **1995**, *28*, 4986-4990 (Chapters 2,3)

M. D. Everaars, A. C. Nieuwkerk, S. Denis, A. T. M. Marcelis, E. J. R. Sudhölter
Superstructures from didodecyldimethylammonium bromide and polyacrylic acid.
Langmuir **1996**, *12*, 4042-4043

A. C. Nieuwkerk, A. Koudijs, A. T. M. Marcelis, E. J. R. Sudhölter
Ion pair amphiphiles from sodium dodecyl sulfate and ammonium amphiphiles carrying functionalized azobenzene units.
Liebigs Annalen/Recueil **1997**, 1719-1724 (Chapter 7)

A. C. Nieuwkerk, A. T. M. Marcelis, E. J. R. Sudhölter
Chromophore labelling as a tool to study interactions between maleic acid copolymers and ammonium surfactants.
Langmuir **1997**, *13*, 3325-3330 (Chapter 4)

A. C. Nieuwkerk, A. T. M. Marcelis, E. J. R. Sudhölter
Interactions between hydrophobically modified poly(maleic acid-*co*-alkyl vinyl ether)s and dodecyltrimethylammonium bromide.
Progress in Colloid and Interface Science, submitted for publication (Chapter 4)

A. C. Nieuwkerk, E. J. M. van Kan, A. Koudijs, A. T. M. Marcelis, E. J. R. Sudhölter
Polyelectrolytes carrying pendant (cyanobiphenylyl)oxy chromophores. Synthesis and behavior in aqueous solution.
To be submitted (Chapters 2,3)

A. C. Nieuwkerk, E. J. M. van Kan, P. Kimkes, A. T. M. Marcelis, E. J. R. Sudhölter
Monolayer formation and film forming properties of maleic anhydride based copolymers.
To be submitted (Chapter 6)

A. C. Nieuwkerk, E. J. M. van Kan, A. Koudijs, A. T. M. Marcelis, E. J. R. Sudhölter
Interactions between maleic anhydride based copolymers and surfactants both carrying chromophoric labels.
To be submitted (Chapter 5)

A. C. Nieuwkerk, J. W. Streef, E. J. R. Sudhölter
New ferrocene containing ammonium amphiphiles. Synthesis and thermotropic and lyotropic behavior.
To be submitted